MATHEMATICAL MODELS FOR THE PREDICTION OF TEMPERATURE DISTRIBUTIONS RESULTING FROM THE DISCHARGE OF HEATED WATER INTO LARGE BODIES OF WATER

ENVIRONMENTAL PROTECTION AGENCY • WATER QUALITY OFFICE

WATER POLLUTION CONTROL RESEARCH SERIES

The Water Pollution Control Research Series describes the results and progress in the control and abatement of pollution of our Nation's waters. They provide a central source of information on the research, development, and demonstration activities of the Water Quality Office, Environmental Protection Agency, through inhouse research and grants and contracts with Federal, State, and local agencies, research institutions, and industrial organizations.

Inquiries pertaining to the Water Pollution Control Research Reports should be directed to the Head, Project Reports System, Office of Research and Development, Water Quality Office, Environmental Protection Agency, Washington, D.C. 20242.

MATHEMATICAL MODELS FOR THE PREDICTION OF TEMPERATURE DISTRIBUTIONS RESULTING FROM THE DISCHARGE OF HEATED WATER INTO LARGE BODIES OF WATER

by

Robert C. Y. Koh
Loh-Nien Fan
Tetra Tech, Inc.
630 N. Rosemead Blvd.
Pasadena, California 91107

for the

WATER QUALITY OFFICE
ENVIRONMENTAL PROTECTION AGENCY

Program #16130 DWO
Contract #14-12-570

October, 1970

For sale by the Superintendent of Documents, U.S. Government Printing Office
Washington, D.C., 20402 - Price $1.75

EPA Review Notice

This report has been reviewed by the Water Quality Office, EPA, and approved for publication. Approval does not signify that the contents necessarily reflect the views and policies of the Environmental Protection Agency, nor does mention of trade names or commercial products constitute endorsement or recommendation for use.

TABLE OF CONTENTS

LIST OF FIGURES

LIST OF SYMBOLS

For simplicity, symbols of secondary importance which appear only briefly in the text are omitted from the following list.

Chapter 3.

C_D	drag coefficient
C'_D	$\frac{3}{8} C_D$
D_o	jet diameter
E	entrainment function
F	density deficiency flux
F_1	initial value for density deficiency flux
G	temperature deficiency flux
G_1	initial value for temperature deficiency flux
K	coefficient
L	jet spacing
M	kinematic momentum flux
M'	momentum flux
M_1	initial value of kinematic momentum flux
Q	volume flux

Q_1	initial value of volume flux
Q_o	discharge
T	centerline temperature
T_a	ambient temperature
T^*	temperature
T_1	initial value of centerline temperature
a	thickness of spreading layer
a_o	initial thickness of spreading layer
b	jet characteristic width or radius of spreading layer
b_o	initial radius of spreading layer
d_j	depth of jet
f	buoyancy force
g	gravitational acceleration
p	pressure
q_o	discharge
s	coordinate along jet path
t	time

u	velocity along jet
u	centerline velocity along jet
x	horizontal coordinate
y	vertical coordinate
α	entrainment coefficient
α_s	entrainment coefficient for slot jet
α_r	entrainment coefficient for round jet
β	dimensionless radius of spreading layer
ϵ	eddy viscosity
η	coordinate normal to s
θ	angle of jet trajectory
θ_o	initial angle of jet discharge
ρ	centerline density
ρ_o	ambient reference density
ρ_a	ambient density
ρ^*	density
ρ_1	jet discharge density

λ_s	spreading ratio for slot jet
λ_r	spreading ratio for round jet
τ	dimensionless time

Chapter 4.

F	densimetric Froude number $= U^2/g \frac{T}{\rho_o} h$
F_o	source densimetric Froude number $= U_o^2/ g \frac{T_o}{\rho_o} h_o$
F_2	value of F after an internal hydraulic jump
F_{ocr}	critical value of densimetric Froude number
K	surface heat exchange coefficient
K_{cr+}	upper critical value of K above which jet type solution exists
K_{cr-}	lower critical value of K below which the source is inundated
R	Reynolds number $= \frac{Uh}{\varepsilon}$
Ri	Richardson number $= \frac{1}{F}$
Ri_{cr}	critical Richardson number
T	density deficiency
T_o	source density deficiency

U	velocity
U_o	source velocity
e	entrainment coefficient
e_o	entrainment coefficient for $F = \infty$
g	gravitational acceleration
h	thickness of surface jet
h_o	initial thickness of surface jet
k	dimensionless surface heat exchange coefficient
k_{cr+}	upper critical value of k
k_{cr-}	lower critical value of k
p	pressure
q_o, q_2	discharge
r	radial coordinate
s	$\frac{1}{Rk}$
u	horizontal velocity or dimensionless velocity
v	vertical velocity
x	horizontal coordinate
y	vertical coordinate
z	vertical coordinate in axisymmetric case

α, α_1, α_2	coefficients
γ	dimensionless coefficient, $= \frac{2F_o}{R}$
η	free surface elevation
θ	density deficiency
τ	shear stress (kinematic)
τ_s	shear stress at free surface (kinematic)
τ_i	shear stress at interface (kinematic)
ϵ	shear coefficient
ρ	density
ρ_o	ambient density
ρ_1	jet density

Chapter 5. (Note: Primed quantities are dimensionless)

A	dissipation parameter ($K_z = A\sigma_z^{4/3}$)
A_L	dissipation parameter ($K_z = A_L L^{4/3}$)
C_h	specific heat of water
E	equilibrium temperature
F_{CO}	source strength
H_a	heat content of ambient above a given reference level

H_t	total heat content above a given reference level
K_x	longitudinal diffusion coefficient (horizontal)
K_y	vertical diffusion coefficient
K_{y1}	vertical diffusion coefficient at sea surface
K_z	lateral diffusion coefficient (horizontal)
K_E	surface heat exchange coefficient
K_e	kinematic surface heat exchange coefficient $(K_E/\rho C_h)$
K_d	decay coefficient
L_o	source width
L	plume width
R_i	Richardson number $\left(\frac{\frac{g}{\rho}\left\|\frac{d\rho}{dy}\right\|}{(\frac{du}{dy})^2}\right)$
T	temperature excess
T_a	surface ambient water temperature
T_p	surface water temperature
c	concentration
c_o	zeroth moment of c
c_1	first moment of c
c_2	second moment of c
c_{max}	maximum value of c in z

g	gravitational acceleration
h_o	source thickness
h_b	depth of water
t	time
u	velocity in x-direction
u_o	characteristic velocity
v	velocity in y - direction
w	horizontal coordinate, in direction of current
x_t	terminal x of interest
y_{K1}, y_{K2}, y_{K3}, y_{K4},	y - coordinates in defining K_y - profiles (see Fig. 5.7)
y_{e1}, y_e	y - coordinates in defining u - profiles (see Fig. 5.7)
y_o	source level
z	horizontal coordinate, transverse to current
β_1, β_2	coefficients in defining K_y profile (see Fig. 5.7)
ϵ	density gradient
ρ	density
σ_z	plume width characteristic

σ_0 source width characteristic

λ' dimensionless dissipation parameter = $\dfrac{Ax_t}{\left\{\sigma_z^{2/3}(o, y_o)u_o\right\}}$

CHAPTER 1 INTRODUCTION

The rise in the production of electric power has resulted in the attendant generation of large quantities of waste heat. This waste heat is usually disposed of either to the atmosphere through cooling towers or ponds or to adjacent bodies of water. In order to properly manage the vast quantities of waste heat which will be produced in the future, it is necessary to develop a body of knowledge on the transport behavior and the effects of heat on the total environment. One important item in this necessary body of knowledge is the ability to predict the temperature distribution in the environment given the method of waste heat discharge and the characteristics of the environment. The present investigation is concerned with the development of prediction methods in the case when the waste heat is discharged into a large body of water. In this case, two limiting schemes can be envisioned for the method of discharge of heated water. First, one may employ a multiport diffuser submerged at some depth to promote much initial dilution such as is done for sewage. Alternatively, the other extreme would be to "float" the warm water on the surface, resulting in a minimum of initial dilution while maximizing the rate of heat loss to the atmosphere.

In order to properly evaluate the effects of various discharge schemes on the environment, it is necessary to be able to predict the resulting temperature distribution given the discharge scheme. This would also provide a rational basis for the design of the discharge structure.

Of importance in this overall problem of excess temperature prediction are the following phenomena and their interrelationships:

a) <u>momentum of the discharge.</u> For discharge schemes employing relatively large efflux velocities, the behavior of the effluent near the source is strongly influenced by this momentum and the mixing phenomenon may resemble that in a jet.

b) <u>buoyancy of the discharge</u>. Since the effluent is warmer (and hence lighter) than that of the receiving waters, there is a tendency for it to float on top of the ambient cooler (and hence heavier) water.

c) dispersion due to ambient turbulence. Even in the absense of momentum and buoyancy, the introduction of any miscible tracer into a body of water would result in the dispersion of the tracer due to existing turbulence in the ambient.

d) ambient density stratification. The water in a typical lake, reservoir or the ocean is often density stratified particularly in the summer months. The stable stratification has the profound effect of suppressing vertical turbulence and dispersion. In addition, the warm effluent, if discharged at the surface, tends to float on top of the cooler ambient and enhance the existing stratification.

e) ambient current structure. The effluent, other than undergo motions induced by its own momentum and buoyancy, would also be advected by any ambient currents which may be there. These currents may change with time and location.

f) solid boundaries. The presence of boundaries (both the shore and the bottom) also affects the dispersion of the effluent and the resulting temperature distribution in the local environment.

g) surface heat exchange. The warm effluent exposed to the atmosphere would gradually lose heat to the atmosphere, altering the temperature and density of the water, particularly when there is wind.

When heated cooling water is released from a power plant through a discharge structure, all the mechanisms discussed above and their interrelationships play a role in influencing the resulting temperature distribution in the receiving water. However, different mechanisms would dominate in different regions of the induced flow field. For example, near the source of discharge, it can be expected that the momentum and buoyancy of the effluent would be important in influencing the mixing process. On the other hand, far from the source, it may be imagined that the ambient currents and turbulence would be dominating factors and the dispersion may be thought of as more or less passive. In between, all the mechanisms may contribute to the dispersion process.

The phenomenon of dispersion and mixing of one fluid with another has been studied by numerous investigators. There is, for example, a body of knowledge on the dispersion of sewage effluent discharged from outfalls. These can be applied, with some modifications, to the problem of the transport behavior of heated water discharged below the surface. Also there are some laboratory studies on the dispersion of heated water discharged at the surface into a laboratory tank containing cooler water. These investigations will now be briefly summarized.

a) Dispersion of Sewage Effluent. Present methods of ocean sewage disposal typically discharges the effluent through a multiport outfall diffuser submerged at about 200 ft. depth. The mixing processes undergone by the effluent can be divided into three separate phases. First, the effluent undergoes jet diffusion through entrainment of the ambient water as it rises in the form of a buoyant jet or plume. Second, on reaching its terminal level of ascent which may be the surface it spreads out horizontally due to the density difference or difference in density stratification. Third, it further diffuses in the prevailing ocean current. The phenomenon of buoyant jets and plumes has been studied by many investigators including Abraham (1963), Brooks and Koh (1965) and Fan (1967). Almost all those investigations are for the case when the ambient fluid is motionless.

The further passive diffusion of the diluted effluent in the prevailing current has been studied by Brooks (1960) for the case of vertical uniformity and constant current velocity with the lateral dispersion characterized by a power dependence on the plume width. Edinger and Polk (1969) analyzed the similar problem including vertical variations but all dispersion coefficients and currents were assumed constant.

The second phase of the horizontal spreading phenomenon has, to date, not been studied to nearly the same extent. Some small scale laboratory experiments have been performed by Sharp (1969), for the case when the spreading is on the surface of a quiescent laboratory tank.

b) Studies on Thermal Dispersion on the Surface. The growing concern over thermal pollution has lead to several laboratory and theoretical investigations of the dispersion of heated water discharged on the surface of a body of cooler ambient water. Jen, Wiegel and Mobarek (1966), Hayashi and Shuto (1967), and Stefan and Schiebe (1968) performed laboratory experiments where the warm water was discharged from a finite source horizontally into a quiescent cooler ambient. Measurements were made for a variety of cases. Wada (1966) and Hayashi and Shuto further advanced a theory for this problem. However, it is applicable only for extremely low discharges and small temperature differences. The two-dimensional case of the same problem was also investigated experimentally by Stefan and Schiebe with several interesting results.

From the above brief summary of previous work on the problem of prediction, it is clear that no general method exists by means of which the temperature distribution resulting from waste heat discharge can be predicted. It is the purpose of the present investigation to advance the status of knowledge on this problem. It should be pointed out that no general prediction method is developed in this report. Rather, several simpler prediction models are developed each applicable under differing circumstances. It is believed that these models bring us closer to the time when a general model may be formulated.

It will become obvious on reading the subsequent chapters of this report that the general mixing and dispersion phenomenon which ensues following the discharge of heated cooling water into a large body of water is highly complex and thus difficult to analyze. Not only is the hydrodynamical aspects complicated, the prevailing ambient conditions are usually not deterministic and can only be statistically described. Moreover, the interplay of the many mechanisms such as source momentum, buoyancy, surface heat loss, ambient currents and so on, make the problem difficult to describe even qualitatively. Therefore, before any attempt is made to develop a general prediction model, it is necessary to examine the significance and interrelationships between these mechanisms taken several at a time. This then is the philosophy of the present investigation. It is found that the interrelationship between these mechanisms are such that the flow field is sometimes entirely different from what may be intuitively expected.

This report has been divided into several chapters. Chapter 3 deals with the initial and intermediate phases of mixing in the event the discharge is made at depth. The problem of a row of equally spaced round buoyant jets discharging at an arbitrary angle into an arbitrarily density-stratified body of water is solved in Sec. 3.2. The unsteady surface spreading of a warm fluid on top of a cooler ambient is analyzed in Sec. 3.3.

Chapter 4 deals with the case when the discharge is made at the surface. The two-dimensional case is treated in detail while the axisymmetric case is also examined. The effects of source momentum, source buoyancy, interfacial shear, surface heat exchange and entrainment are all included. It is found that the flow field can be entirely different depending on the relative importance of these mechanisms. In some cases, the flow field is like a jet while in others, it is like a two-layered stratified flow. Under certain conditions, the flow field consists of a jet type region near the source followed by a stratified flow region with an internal hydraulic jump joining the two. Given the source characteristics and the ambient conditions, the model developed can predict the flow field and the temperature distribution and also locate the hydraulic jump, if it occurs.

In Chapter 5, two mathematical models have been developed for the case of passive turbulent diffusion from a continuous source in a unidirectional current. The vertical dispersion is allowed to be an arbitrary prescribed function of the vertical coordinate. The horizontal dispersion is assumed to be proportional to the 4/3 power of the plume width. In Section 5.3, a model is developed for the case of a steady release into a steady environment with a shear current (PTD). In Section 5.4, a model is developed for the case of a time varying release into a time varying environment (UTD). In the latter model, the current is unsteady but uniform.

Most of the models developed in this investigation represent generalizations of previously existing models. For example, in Chapter 3, the previous analyses on a single buoyant jet has been generalized to include a row of jets which interferes and to include an arbitrary ambient density stratification. In Chapter 5, the problem of dispersion from a continuous source in a current has been generalized to include arbitrary vertical distributions for current and vertical diffusivity. Previous models have assumed constant current and constant diffusivities. In these cases, the solutions found are as expected in the sense that they are qualitatively the same as those previously found. The model developed in Chapter 4, on the horizontal surface buoyant jet, however, gives results which are qualitatively different from previous investigations on either the ordinary jet or the submerged buoyant jet. These results should be verified in the laboratory. Some laboratory experiments on this phenomenon have been reported by Stefan and Schiebe (1968), which showed some of the qualitative features found in this investigation. These should be analyzed in more detail in the light of the present findings.

CHAPTER 2. CONCLUSIONS & RECOMMENDATIONS

In this report, several mathematical models have been developed for predicting the distribution of excess temperature resulting from the discharge of heated cooling water from power plants into large bodies of water. The main conclusions and recommendations are as follows:

a) Initial mixing for subsurface discharge.

1. The flow field and mixing resulting from a row of equally spaced round buoyant jets discharging at an arbitrary angle into a quiescent ambient with arbitrary density and temperature stratification is formulated. A computer program RBJ (Appendix A) has been written to obtain the solution given the jet characteristics and the ambient conditions.

2. The flow field consists of two zones. Near the source, the individual round jets behave as if they were single jets. Further away, they merge together and resemble a two-dimensional slot jet.

3. The transition from one zone to the other is taken to be either 1) when the round jet width is equal to the jet spacing, or 2) when the entrainment based on round jet analysis and slot jet analysis are equal.

4. It is found that the two transitions give virtually identical results except in the small region between the two transition points.

5. Due to the relatively large dilution ratios and the fact that the temperature excess of the discharge is usually only 10 to 20^{o}F, a very small density stratification is sufficient to prevent the discharge from reaching the surface. In that event, all the temperature excess is assimilated in the ambient subsurface water.

It is recommended that

1. A parametric study be performed based on the model developed (RBJ) to obtain the resulting temperature excess distribution in a variety of cases.

2. The model be extended to include end effects. The model developed assumes infinitely many equally spaced round jets. Practical multiport diffusers are of finite length. Thus it is recommended that the effects of the end jets be analyzed. It can be expected that the effects would be most important for short diffusers. However, the model RBJ should give conservative results.

3. The model be extended to include an ambient current. Presence of ambient current would further contribute to the mixing of the effluent with the receiving waters. This effect should be analyzed by incorporating the current into the model guided by available experiments.

4. The model be verified by laboratory investigation. Although there has been much laboratory investigation on single buoyant jets in linearly stratified ambient, there is little on multiple jets in non-linearly stratified water. Experiments should be performed to verify the findings from this model.

b) Intermediate phase for subsurface discharge.

1. In the event the buoyant jet reaches the free surface, a model is developed to obtain the spreading of the buoyant fluid on the ambient (Sec. 3. 3).

2. In the two-dimensional case, the horizontal extent of the spreading layer is found to grow (after a brief initial period) at first linearly with time t gradually becoming proportional to $t^{4/5}$.

3. In the axisymmetric case, the radius of the spreading layer is found to grow (after a brief initial period) as $t^{3/4}$ at first gradually becoming proportional to $t^{1/2}$.

It is recommended that

1. A laboratory investigation be performed to verify the model and to obtain the coefficients needed.

c) Surface horizontal buoyant jet.

1. The flow field induced and the dispersion process in a horizontal buoyant jet discharged at the surface is investigated in Chapter 4. The interplay of source momentum, source buoyancy, interfacial shear, entrainment, and surface heat loss have all been incorporated in the model. The two-dimensional case has been treated in detail.

2. The flow field is found to possess features different from that of either an ordinary non-buoyant jet or a fully submerged buoyant jet.

3. The type of flow field is found to depend on the relative magnitudes of three parameters: F_o, the source densimetric Froude number, k, the dimensionless surface heat exchange coefficient, and R, the source Reynolds number.

4. The parameter space can be divided into three regions such that given F_o and R for example, there exist two critical values for k, $k_{cr+} > k_{cr-}$ such that if $k > k_{cr+}$, the flow field is of jet type. If $k < k_{cr-}$, the source is inundated. For $k_{cr-} < k < k_{cr+}$, the flow field consists of a jet type region near the source followed by an internal hydraulic jump. The flow field after the jump resembles that in a two-layered stratified flow.

5. The finding in 4. is of importance from design considerations since; a) the temperature distribution is dependent on the type of flow field, and b) inundation of the source may lead to short circuiting the intake and discharge of cooling water.

It is recommended that

1. Available laboratory experiments be analyzed to verify the findings and determine the coefficients.

2. Further laboratory experiments be performed to supplement those already available.

3. The analogous axisymmetric problem (Sec. 4.3) be analyzed in detail to obtain the critical relations in parameter space.

4. The analysis be extended to the three-dimensional case.

d) Passive diffusion in a current.

1. Two mathematical models have been developed in Chapter 5 resulting in two computer programs; PTD (Appendix C) and UTD (Appendix D). In both models, longitudinal dispersion is ignored. Lateral dispersion is assumed to follow a 4/3 law. The vertical diffusion coefficient is allowed to be an arbitrary function of the vertical coordinate.

2. Program PTD treats the case of steady release of contaminant into a steady uni-directional shear current. Program UTD treats the case of a time-variable release into a time-varying uniform current. The surface heat exchange coefficient, assumed constant in PTD, is allowed to be time varying in UTD.

3. Results from the models are as would be expected. Larger diffusion coefficients result in larger dispersion.

4. The presense of current shear was found to enhance the dispersion process.

It is recommended that

1. The models be applied to a variety of cases to further obtain the quantitative dependence of the dispersion process on the parameter.

2. The model be extended to include the effects of longitudinal diffusion and a time dependent current shear. Moreover, the current should be allowed to exist in two directions, so that the current direction as well as magnitude are functions of depth.

   The models should also be extended to include the possibility of current reversals and times of slack (no current). The extension of the models to include those effects can be achieved by 1) formulating the dispersion model for an instantaneous source in a general ambient and 2) superposing the solutions to obtain the resulting contaminant distribution.

CHAPTER 3 INITIAL MIXING AND SURFACE SPREADING DUE TO SUBSURFACE DISCHARGE

3.1 Introduction

The heated cooling water containing the waste heat from a power plant is often discharged into a neighboring body of water. The discharge may be made at the surface or submerged at some depth. These may be thought of as representing two different philosophies of alleviating the thermal pollution problem. If the discharge is made at the surface then it is possible to design the discharge structure in such a way that minimal mixing occurs between the effluent and the ambient water. This promotes a comparatively high rate of heat dissipation to the atmosphere. On the other hand, if the discharge is made at depth, then it is possible to promote much initial mixing reducing the temperature rise in the ambient. In this case, however, the rate of heat dissipation to the atmosphere is correspondingly much lower. Of course, it is also possible to design a surface discharge scheme which results in much initial mixing. The subject of surface discharge will be treated in Chapter 4 of this report where it will be shown that proper design to achieve given goals may be more difficult than it first appears.

In this chapter, we shall investigate some aspects of the flow and mixing phenomenon when the discharge is made at depth. Since the heated water is slightly less dense than the ambient water, the efflux would tend to rise towards the surface. The general mixing and flow field can be conveniently divided into three phases: an initial phase of jet mixing where the momentum and buoyancy of the efflux are of importance in governing the flow; a final phase of passive turbulent diffusion where the ambient turbulence and currents are dominant in the dispersion process; and an intermediate phase joining the two. The final phase of passive turbulent diffusion will be investigated in Chapter 5. In this chapter, we shall investigate the initial phase of jet mixing and the intermediate phase.

3.2 Initial Mixing Phase: Multiple Submerged Buoyant Jets Discharged into an Arbitrarily Stratified Ambient

The mixing phenomenon in buoyant jets and plumes have been studied by numerous investigators. Morton, Taylor and Turner (1956) applied an integral method to the problem of a buoyant plume discharged as a point source into a linearly stratified ambient fluid. Brooks and Koh (1965) analyzed the two-dimensional buoyant jet problem with application to the design of a submerged ocean outfall diffuser. Fan (1967) examined the more general case where the angle of discharge is arbitrary. Abraham (1963) examined the same problem as Fan but using a slightly different mechanism of entrainment. All these studies assume 1) similarity in the flow pattern, 2) density differences are small so that the Boussineq approximation is valid, 3) an entrainment mechanism which depends only on the local mean flow, and 4) the ambient fluid is motionless.

For application to the practical situation, it is necessary to generalize the models developed in several respects. First, all the previous studies are for a single jet (either axisymmetric or two-dimensional). In a practical case, there may be many jets spaced by a certain distance from one another. Thus after an initial period, these jets would merge and interfere with each other. Second, the ambient density stratification is most likely not linear. Third, the ambient fluid may not be motionless in the vicinity of the discharge. Finally, for application to thermal discharges, it must be realized that the ambient density stratification and the thermal stratification may be different as, for example, in the case when salinity variations are also contributing to the density stratification.

In this chapter, a general integral model is first developed which is independent of the geometry of the jet (i.e., equally applicable to two-dimensional or axisymmetric cases). The ambient density stratification and temperature stratification are considered as independent and arbitrary (may be nonlinear). This model is then specialized to either the two-dimensional case of a slot jet or the axisymmetric case of a round jet. The case of a row, of equally spaced round jets, is then examined. Near the source, before jet interference, the individual round jets are more or less separate and the axisymmetric case applies. At some point, the individual jets would begin to merge and finally the two-dimensional case would apply. The transition from one to the other occurs in an intermediate zone where neither axisymmetry or two-dimensionality obtain. In the model to be developed, the transition is taken to be sudden. However, two different transition criteria were used and the results are found to be virtually the same based on either criteria.

3.2.1 Formulation

Consider a jet oriented at angle θ_o to the horizontal issuing fluid of density ρ_1 and temperature T_1 into an ambient of density stratification $\rho_a(y)$ and temperature stratification $T_a(y)$. Let Q_1 be the discharge, M_1 the momentum flux, F_1 the density deficiency flux, and G_1 the temperature deficiency flux at the source. Figure 3.1 illustrates the general behavior of such a jet. The bending of the jet path is a result of the fact that the discharge is buoyant. Define u^* as the velocity, T^* the temperature and ρ^* the density of the fluid. Since the ambient is motionless, u^* is assumed to be along the jet path. Let s be the coordinate along the jet path, A-plane be the plane perpendicular to the jet path, and θ the angle of the jet path with respect to the horizontal. We now define the volume flux Q, momentum flux M, density deficiency flux F and temperature deficiency flux G as

$$Q = \int_A u^* \, dA, \tag{3.1}$$

$$M = \frac{M'}{\rho_o} = \frac{1}{\rho_o} \int_A u^{*2} \rho^* dA \approx \int_A u^{*2} dA \tag{3.2}$$

$$F = \int_A (\rho_a - \rho^*) \, u^* \, dA \tag{3.3}$$

Note that M' is the true momentum flux while M is the kinematic momentum flux.

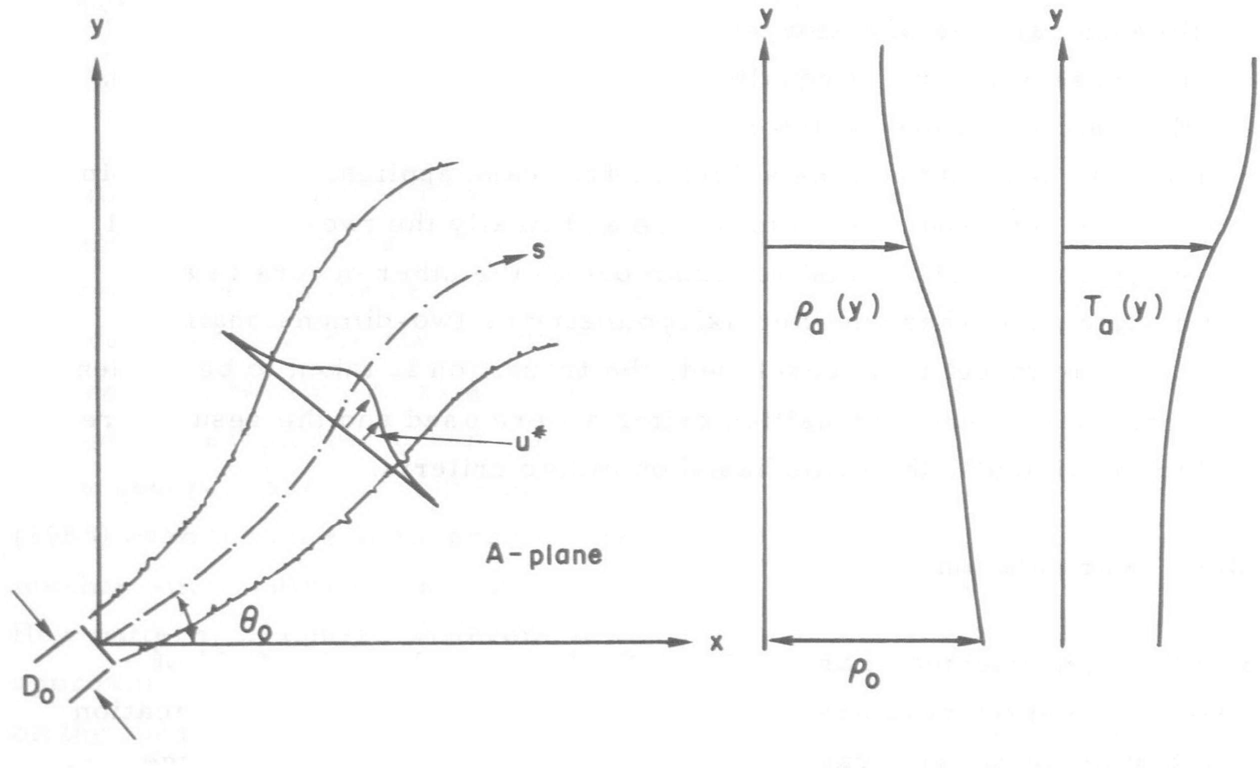

Figure 3.1 Definition sketch

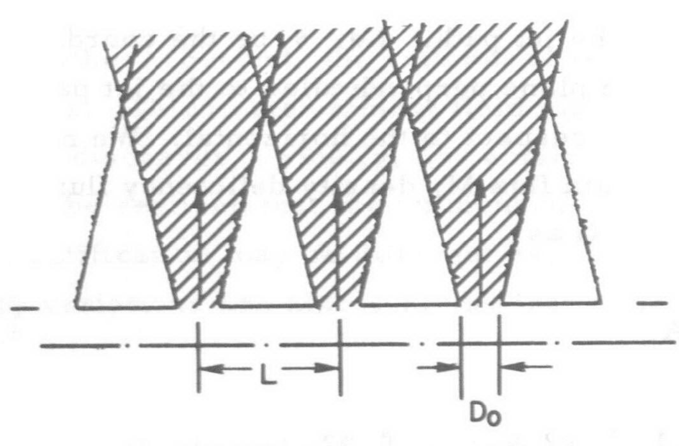

Figure 3.2 Jet interference

$$G = \int_A (T_a - T^*) u^* \, dA \qquad (3.4)$$

We note that in the vertical direction, a buoyancy force exists due to the density difference between the jet fluid and the ambient fluid tending to bend the jet. This force f is

$$f = g \int_A (\rho_a - \rho^*) \, dA \qquad (3.5)$$

The conservation equations can now be written in terms of the variables. The conservation of mass equation is

$$\frac{dQ}{ds} = E \qquad (3.6)$$

where E is the rate of entrainment of ambient fluid. Note that strictly speaking, since the density is variable we should really have, instead of Eq. (3.6)

$$\frac{d}{ds}\left\{ \int_A u^* \rho^* \, dA \right\} = E \rho_a \qquad (3.7)$$

However, all density differences are small and we may approximate the Eq. (3.7) by (3.6)

The conservation of horizontal momentum flux is

$$\frac{d(M \cos \theta)}{ds} = 0 \qquad (3.8)$$

For the vertical momentum, we must include the buoyancy force. Thus

$$\frac{d}{ds} (M' \sin \theta) = f \qquad (3.9)$$

The conservation of density deficiency flux equation reads

$$\frac{d}{ds}\left\{ \int_A u^* (\rho_o - \rho^*) \, dA \right\} = E(\rho_o - \rho_a) \qquad (3.10)$$

where ρ_o is a reference density (e.g., $\rho_o = \rho_a(0)$). Equation (3.10) can be written

$$\frac{d}{ds}\left\{\int_A u^*(\rho_o - \rho_a)\, dA + \int_A u^*(\rho_a - \rho^*)\, dA\right\} = E(\rho_o - \rho_a)$$

or

$$(\rho_o - \rho_a)\frac{dQ}{ds} + Q\left(-\frac{d\rho_a}{ds}\right) + \frac{dF}{ds} = E(\rho_o - \rho_a) \tag{3.11}$$

Using Eq. (3.6), we finally have

$$\frac{dF}{ds} = \frac{d\rho_a}{ds} Q \tag{3.12}$$

Similarly, the conservation of temperature deficiency flux equation reads

$$\frac{d}{ds}\left\{\int_A u^*(T_o - T^*)\, dA\right\} = E(T_o - T_a) \tag{3.13}$$

which reduces, with Eq. (3.6), to

$$\frac{dG}{ds} = \frac{dT_a}{ds} Q \tag{3.14}$$

Equations (3.6), (3.8), (3.9), (3.12) and (3.14) constitutes five equations for the five unknowns Q, M, θ, F, G, as functions of s once we can express E and f in terms of known quantities or these unknowns. To do this we will make two more assumptions. First, we shall assume similarity of the shapes of the velocity profile, temperature deficiency profile and density deficiency profile in the plane A. In particular, it will be assumed that the profiles are Gaussian. Thus, in the two-dimensional case (slot jet) we assume

$$u^*(s, \eta) = u(s)\, e^{-\eta^2/b^2(s)} \tag{3.15}$$

$$\rho_a - \rho^*(s, \eta) = [\rho_a - \rho\ (s)]\, e^{-\eta^2/\lambda_s^2 b^2} \tag{3.16}$$

$$T_a - T^*(s,\eta) = [T_a - T(s)]\, e^{-\eta^2/\lambda_s^2 b^2} \tag{3.17}$$

where u(s), $\rho(s)$, and T(s) are the values along the jet centerline. η is the coordinate normal to s, b(s) is the characteristic jet width, and λ_s is a turbulent Schmidt number for the two-dimensional case. Similarly in the axisymmetric case, we take

$$u^*(s,r) = u(s)\, e^{-r^2/b^2} \tag{3.18}$$

$$\rho_a - \rho^*(s,r) = [\rho_a - \rho(s)]\, e^{-r^2/\lambda_r^2 b^2} \tag{3.19}$$

$$T_a - T^*(s,r) = [T_a - T(s)]\, e^{-r^2/\lambda_r^2 b^2} \tag{3.20}$$

Secondly, we shall assume that the entrainment function E is proportional to the jet characteristic velocity u and the jet boundary ($2\pi b$ or 2L) and the proportionality constant is α (α_r for round jet and α_s for slot jet).

Substituting these expressions into the definitions for Q, M, F, G and f (Eqs. (3.1) through (3.5)) will give Q, M, F, G and f expressed in terms of the quantities u, ρ, T and b. For example, substituting Eq. (3.15) into (3.1) gives

$$Q = L\int_{-\infty}^{\infty} u(s)\, e^{-\eta^2/b^2}\, d\eta$$

where L is the length of the jet. Thus

$$Q = Lub\int_{-\infty}^{\infty} e^{-\xi^2}\, d\xi = \sqrt{\pi}\, ubL$$

Similarly, substituting Eqs. (3.15) and (3.16) into Eq. (3.3) gives

$$F = L\int_{-\infty}^{\infty} u\, e^{-\eta^2/\lambda_s^2 b^2 - \eta^2/b^2} (\rho_a - \rho)\, d\eta$$

$$= Lu(\rho_a - \rho)\int_{-\infty}^{\infty} e^{-(\eta^2/b^2)(1/\lambda_s^2+1)}\, d\eta$$

$$= Lu(\rho_a - \rho)\, b\sqrt{\frac{\lambda_s^2 \pi}{1+\lambda_s^2}}$$

In this fashion, Table 3.1 may be constructed;

TABLE 3.1

	For Round Jet	For Slot Jet of Length L
Volume Flux Q	$\pi u b^2$	$\sqrt{\pi}\ ubL$
Momentum Flux $M = \frac{M'}{\rho_o}$	$\pi u^2 b^2/2$	$\sqrt{\pi/2}\ u^2 bL$
Density Deficiency Flux F	$\frac{\lambda_r^2}{1+\lambda_r^2} \cdot \pi u b^2(\rho_a - \rho)$	$\sqrt{\frac{\pi\lambda_s^2}{1+\lambda_s^2}}\ ub(\rho_a - \rho)L$
Temperature Deficiency Flux G	$\frac{\lambda_r^2}{1+\lambda_r^2}\ \pi u b^2(T_a - T)$	$\sqrt{\frac{\pi\lambda_s^2}{1+\lambda_s^2}}\ ub(T_a - T)L$
Buoyancy Force f	$\pi\lambda_r^2 b^2 (\rho_a - \rho) g$	$\sqrt{\pi}\ \lambda_s bLg(\rho_a - \rho)$
Entrainment Function E	$2\pi\alpha_r ub$	$2\alpha_s\ uL$

This table gives the transformation from the variables u, b, etc. to the variables Q, M, etc. The inverse transformation is given in Table 3.2. Moreover, it is possible to express E and f now in terms of Q, M, etc. as shown in Table 3.3

The problem under consideration in this chapter is the mixing processes involved for a row of round buoyant jets spaced a distance L apart. Initially, the jets are separate round jets. However, after a while, they begin to merge and form more nearly a two-dimensional

TABLE 3.2

	Round Jet	Slot Jet
Centerline Velocity u	$2M/Q$	$\sqrt{2}\, M/Q$
Norminal Half Width b	$Q/\sqrt{2\pi M}$	$Q^2/[\sqrt{2\pi}\, LM]$
Density Deficiency $\rho_a - \rho$	$\frac{1+\lambda_r^2}{\lambda_r^2}\, F/Q$	$\sqrt{\frac{1+\lambda_s^2}{\lambda_s^2}}\, F/Q$
Dilution Ratio S	Q/Q_1	Q/Q_1
Temperature Deficiency $T_a - T$	$\frac{1+\lambda_r^2}{\lambda_r^2}\, G/Q$	$\sqrt{\frac{1+\lambda_s^2}{\lambda_s^2}}\, G/Q$

TABLE 3.3

	Round Jet	Slot Jet
E	$2\sqrt{2\pi}\, \alpha_r \sqrt{M}$	$2\sqrt{2}\, \alpha_s\, LM/Q$
f	$\frac{1+\lambda_r^2}{2M}\, gQF$	$\frac{\sqrt{1+\lambda_s^2}\, QgF}{\sqrt{2}\, M}$

slot jet (see Fig. 3.2). Thus in the calculations, it is necessary to provide a criterion whereby the round jet analysis is switched to that for a slot jet. Two such criteria are proposed. First, we may assume that transition occurs when the width of the round jet becomes equal to the jet spacing. This shall be designated transition 1. Referring to Table 3.2, this occurs when

$$\frac{Q2\sqrt{2}}{\sqrt{2\pi M}} = L \quad \text{or} \quad \frac{Q}{\sqrt{M}} = L\,\frac{\sqrt{\pi}}{2} = 0.885\ L \tag{3.21}$$

Here the "jet width" has been taken to be $2\sqrt{2}\,b$. Alternatively, we may assume that transition occurs when the entrainment as calculated by the round jet theory or the slot jet theory becomes equal. This shall be designated transition 2. Referring to Table 3. 3, we see that this occurs when

$$2\sqrt{2\pi}\ \alpha_r \sqrt{M} = 2\sqrt{2}\,\alpha_s\ LM/Q$$

or

$$\frac{Q}{\sqrt{M}} = \frac{\alpha_s}{\alpha_r \sqrt{\pi}} L$$

Since experimental values for α_s and α_r are 0.16 and 0.082 respectively, this is

$$\frac{Q}{\sqrt{M}} = \frac{0.16}{0.082\sqrt{\pi}} L = 1.1\ L \tag{3.22}$$

This occurs somewhat later than the first transition. Of the two transition criteria, it is felt that the second is more reasonable since, in the first one, it is necessary to define the "jet width" which is somewhat arbitrary. It has been found, however, that the two criteria gave virtually the same results except for the region between transition 1 and 2. Thus the solution is not sensitive to exactly where the transition is.

It should be noted that the independent variable of integration is s, the distance along the jet path. However, the ambient conditions ρ_a and T_a are usually only given as functions of y. Thus the following two equations are needed to allow conversion between s and x, y:

$$\frac{dx}{ds} = \cos\theta \tag{3.23}$$

$$\frac{dy}{ds} = \sin\theta \tag{3.24}$$

The system of Eqs. (3.6), (3.8), (3.9), (3.12), (3.14), (3.23) and (3.24) constitute seven ordinary differential equations for the seven unknowns,

Q, M, θ, F, G, x and y as function of s. These equations may be solved given the initial values of the unknowns at $s = 0$.

The initial conditions are given by the source conditions, namely, u_o, the jet velocity, D_o, the jet diameter, T_1, the jet temperature, ρ_1, the jet density, θ_o, the jet discharge angle. However, since the formulation is in terms of the flux quantities Q, M, F, and G, these jet characteristics must be converted to initial values in these variables. Moreover, it is well known that there exists a zone of flow establishment extending a few jet diameters during which the top hat profiles of velocity, density deficiency and temperature excess change gradually to Gaussian form. In this formulation, we shall start the integration from the beginning of the zone of established flow. Thus it is necessary to relate the jet characteristics to the flux quantities at this point. Albertson, et. al (1950), in their experimental investigations on the round jet found that the zone of flow establishment extends a distance of 6.2 jet diameters. Equating the momentum flux at the beginning and end of the zone of flow establishment, (assuming that the buoyancy force is negligible in such a short region), we get

$$\frac{\pi}{4} D_o^2 u_o^2 = \int_0^\infty u^{*2} \, 2\pi r dr = \frac{\pi b_o^2 u_o^2}{2}$$

Thus the initial value for Q is

$$Q_1 = \pi b_o^2 u_o = \frac{\pi}{2} D_o^2 u_o$$

In other words, the volume flux at the beginning of the zone of established flow is twice that at the source.

By assuming further that the ambient density is uniform in the zone of flow establishment, we may equate the density deficiency flux at the beginning and end of this zone to get

$$\frac{\pi}{4} D_o^2 u_o(\rho_a - \rho_1) = \int_0^\infty u^*(\rho_a - \rho^*)\, 2\pi r dr$$

$$= \frac{\lambda_r^2}{1+\lambda_r^2} \pi b_o^2 u_o(\rho_a - \rho)$$

Thus the initial value for F is

$$F_1 = \frac{\pi}{4} D_o^2 u_o(\rho_a - \rho_1)$$

However, the centerline density deficiency is

$$\rho_a - \rho = \frac{1+\lambda_r^2}{2\lambda_r^2} (\rho_a - \rho_1)$$

For $\lambda_r = 1.16$, $\rho_a - \rho = 0.87\ (\rho_a - \rho_1)$.

Similarly,

$$G_1 = \frac{\pi}{4} D_o^2 u_o(T_a - T_1)$$

and the centerline temperature excess is

$$T_a - T = \frac{1+\lambda_r^2}{2\lambda_r^2} (T_a - T_1) = 0.87(T_a - T_1)$$

The temperature excess and density deficiency are thus already decreased to 87% of their values at the jet efflux due to their faster spreading. In other words, the zone of flow establishment for temperature and density are shorter than that for velocity. Since we are starting the calculations at the end of the zone of flow establishment for velocity, the temperature excess and density deficiency have already undergone some decrease, namely 13%. Note that if $\lambda_r = 1$ (same spreading and length of zone of flow establishment) then this decrease would be absent. This phenomenon is shown schematically in Fig. 3.3.

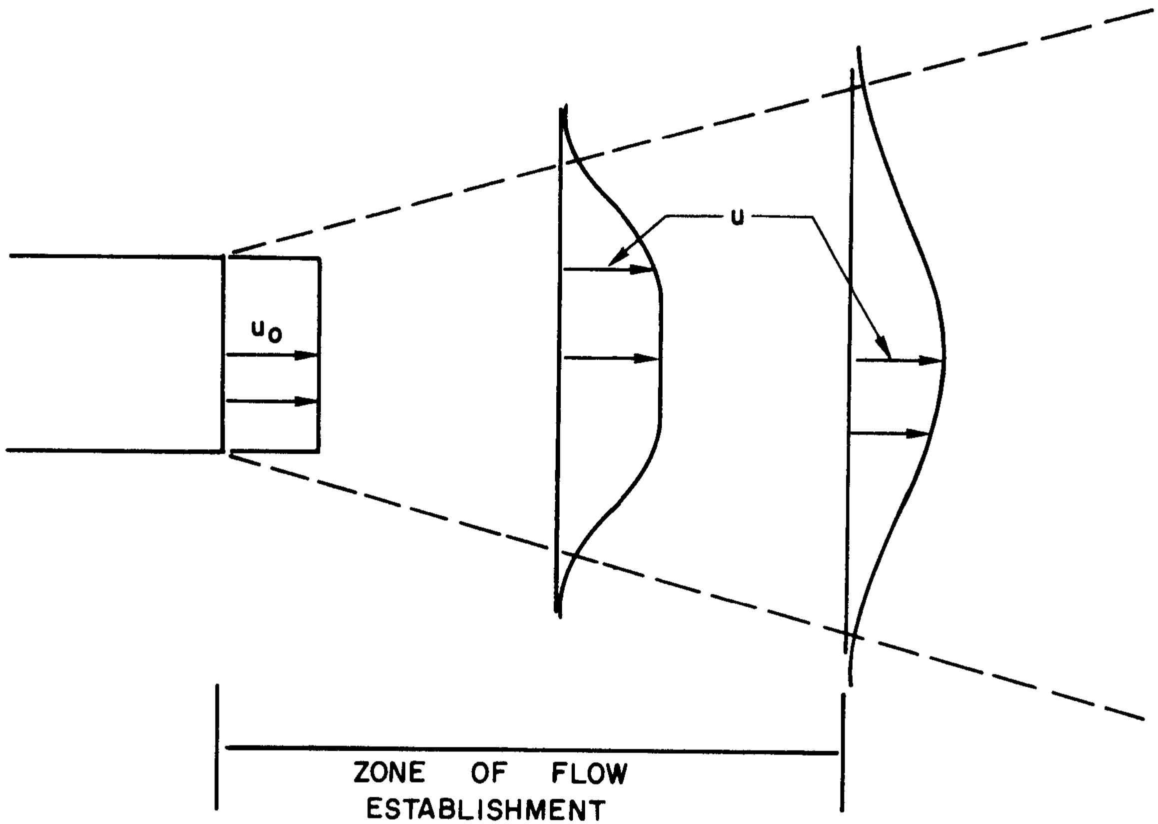

Figure 3.3 Zone of flow establishment in a submerged jet.

3.2.2 Method of Solution and Examples

A computer program RBJ has been written in Fortran IV language to solve the problem formulated in the previous section. A listing of the program is included as Appendix A. The method of solution is to first obtain the initial conditions Q_1, M_1, F_1, G_1, from the given source characteristics. Then the Eqs. (3.6), (3.8), (3.9), (3.12), (3.14), (3.23) and (3.24) are integrated with E and f as given by those for the round jet (column 2, Table 3.3). When transition is reached, given by either Eq. (3.21) or (3.22), one simply continues the solution but with E and f as given by those for the slot jet (column 3, Table 3.3). The results obtained are then converted from the variables Q, M, F, G,... to the physical variables u, ρ, T, and W, the jet width which is taken to be $2\sqrt{2}$ b. The conversion is effected by the relations in Table 3.2.

The inputs to the program consists of the following:

u_o	=	jet velocity
D_o	=	jet diameter
T_1	=	jet temperature
ρ_1	=	jet density (in gm/c.c.)
θ_o	=	jet discharge angle with respect to the horizontal, (in degrees)
d_j	=	jet discharge depth
L	=	jet spacing
α_r	=	entrainment coefficient for a round jet (usually taken to be 0.082) *
α_s	=	entrainment coefficient for a slot jet (usually taken to be 0.16) *
λ_r	=	spreading ratio for a round jet (usually taken to be 1.16) *
λ_s	=	spreading ratio for a slot jet (usually taken to be 1.0)*
g	=	gravitational acceleration

The program is written in such a fashion that all the quantities are dimensional. However, any consistant system of units may be used (FPS, MKS, or CGS), except that density is always in units of gm/cc. The specification

* See Fan (1967)

of g, the gravitational acceleration is utilized as the indicator for the units. Thus, for example, if g is specified to be 32.2, then the system of units which should be used is the FPS system.

In addition to the inputs above, it is also necessary to specify the density and temperature profiles in the ambient. This is accomplished by specifying a table of depth, temperature, and density. The program linearly interpolates between specified values to arrive at the values for intermediate points. For example, if the ambient is linearly stratified in temperature and density, then only two points need to be specified one at the surface, and one at the jet depth. When the two values coincide, then the ambient is uniform.

Output quantities from the program consist of x, y, jet width, dilution, jet temperature, jet density, ambient density, ambient temperature, and temperature excess. The quantity jet width is taken to be $2\sqrt{2}$ b. Dilution is the ratio of volume flux Q to that at the beginning of the zone of established flow. Jet temperature, density and temperature excess are all centerline values. These should be kept in mind when interpreting the results.

Example cases have been solved using the program RBJ and these cases are summarized in Table 3.4. The solutions are shown graphically in Figs. 3.4 to 3.6. The effect of the various parameters can be readily seen from the figures. Figure 3.4 shows that the jet path for various value of L, the jet spacing and D_o, the jet diameter in a uniform environment. It is readily seen that, as expected, decreasing D_o or increasing L, implying delayed jet intereference, bends the jet upwards. Figure 3.5 shows the jet excess temperature as a function of the vertical coordinate. It is seen that the transition point is not of import except for a short zone between the two transition points. Otherwise, the predictions of excess temperature based on the two transition points are virtually identical. It should be noted that in Fig. 3.5, the scale on y starts at y = 1. The jets have already travelled horizontally quite a distance before reaching y = 1 (see Figure 3.4). Thus they have already achieved a significant reduction in Δ T through entrainment. Also note that in most cases in Figure 3.5, transition occured before y = 1. Since the excess temperature at discharge is usually only a matter of 10 or 20^{o}F, and since the dilution is usually quite large in a submerged jet, only a very small density stratification is needed to suppress the jet from reaching the surface. This can be seen in Fig. 3.6. In these cases there is a temperature difference of but 0.8°F over a distance of 60 ft., yet when the jet temperature was 82.4°F (jet efflux excess temperature = 12.2°F), the jet never even reached a vertical distance of 60 ft. When the jet temperature is 89.2°F (jet efflux excess temperature = 20°F), the jet does reach above the 60 ft. level. However, it is stopped by the thermocline. It can be expected that if the ambient is stratified, even very slightly, it would not be difficult to design an outfall diffuser to always keep the discharge submerged.

TABLE 3.4

	D_o	u_o	T_1	d_j	L	Ambient T_a (y)
1	0.5	12.5	89.2	100	5	uniform 77°
2	0.5	12.5	89.2	100	10	uniform 77°
3	0.25	12.5	89.2	100	5	uniform 77°
4	1	12.5	89.2	100	5	uniform 77°
5	1	12.5	89.2	100	10	uniform 77°
6	1	12.5	89.2	100	20	uniform 77°
			Non-uniform Ambient			
7	0.5	12.5	89.2	100	5	
8	0.5	12.5	82.4	100	5	

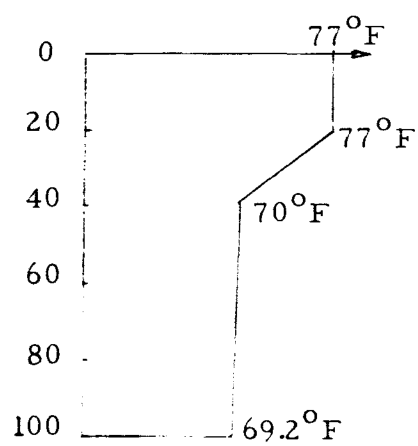

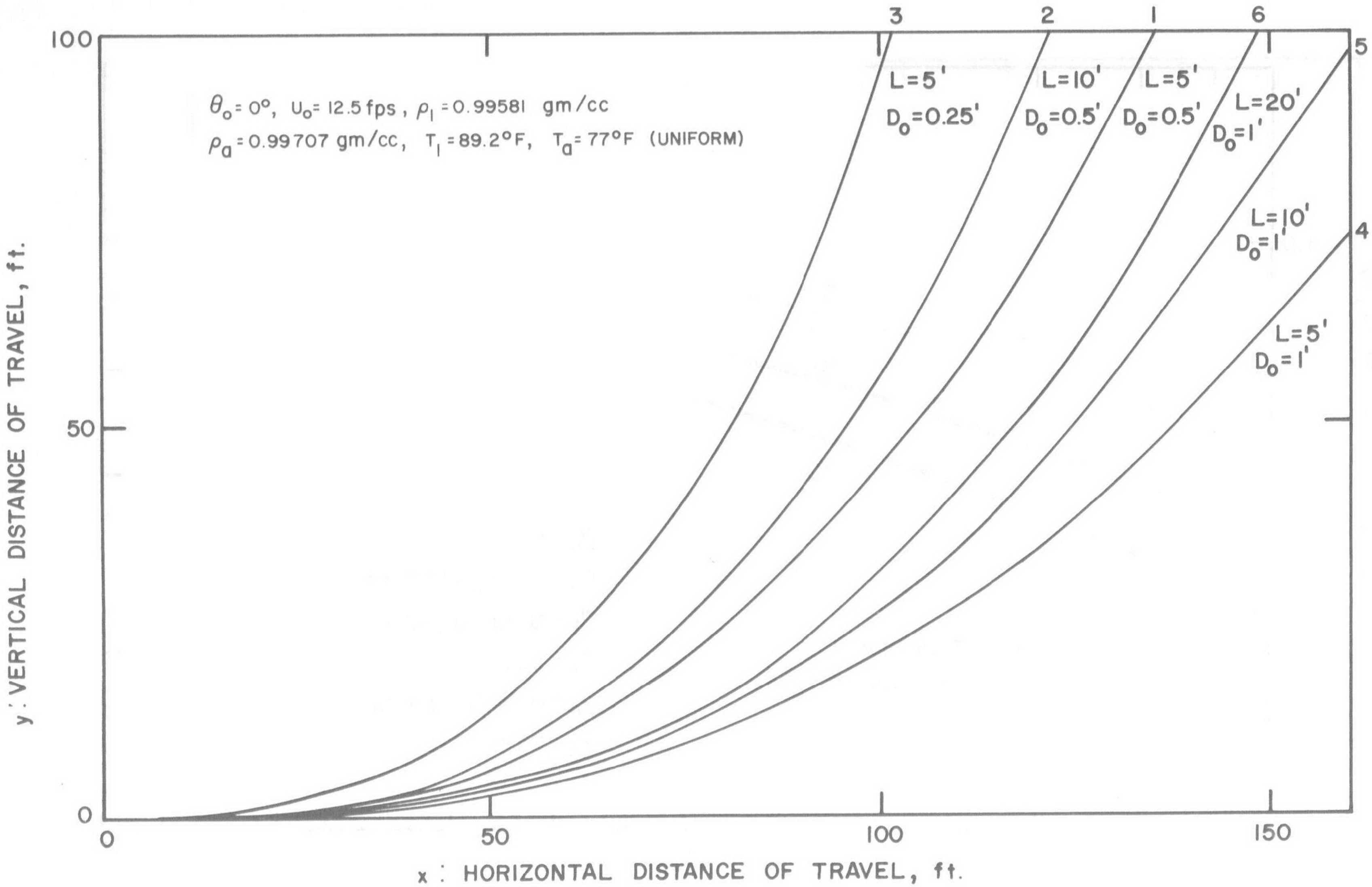

Figure 3.4 Predicted trajectories of multiple buoyant jets in a uniform environment.

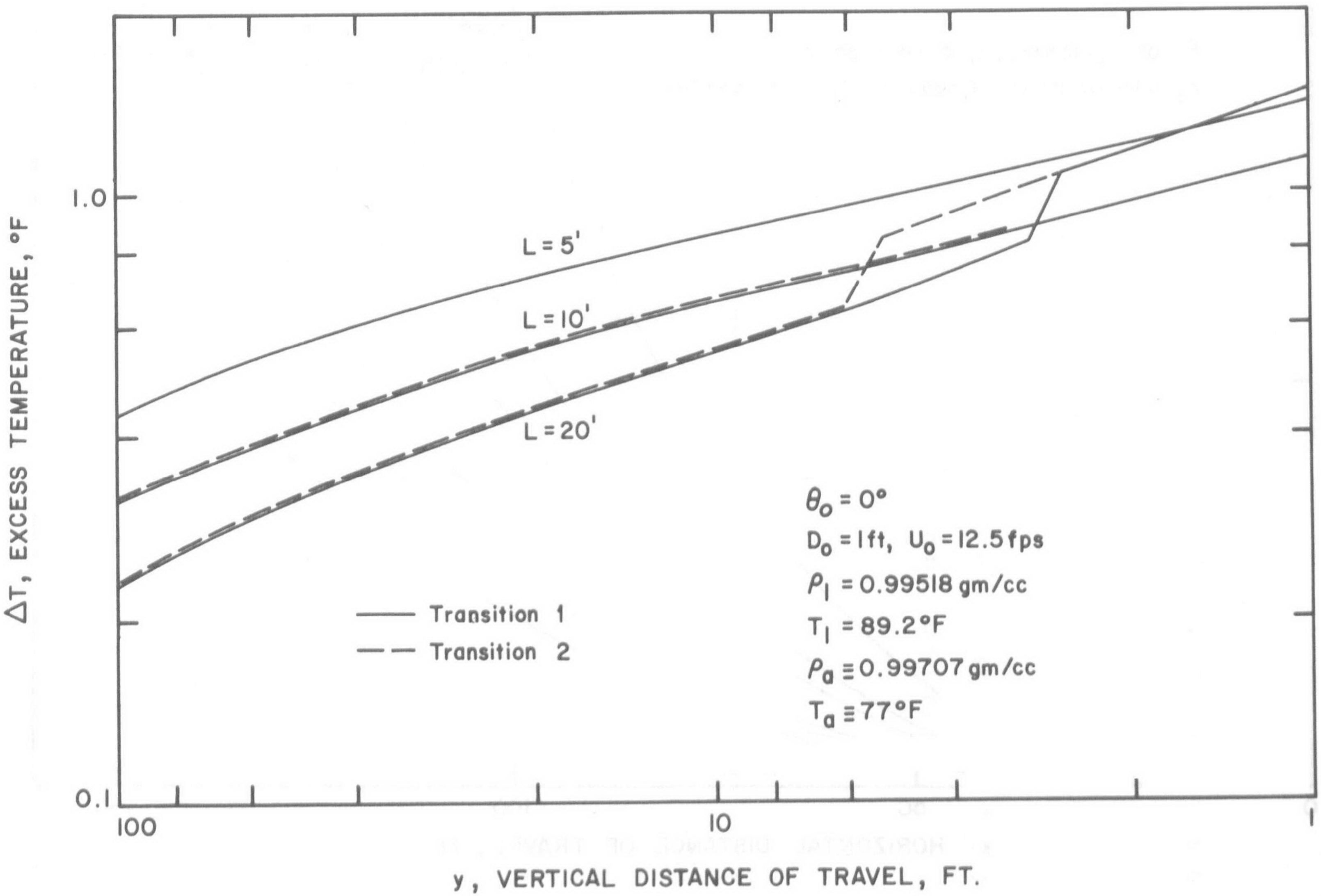

Figure 3.5a Predicted jet centerline excess temperature of multiple buoyant jets in uniform environment.

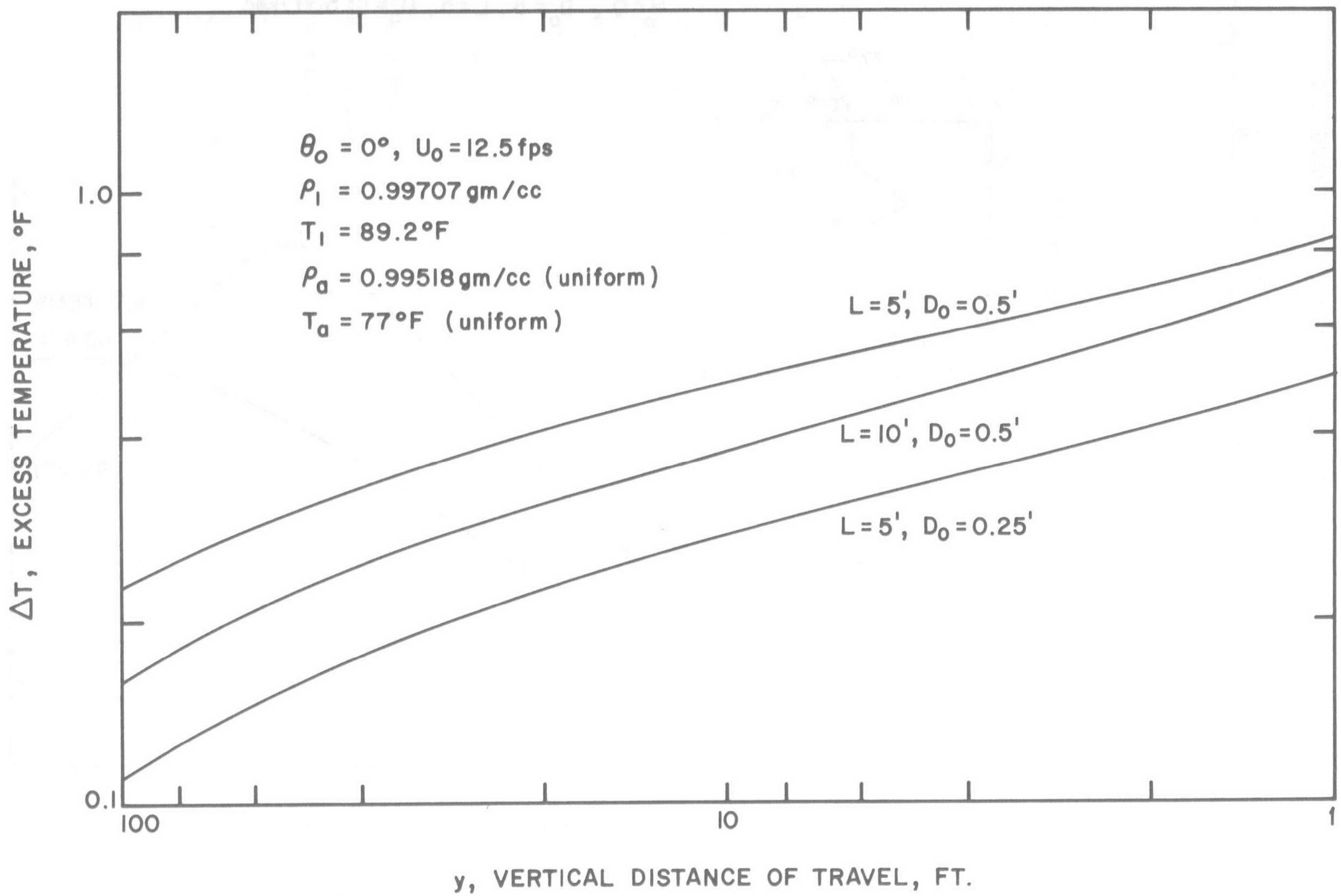

Figure 3.5b Predicted jet centerline excess temperature of multiple buoyant jets in uniform environment.

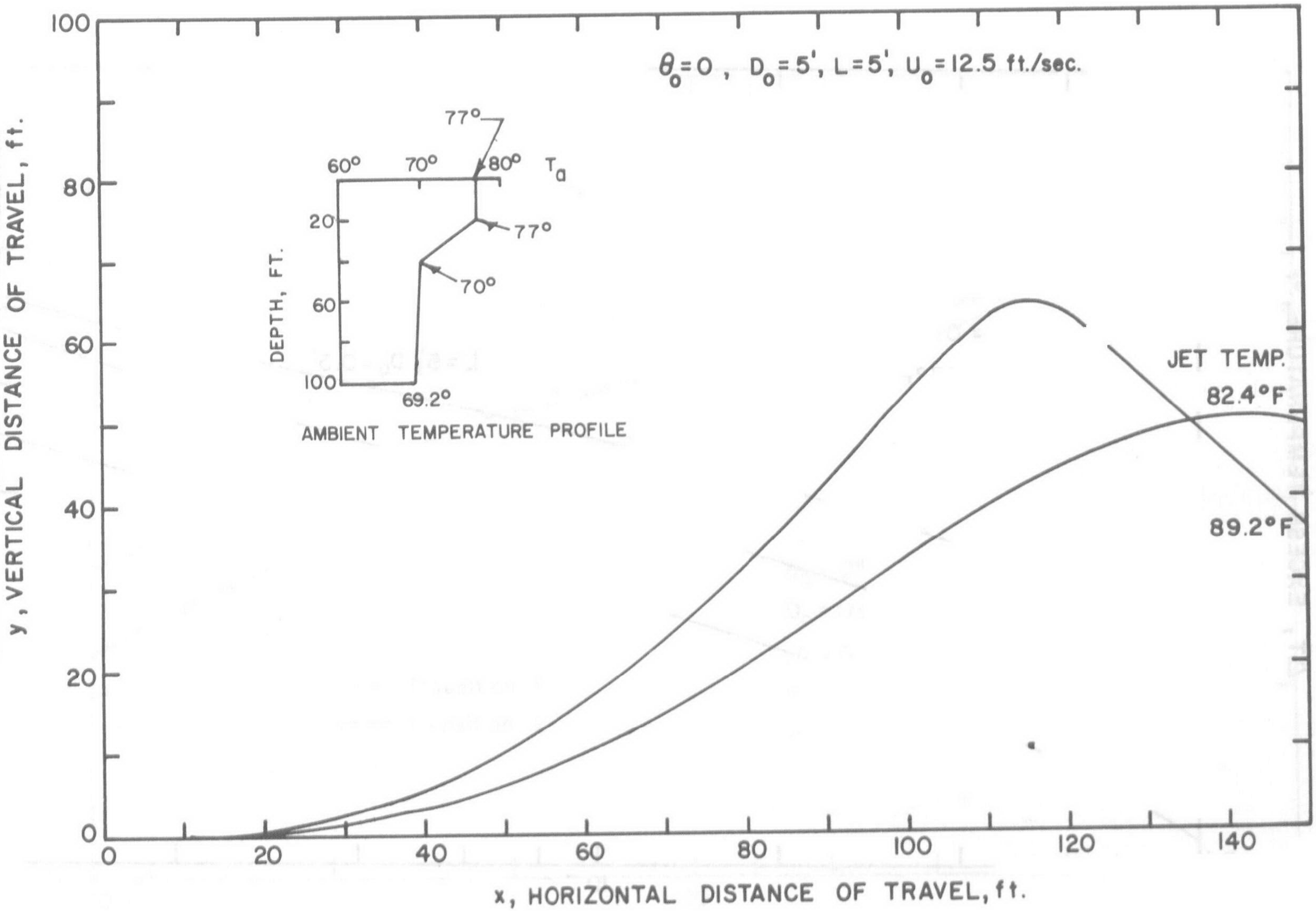

Figure 3.6 Predicted trajectories of multiple buoyant jets in stratified environment.

3.3 Time Dependent Surface Spreading of a Buoyant Fluid

When the warm efflux discharged at some depth reaches the surface of the ambient fluid, it may still possess some buoyancy and will thus spread on the surface. The phenomenon of surface spreading can be likened to that of a surface horizontal buoyant jet, which is treated in Chapter 4. There it was found that if surface heat exchange is absent, no steady state solutions may be found. In this section, the unsteady surface spreading problem will be investigated. The analysis to be presented is very approximate and should be viewed as providing only an order of magnitude estimate of the phenomenon. No detailed flow field will be derived. Only the gross properties of the spreading pool of buoyant fluid will be obtained. The analysis further incorporates several coefficients on which no data is available. Experiments on this phenomenon should be performed in the future to verify the findings and provide estimates of the coefficients.

In this investigation, no surface heat exchange or entrainment of ambient fluid will be included. In Chapter 4, it will be found that it is when surface heat exchange is absent that a steady state solution cannot be found. Moreover, the spreading layer thickens with time so that after an initial period, entrainment may also be ignored.

3.3.1 Two-Dimensional Case

We assume that at time $t = 0$, a line source of strength $2q_o$ per unit length injects lighter fluid of density ρ onto a heavier quiescent ambient fluid of density ρ_o as shown in Fig. 3.7. We make the following assumptions:

1. no entrainment of ambient fluid occurs;
2. as the buoyant fluid spreads, the shape of the interface is similar from one instant to another; and
3. the pressure distribution is hydrostatic.

Under these assumptions, we now examine the motion of the pool as a whole. Consider a half of the spreading pool at time t as shown in Fig. 3.8. For simplicity, the similar shape will be taken to be rectangular. It will become

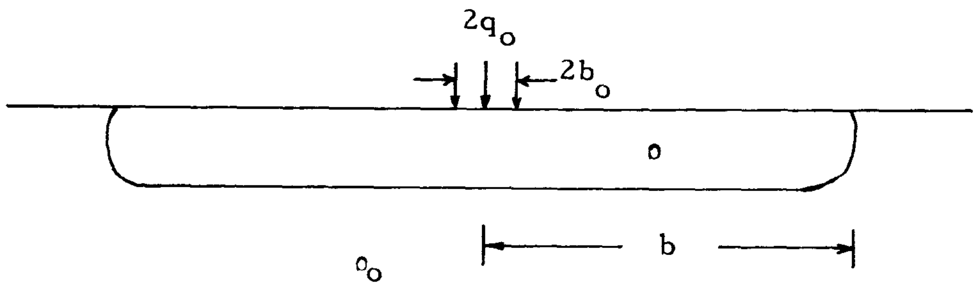

Figure 3.7 Definition sketch.

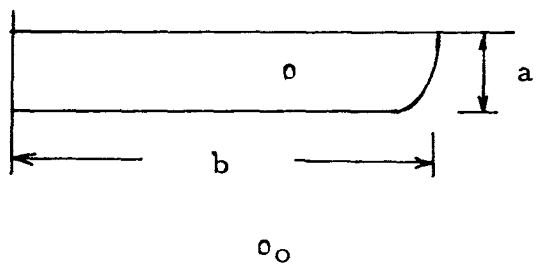

Figure 3.8 Definition sketch.

obvious later that taking it to be some other shape will not change the basic features of the resulting equations but will only change some of the numerical coefficients.

We now write the equation of motion for the buoyant fluid as a whole. The time rate of change of the momentum of the center of mass is

$$\frac{d}{dt}\left\{\rho\, a\, (\tfrac{1}{2} b')\, b\right\}$$

where the symbols are as defined in Fig. 3.7. The driving force is the pressure difference induced by the density difference. It can easily be demonstrated that this is

$$\tfrac{1}{2}\, g(\Delta\rho)\, a^2$$

where $\Delta\rho = \rho_o - \rho$. The resistive forces of shear and hydrodynamic drag are respectively

$$\tau(b - b_o)$$

and

$$C_D \tfrac{1}{2}\, \rho_o (b')^2 a$$

Now we assume $\tau = \frac{b'}{a}\varepsilon$ where ε is an effective viscosity coefficient. The equation of motion of the spreading pool is then

$$\frac{\rho}{2}\frac{d}{dt}[abb'] = \tfrac{1}{2}g(\Delta\rho)a^2 - C_D\rho_o \frac{a}{2}(b')^2 - \frac{\varepsilon}{a}b'(b - b_o) \qquad (3.25)$$

For $\Delta\rho << \rho$, Eq. (3.25) reduces to

$$\frac{1}{2}\frac{d}{dt}\left[ab\frac{db}{dt}\right] = \tfrac{1}{2}g'a^2 - \frac{C_D}{2}a(b')^2 - \frac{\varepsilon}{\rho}\frac{(b-b_o)}{a}b' \qquad (3.26)$$

where $g' = \frac{\Delta\rho}{\rho}g$. Now, for no entrainment, we have the continuity relation

$$ab = q_o t \tag{3.27}$$

Hence Eq. (3.26) can be written

$$\frac{1}{2} \frac{d}{dt}\left[q_o t \frac{db}{dt} \right] = \frac{1}{2} g' \frac{q_o^2 t^2}{b^2} - \frac{C_D}{2} \frac{q_o t}{b} \left(\frac{db}{dt} \right)^2 - \left(\frac{\varepsilon}{\rho} \right) \frac{b(b-b_o)}{q_o t} \frac{db}{dt} \tag{3.28}$$

This equation can be solved for b as a function of time t for given initial conditions. The terms in Eq. (3.28) represent, respectively, the local inertia, the pressure driving force induced by the density difference, the hydrodynamic drag and the shear.

It can be expected that after a brief initial period (for which this analysis is probably not valid), the inertia term $\frac{d}{dt}(q_o t \frac{db}{dt})$ probably becomes negligible. This initial period is followed by one when the hydrodynamic drag is balanced by the driving pressure with the shear of secondary importance. Then the equation is

$$\frac{1}{2} g' a^2 = \frac{C_D}{2} a(b')^2 \tag{3.29}$$

Note that this implies

$$\frac{\left(\frac{db}{dt} \right)^2}{g'a} = \frac{1}{C_D} \tag{3.30}$$

The left hand side is simply a densimetric Froude number. In studies of density currents (such as turbidity currents and cold fronts), it has been found that this Froude number is constant and equal to approximately 2 corresponding to $C_D = 0.5$, a very reasonable number. Moreover, this equation gives rise to the solution

$$b = [2g' q_o]^{1/3} t \tag{3.31}$$

where upon

$$a = \frac{q_o t}{b} = \frac{q_o}{(2g'q_o)^{1/3}} = \frac{q_o^{2/3}}{(2g')^{1/3}} = \text{constant} \tag{3.32}$$

For large time, it can be expected that the shear term dominates as the resistive mechanism so that the pertinent equation is approximately

$$\tfrac{1}{2} g'a^2 = \frac{\varepsilon}{\rho} \frac{b}{a} \frac{db}{dt} \tag{3.33}$$

With $ab = q_o t$, we get

$$b^4 \frac{db}{dt} = \frac{1}{2} \frac{g'\rho}{\varepsilon} q_o^3 t^3 \tag{3.34}$$

with solution

$$b = \left[\frac{5\rho g' q_o^3}{8\varepsilon} \right]^{1/5} t^{4/5} \tag{3.35}$$

and

$$a = \left[\frac{5\rho g' q_o^3}{8\varepsilon} \right]^{-1/5} q_o t^{1/5} \tag{3.36}$$

In summary, b, the horizontal extent of the spreading pool, increases (after a brief initial period) linearly with distance while the thickness is essentially constant. When the spreading has proceeded far enough for viscous effects to dominate, the spreading rate decreases to $t^{4/5}$ while the thickness increases but slowly ($t^{1/5}$). As time $t \to \infty$, the thickness would tend to infinity.

We now note that if the similarity shape is not a rectangle but is some other shape, the same dependence on time will be found. Only the numerical factors in the proportionality constants will be different.

3.3.2 Axisymmetric Case

We now derive the equation for the axisymmetric case. Basically this is the same physical phenomenon and hence the same assumptions will be made. Thus, instead of a line source as in the two-dimensional case, a small circular source is taken to be emitting buoyant fluid onto a heavier motionless ambient as shown in Fig. 3.9. Under the same assumptions as in the previous section, we consider a slice of the spreading pool at time t as shown in Fig. 3.10. Instead of assuming a rectangular cross-sectional shape, we shall assume an ellipsoidal shape. The driving pressure force on the section shown in Fig. 3.10 can be found by integrating the pressure, thus

$$\Delta F = \int_A (p - p_o)\, dA$$

where p is the pressure in the buoyant surface fluid and p_o that in the ambient and A is the projected area over which the pressure acts (see Fig. 3.10).

Since pressure at the interface must be single-valued, it follows that

$$p = \rho g a - \rho g x \qquad 0 < x < a$$

$$p_o = \begin{cases} \rho g a - \rho_o g x & 0 < x < a\left(1 - \dfrac{\Delta\rho}{\rho_o}\right) \\ 0 & a\left(1 - \dfrac{\Delta\rho}{\rho_o}\right) < x < a \end{cases}$$

$$dA = \frac{(b\,d\theta)\, x}{a\left(1 - \dfrac{\Delta\rho}{\rho_o}\right)}\, dx$$

Hence

$$\Delta F = \int_0^{a\left(1-\frac{\Delta\rho}{\rho_o}\right)} (\rho_o - \rho) g x \frac{b\,d\theta}{a\left(1-\dfrac{\Delta\rho}{\rho_o}\right)}\, x\,dx + \int_0^{a\frac{\Delta\rho}{\rho_o}} \rho g x \frac{b\,d\theta\, x}{a\dfrac{\Delta\rho}{\rho_o}}\, dx$$

$$= \frac{(\Delta\rho)\, g b\, d\theta}{a\left(1-\dfrac{\Delta\rho}{\rho_o}\right)} a^3 \frac{\left(1-\dfrac{\Delta\rho}{\rho_o}\right)^3}{3} + \frac{\rho g b\, d\theta}{3} a^2 \left(\frac{\Delta\rho}{\rho_o}\right)^2$$

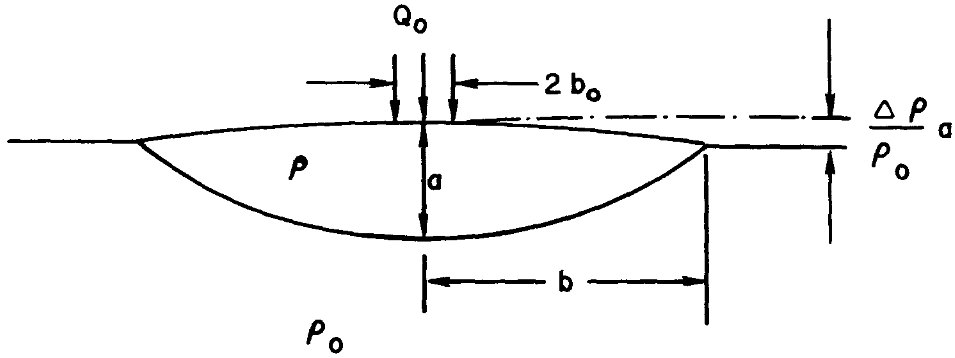

Figure 3.9 Definition sketch

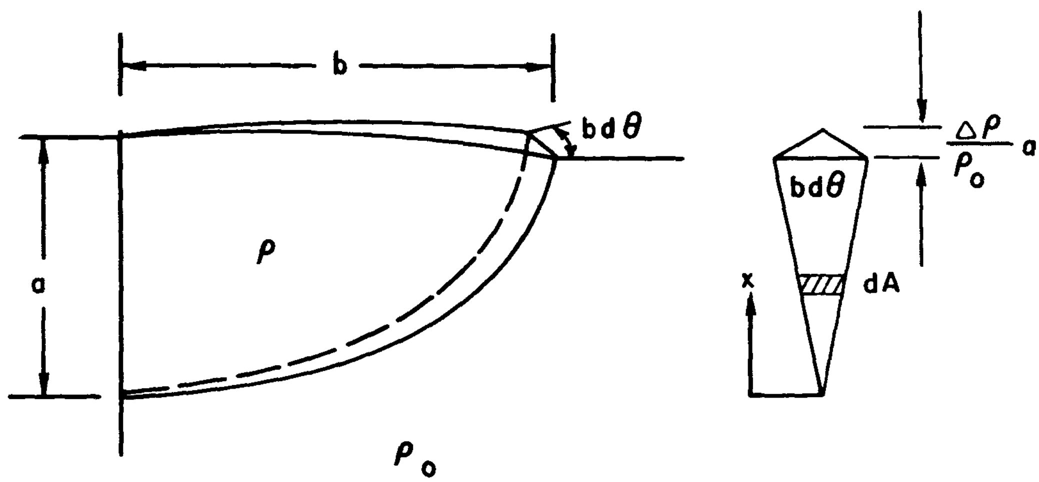

Figure 3.10 Definition sketch

For $\frac{\Delta\rho}{\rho_o} << 1$, we have

$$\Delta F = (\Delta\rho) g b \, d\theta \, \frac{a^2}{3} \tag{3.37}$$

The time rate of increase of momentum of the slice is

$$\frac{d}{dt}\left\{\rho \frac{\pi a b^2}{16} \frac{db}{dt}\right\} d\theta$$

The shear and hydrodynamic drag forces are respectively

$$\varepsilon \frac{(b^2 - b_o^{\,2})}{a} \frac{db}{dt} \, d\theta$$

and

$$C_D \frac{\rho a b}{4} \left(\frac{db}{dt}\right)^2 d\theta$$

so that the equation of motion is

$$\frac{d}{dt}\left\{\rho \frac{\pi a b^2}{16} \frac{db}{dt}\right\} = \frac{\Delta\rho}{3} g a^2 b - C_D \rho \frac{ab}{4} \left(\frac{db}{dt}\right)^2 - \varepsilon \frac{(b^2 - b_o^{\,2})}{a} \frac{db}{dt} \tag{3.38}$$

The continuity equation is

$$a\, b^2 = \left[\frac{2\pi}{3}\right] Q_o t \tag{3.39}$$

Equations (3.38) and (3.39) can be solved for given parameters and given initial conditions.

Again, if we assume that after a brief initial period, the local inertia is negligible, so that the driving force is balanced by the hydrodynamic drag, we get

$$\frac{1}{3} g' \, a^2 b = C_D \frac{ab}{4} (b')^2 \tag{3.40}$$

where $g' = g \frac{\Delta\rho}{\rho_o}$

or

$$\frac{(b')^2}{ag'} = \frac{4}{3C_D} \tag{3.41}$$

The left hand side is again a densimetric Froude number. Since the continuity equation is $a\,b^2 = [\frac{2\pi}{3}]Q_o t$, we have

$$b^2\left(\frac{db}{dt}\right)^2 = \frac{4}{3C_D}\,g'\,[\frac{2\pi}{3}]\,Q_o t$$

Letting $\frac{4[\frac{2\pi}{3}]}{3C_D} \equiv \alpha^2$, we get

$$b\,\frac{db}{dt} = \alpha\sqrt{g'Q_o}\,\sqrt{t} \tag{3.42}$$

If at time $t = 0$, $b = b_o$, therefore the solution to Eq. (3.42) is simply

$$b = \sqrt{b_o^{\,2} + \frac{4\alpha\sqrt{g'Q_o}}{3}\,t^{3/2}} \tag{3.43}$$

Thus, after a brief initial period, the diameter of the spreading pool grows as $t^{3/4}$. The thickness a is

$$a = \frac{[\frac{2\pi}{3}]Q_o t}{b^2} = \frac{[\frac{2\pi}{3}]Q_o t}{b_o^{\,2} + \frac{4\alpha\sqrt{g'Q_o}}{3}\,t^{3/2}} \tag{3.44}$$

which first increases and then decreases with time.

We next examine the solution for large time when the dominating resistive force is the shear. In this case, the Eq. (3.38) reduces approximately to

$$\frac{g'}{3}\,a^2 b = \left(\frac{\varepsilon}{\rho}\right)\frac{b^2}{a}\,\frac{db}{dt} \tag{3.45}$$

Using the continuity Eq. (3. 39) and letting $\alpha_1 = \dfrac{g' Q_o{}^3 [\frac{2\pi}{3}]^3}{3} \dfrac{\rho}{\epsilon}$, we get

$$\alpha_1 t^3 = b^7 \frac{db}{dt}$$

with solution

$$b = (2\alpha_1)^{1/8} t^{1/2} \tag{3.46}$$

The thickness a is then

$$a = \frac{[\frac{2\pi}{3}] Q_o t}{b^2} = \frac{[\frac{2\pi}{3}] Q_o}{(2\alpha_1)^{\frac{1}{4}}} = \text{constant} \tag{3.47}$$

Thus, after a brief initial period, the diameter of the spreading pool would grow as $t^{3/4}$ gradually decreasing to $t^{1/2}$ while the thickness first increases and then decreases tending to a constant value

$$\frac{[\frac{2\pi}{3}] Q_o}{(2\alpha_1)^{\frac{1}{4}}} .$$

3. 3. 3 Comparison with Experiments

The theory presented in the previous section on the axisymmetric time dependent surface spreading can be compared with the experiments by Sharp (1969). Sharp reported on the growth of the radius of the spreading pool resulting from the surfacing of buoyant jets discharged at the bottom of a laboratory tank. These results are summarized in Table 3. 5.

TABLE 3.5

$\dfrac{b(g')^{1/5}}{Q_o^{2/5}}$	$\dfrac{t(g')^{3/5}}{Q_o^{1/5}}$
1.5	1
2.3	2
3.4	4
4.3	6
5.2	8
5.4	10
8.8	20
11.9	30
14.4	40
16.5	50

For $b_o << b$, Eq. (3.43) (viscous effects negligible) can be written

$$b = \left(\frac{4\alpha}{3}\right)^{\frac{1}{2}} (g'Q_o)^{\frac{1}{4}} t^{3/4}$$

or putting it in Sharp's notation

$$\frac{b(g')^{1/5}}{Q_o^{2/5}} = \left(\frac{4\alpha}{3}\right)^{\frac{1}{2}} \left\{\frac{t(g')^{3/5}}{Q_o^{1/5}}\right\}^{3/4} \tag{3.48}$$

Figure 3.11 shows Sharp's data together with Eq. (3.48) with $\alpha = 3/4$. It should be noted that for small t and b, the influence of b_o becomes more important and one expects higher measured values of b than given by Eq. (3.48). Since Sharp did not detail the initial values b_o for his various experiments, no estimate can be given as to its influence. It is clear however, that the agreement between Eq. (3.48) and Sharp's data is reasonable.

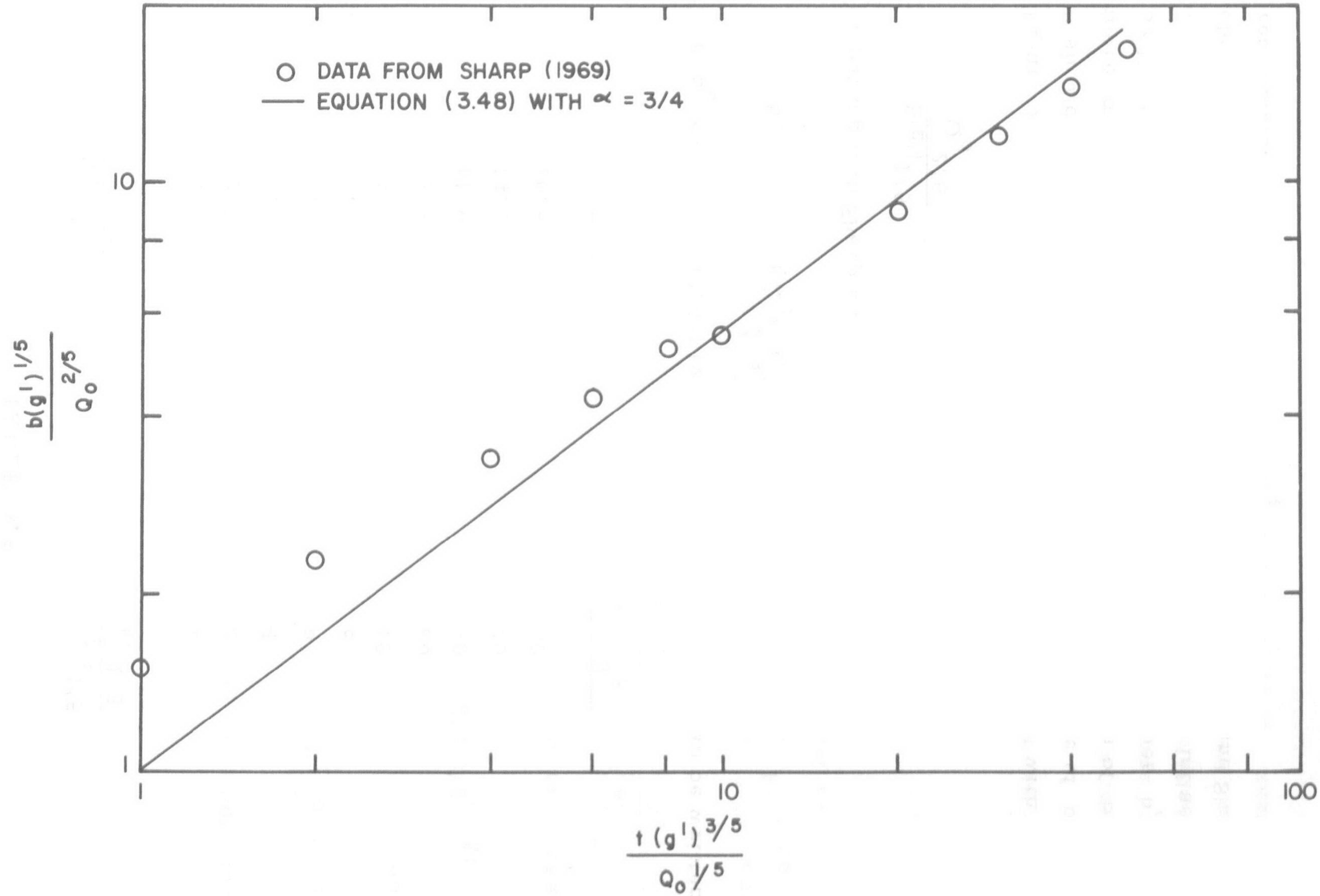

Figure 3.11 Comparison of theory with experiments for the surface spreading of buoyant fluid.

3.3.4 Numerical Solutions

The equations for surface spreading derived in the previous sections can be solved numerically including all the terms. For example, in the axisymmetric case, the Eqs. (3.38) and (3.39) can be combined and by further normalizing the variables by letting $t^* = t/t_o$, $\beta = b/b_o$, where $t_o = \left(\frac{9\, b_o^4}{32\, g' Q_o}\right)^{1/3}$, it can be written

$$\frac{d^2\beta}{dt^{*2}} = -\frac{1}{t^*}\frac{d\beta}{dt^*} + \frac{t^*}{\beta^3} - C'_D \frac{1}{\beta}\left(\frac{d\beta}{dt^*}\right)^2 - K\,\frac{\beta^2(\beta^2-1)}{t^{*2}}\,\frac{d\beta}{dt^*}$$

where $C'_D = \frac{8}{3} C_D$, $\quad K = \frac{\varepsilon}{\rho}\,\frac{3\, b_o^4}{2\pi Q_o t_o}$.

This equation has been solved for the cases $C'_D = 0.5$, and $K = 0,\ 10^{-4}$, 10^{-3}, 10^{-2} and are reproduced here as Fig. 3.12.

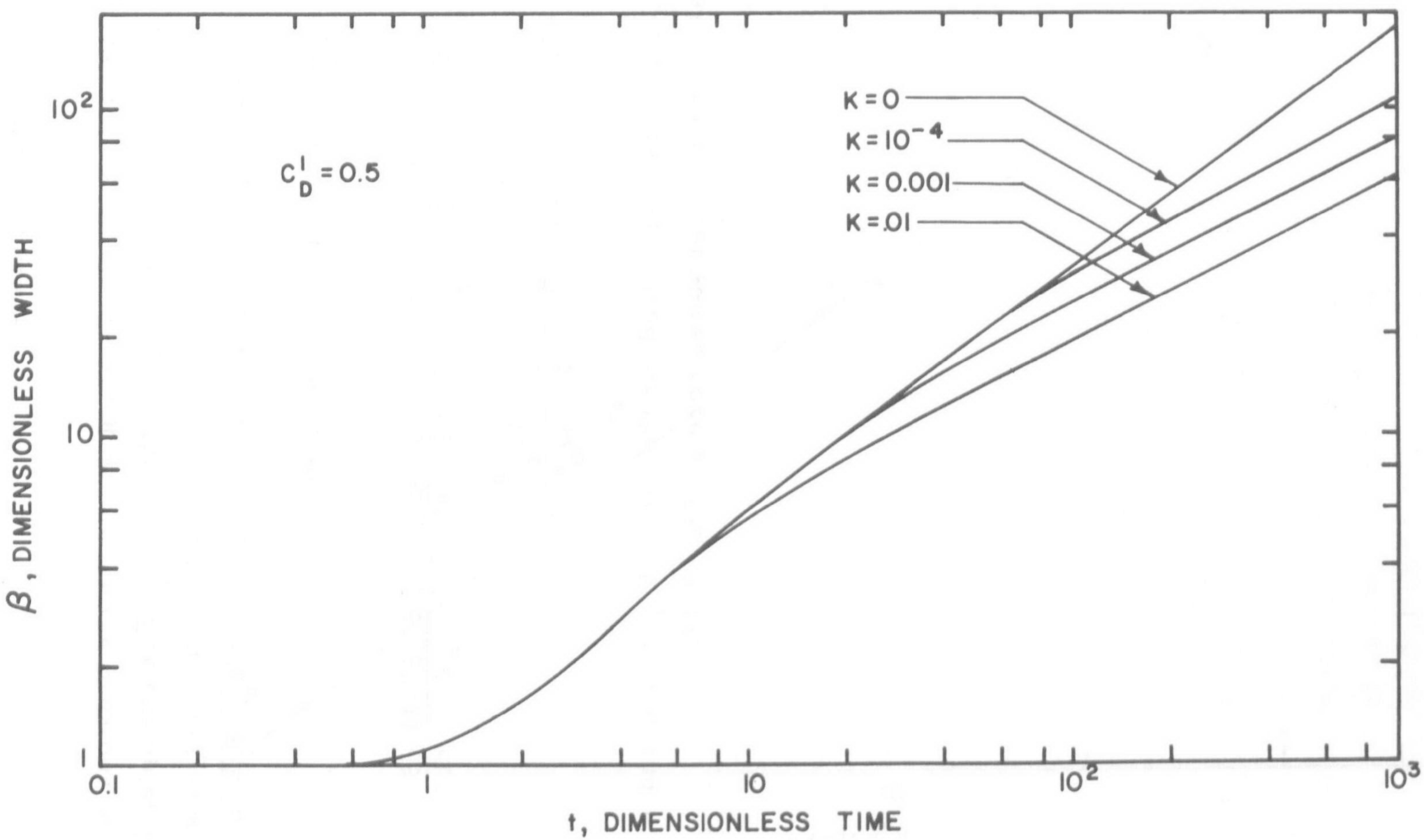

Figure 3.12 Growth of a spreading surface pool of buoyant fluid.

3.4 Summary and Discussion

In this chapter, the initial and intermediate phases of mixing due to the subsurface discharge of warm cooling water is investigated. A mathematical model is developed to describe the initial phase of mixing. In this model, a row of round jets equally spaced at some distance apart is allowed to emit the warm water at depth into an ambient fluid which may be stratified in an arbitrary manner. The model is based on an integral approach similar to the ones used by previous investigators. The phenomenon of jet interference is incorporated in the model. A computer program RBJ based on this model is presented in Appendix A and can be used to obtain the solution in any practical case. It is found that very little stratification is enough to suppress the effluent from reaching the surface.

The intermediate phase of surface spreading of a buoyant fluid on top of a heavier ambient is discussed in Section 3.3. The analysis is very approximate and is performed primarily to obtain the time and length scales of the problem. The results of the analysis can be used to provide a link between the buoyant jet portion of the phenomenon discussed in Section 3.2 and the passive turbulent dispersion portion discussed in Chapter 5. It should be pointed out that application of the analysis requires the knowledge of several coefficients which can only be obtained by experiments. These should be done in the future. Based on typical values for the parameters, it can be inferred from the analysis that the time scale of this intermediate phase is on the order of minutes.

CHAPTER 4 SURFACE HORIZONTAL BUOYANT JETS

4.1 Introduction

In this chapter, we shall investigate the behavior of warm (and hence buoyant) jets discharged horizontally at the water surface. The receiving water is assumed stationary and uniform in density. The two-dimensional case of a slot jet is analysed in detail. The axisymmetric case is also examined. The phenomena of entrainment, source buoyancy and momentum, interfacial shear and surface heat exchange and all included in the model. A number of interesting results are found. In particular, it will be seen that the behavior of such jets can be drastically different from either an ordinary nonbuoyant jet or a fully submerged buoyant jet.

The behavior of ordinary nonbuoyant jets has been studied quite extensively. For example, Albertson, et al. (1950) have performed a series of laboratory experiments on both slot jets and round jets. The detailed results will not be repeated here since they are well known. It is found that the flow field can be conveniently divided into two zones: the zone of flow establishment near the source where the finite size of the source is important followed by the zone of established flow where only the source momentum flux is of importance. In the zone of established flow, the velocity distributions were found to be similar from one station to another with the shape well approximated by a Gaussian profile. It was also found that the momentum flux stays constant with distance downstream while the mass flux increases with distance downstream due to entrainment of ambient fluid.

Investigations into the behavior of submerged buoyant jets and plumes have also been studied quite extensively being stimulated by practical problems in engineering and meteorology, and more recently by the advent of multiport submerged sewage outfall diffusers. Such studies have typically employed an integral approach assuming similarity of velocity and buoyancy profiles and assuming a certain entrainment mechanism. The primary effect of the jet buoyancy is in supplying an added force so that the flux of vertical momentum is no longer constant as was the case in nonbuoyant jets but is related to the buoyancy force. Thus, in the case of a horizontal buoyant jet, the jet path is deduced to bend upwards due to this buoyancy. These studies include Abraham (1963), Brooks and Koh (1965) and Fan (1967), among many others.

An analysis of the problem of a row of submerged buoyant jets discharging into an ambient fluid with an arbitrary density stratification is presented in Chapter 3 of this report.

In the problem to be considered in this chapter, the buoyant source is situated at the surface and is discharging horizontally. For a source with sufficiently strong initial momentum, it is expected that near the source the behavior might resemble that encountered in ordinary submerged jets. However, further away, as the momentum diffuses through jet mixing, the influence of the buoyancy would manifest itself in modifying the horizontal momentum making this problem fundamentally different from the submerged buoyant jet analysed heretofore. Another way of visualizing the difference is as follows. If a source of pure buoyancy exists at some depth, the resulting flow field is primarily vertical towards the water surface. However, if a source of buoyancy exists at the water surface, the resulting flow must be horizontal. The driving force horizontally is due to the buoyancy which modifies the pressure distribution which in turn provides the driving force for the horizontal spreading.

Another important point of departure between ordinary submerged buoyant jets and the surface buoyant jet considered herein is that in the present case, one needs to include in the formulation the effects of interfacial shear. Some distance away from the source, after the momentum has diffused, the buoyant fluid tends to simply float on the denser ambient. Shear forces at the interface then play an important role in the dynamics of the flow. This mechanism is not of import in ordinary submerged jets since in that case, the flow belongs to the class of free turbulent flows with typically Gaussian velocity profiles.

In the following sections of this chapter, the two-dimensional case of a warm jet discharging horizontally at the surface of an infinite body of water will be investigated in detail. The interplay of source buoyancy, source momentum, entrainment, interfacial shear and surface heat exchange will be analysed. It will be demonstrated that if the mechanism of surface heat exchange is absent such as in the case when the density difference is induced by salinity, no steady state solution exists. The source will be inundated by the discharge and the depth of inundation will increase with time. When the mechanism of surface heat exchange is included in the formulation, it is found that a steady state solution always exists. It is further found that the general flow field may possess quite different features depending on the relative importance of the various parameters. For example, if the surface heat exchange coefficient K is sufficiently large, then the flow field may resemble that in an ordinary jet. On the other hand, for small values of K, the jet may not be able to persist resulting in an internal hydraulic jump followed by a zone where the flow is essentially that of a two layered stratified flow. The location of the hydraulic jump is dependent not only on the source conditions but also on downstream conditions which in this case of an infinite fluid is replaced by the surface heat exchange and interfacial shear coefficients. Under certain conditions, the source may be inundated and the zone of stratified flow extends all the way to the source. However, with surface heat exchange, a steady state still exists. The depth of inundation is then governed by downstream conditions and is quite independent of the source momentum.

The general flow field can thus be divided into several zones within each different mechanisms dominate, keeping in mind that under certain conditions, not all the zones may be present. At the source, the source momentum may dominate and the flow field is like a jet. However, the buoyancy reduces the entrainment rate so that the rate of increase of the jet thickness decreases. Far from the source, interfacial shear becomes more important and the flow field becomes controlled by downstream constraints such as by a tailgate in a laboratory tank. In between, the flow field may go through an internal hydraulic jump. In the case with heat exchange at the water surface, this mechanism plays the role of downstream control and plays a part in determining the location of the internal hydraulic jump.

Although only the two-dimensional case is reported in detail here, the general qualitative features of the flow field should remain valid for other geometries. For example, in the axisymmetric case, one would expect the possibility of a circular internal hydraulic jump. The equations and some solutions for this case are also included in this chapter although it has not been carried to the same amount of detail.

Previous investigations of related problems also include Wada (1966), Lean and Whillock (1965), Hayashi and Shuto (1967), Jen, Wiegal and Mobarek (1966) and Stefan and Schiebe (1968). Wada (1966) and Hayashi and Shuto (1967) investigated theoretically the temperature distribution when warm water was discharged from a rectangular outlet at the surface of a semiinfinite motionless ambient. The inertia of the fluid was ignored and the temperature distribution is the result only of the dispersion and advection. Basically, the flow pattern was first obtained by ignoring the density differences. Then the temperature distribution was deduced by using the known flow pattern. Thus the analysis can only be applied for very small temperature differences. Also entrainment was ignored thus the analysis becomes less accurate for large Froude numbers. Laboratory experiments were also performed by Hayashi and Shuto. The temperature determined experimentally was found to be consistantly lower than that predicted indicating the effect of entrainment. Lean and Whillock (1965) and Stefan and Schiebe (1968) performed experiments on the two-dimensional surface jet problem. Their results are consistant with the findings in the present investigation. However, insufficient details were reported to allow detailed quantitative comparison. Jen, Wiegal and Mobarek (1966) and Stefan and Schiebe (1968) performed experiments on the three-dimensional surface jet. Jen, et al. dealed primarily with the case when the source densimetric Froude number is relatively large. They found that the jet excess temperature first decreases due to jet mixing followed by a region where it decreased at a faster rate. Stefan and Schiebe (1968) reported on similar experiments for smaller values of the source densimetric Froude numbers. Detailed measurements were reported. However no analysis of the data was included.

This chapter has been divided into several sections. Section 4.2 treats the two-dimensional case in detail. In Sec. 4.2.1, the assumptions and the resulting equations are derived. These equations turn out to be a set of nonlinear differential equations with four parameters. Some general properties of these equations are discussed in Sec. 4.2.2 where it will be shown that the character of the solutions are strongly influenced by the relative magnitudes of the parameters in the system. In particular, it will be seen that for some combination of parameters, a continuous solution does not exist. In Sec. 4.2.2, an approximate relation between the parameters will be derived which specifies the region in parameter space where a continuous solution can be obtained. Section 4.2.3 examines the solution to this system of equations for various values of the parameters. In the event a continuous solution is not possible, it will be shown that an internal hydraulic jump may be developed. The flow field before the jump, the jump conditions, and the flow field after the jump will be derived and discussed. The problem of matching the solutions at the jump is discussed in Sec. 4.2.4. It will be found that for certain combinations of parameters, no jump can be found to match the solutions indicating that the source is actually inundated in these cases. A nomograph will be presented in Sec. 4.2.4 which divides the parameter space into three regions: a) the region of jet-type solution, b) the region where the solution is characterized by the presence of an internal hydraulic jump and c) the region where the source is inundated. Section 4.2.5 summarizes the findings in the previous sections and describes the procedure of finding the solution for given parameters by using a computer program SBJ2 listed in Appendix B.

In Sec. 4.3, the analogous axisymmetric problem is investigated. The equations are derived and some simplified cases solved. The general features of the solution also depends on the relative magnitudes of the parameters. However, the division of parameter space is much more involved and has not been examined in detail. The detailed study of the axisymmetric case paralleling that done for the two-dimensional case should be performed in the future.

4.2 Formulation and Solutions for the Two-dimensional Problem

Consider a two-dimensional surface source of buoyant fluid at the origin as shown in Fig.4.1. Let the density of the ambient fluid, assumed infinite in extent and motionless, be ρ_o. Also, let the source be characterized by a discharge velocity U_o, source dimension h_o and discharge density $\rho_1 < \rho_o$. Assume that the source densimetric Froude number

$$F_o \equiv \frac{U_o^2}{g\left(\frac{\rho_o - \rho_1}{\rho_o}\right) h_o}$$

is sufficiently large so that near the source, it can be expected that the phenomenon is similar to that of an ordinary two-dimensional jet. Thus, except for a zone of flow establishment, one would expect that the velocity distribution is very nearly Gaussian. Entrainment of the ambient fluid would occur along the jet and the jet dimension would grow with distance x. Let $U(x)$, $\rho(x)$, $h(x)$ be the mean velocity, density and thickness of the jet at x. Laboratory experiments by Ellison and Turner (1959) indicate that, unlike an ordinary nonbuoyant jet which expands linearly with x, the buoyancy of the efflux tends to decrease the entrainment rate. In particular, it was found that the entrainment coefficient e is a monotonic decreasing function of the local Richardson number, Ri, defined as where

$$Ri \equiv \frac{g(\rho_o - \rho)}{\rho_o} h/U^2. \qquad\qquad e = \frac{1}{U}\frac{d}{dx}(Uh)$$

Their experimental finding is reproduced here as Fig.4.2, and can be well approximated by the formula

$$e = \begin{cases} 0.075\left[\dfrac{2}{1 + \dfrac{Ri}{0.85}} - 1\right]^{1.75} & 0 \le Ri \le 0.85 \\ 0 & \text{otherwise} \end{cases}$$

It is noted that entrainment ceases for Richardson number exceeding a certain critical value Ri_{cr}. Thus the buoyant jet does not expand linearly with x,

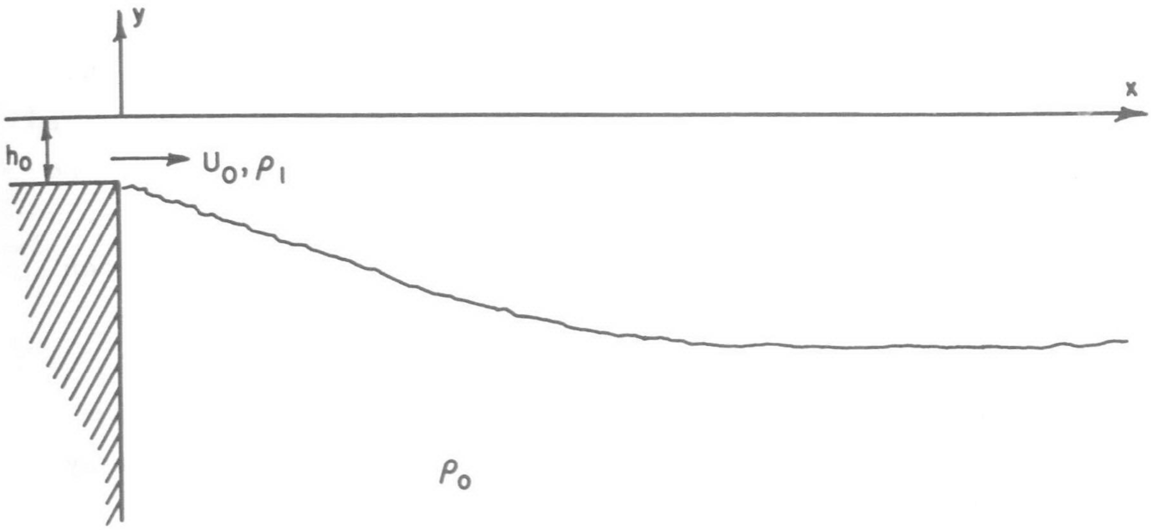

Figure 4.1 Definition sketch.

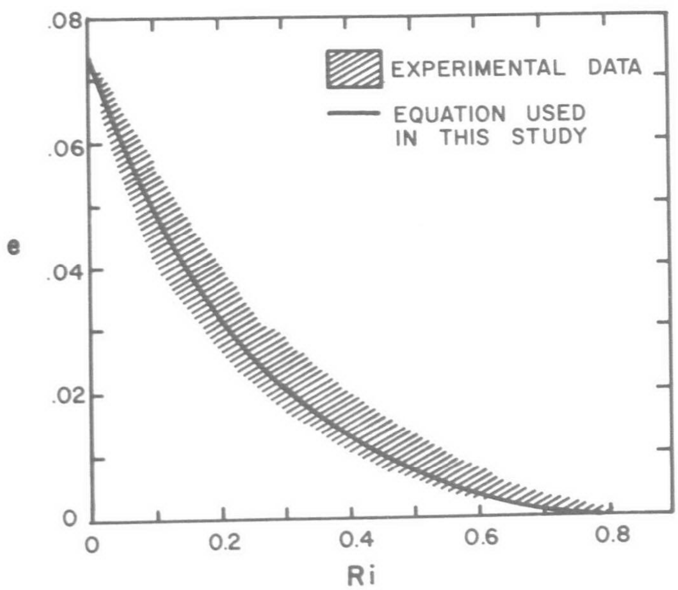

Figure 4.2 Entrainment coefficient e as function of Richardson number Ri.

but rather takes a shape as indicated in Fig.4.1. At some distance from the source, when the local Richardson number reaches the critical value, the jet ceases to expand and the phenomenon resembles a two-layered stratified flow. From that point on (and probably some time before), the flow can no longer be classified as a free turbulent flow and the mechanism of interfacial shear should play a part in determining the flow pattern. It is seen that for the maintanence of positive flow, the interface must possess a slight positive slope in order to overcome the interfacial shear (see Fig. 4.3). This further suggests that at some x = X the interface may meet the free surface, leading to the observation that no steady state solution may exist for this problem.

We now note that as time goes on, X must increase to accommodate the continuing efflux. Thus the maximum thickness of the buoyant fluid would also increase. When this thickness exceeds that which can be provided by the jet through entrainment, an internal hydraulic jump must occur. As X increases further, the jump would occur sooner until a point is reached when the source is inundated. From that point on, the source momentum drops out of the picture entirely.

From the above discussion, it is seen that the phenomenon of a horizontal buoyant jet discharged at the surface of a quiscent fluid of infinite extent may possess features very similar to open channel flow. Near the source, we may encounter jet type flow analogous to supercritical flow in open channels while far away, the phenomenon is similar to subcritical flow in open channels. The subcritical flow region can, therefore, be expected to be influenced by downstream constraints. For example, in the event a laboratory experiment is performed on this phenomenon, the conditions at the downstream end of the tank or flume can strongly influence the flow field.

In this investigation, we are concerned primarily with the case when the buoyancy of the efflux is due to heat. In this case, there is the added mechanism of surface heat exchange between the water and the atmosphere. This mechanism now takes the role of imposing the downstream constraints.

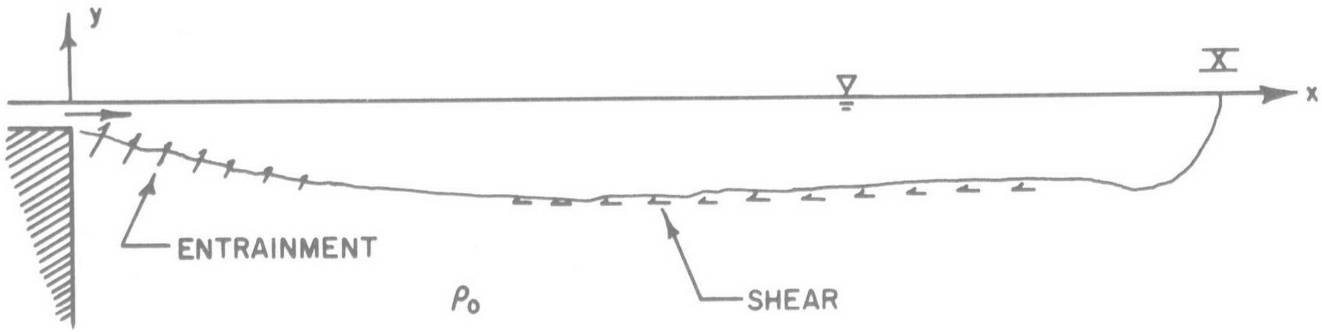

Figure 4.3 Definition sketch.

From the above discussions, it is seen that the flow field induced by a surface horizontal warm jet can, in general, be divided into four zones as shown schematically in Fig.4.4. Zone I is the zone of flow establishment. Zone II is the supercritical region where the flow is basically a jet with decreasing entrainment rate. Zone III is an internal hydraulic jump while Zone IV is the subcritical region where interfacial shear and surface heat exchange play dominant roles.

It should be remarked that not all these zones may be present in any given situation. In particular, as will be shown later, Zones III and IV may be absent if K, the surface heat exchange coefficient, is sufficiently large. In that case, the flow field is similar to that in an ordinary jet. This is reasonable physically since if K is very large, the buoyancy would be lost to the atmosphere quickly and the resulting jet is virtually not buoyant. On the other hand, if K is sufficiently small, it will be seen that the source may be inundated and Zones I, II and III may be absent. Thus, given all the other parameters, there exists two critical values of K; K_{cr+} and K_{cr-} with $K_{cr+} > K_{cr-}$, such that if $K > K_{cr+}$, Zones III and IV are absent and if $K < K_{cr-}$, Zones I, II, and III are absent. For K between K_{cr-} and K_{cr+}, all the zones are present. The model to be developed in the following sections will predict whether all the zones are present and also locate the hydraulic jump when it occurs.

Since the mixing processes involved in the various zones are quite different, the above discussion is of importance in design considerations. For example, if it is desirable to achieve initial jet mixing so that the temperature drops quickly, then the discharge structure must be designed so that the source is not inundated. On the other hand, if maximum surface heat loss is desired then it would be desirable to achieve inundation. However, the depth of inundation should not be too large so as to cause the discharge to interfere with the intake of the cooling water.

The formulation and the solutions to be presented in the following is primarily concerned with Zones II and IV with a brief discussion of Zone III.

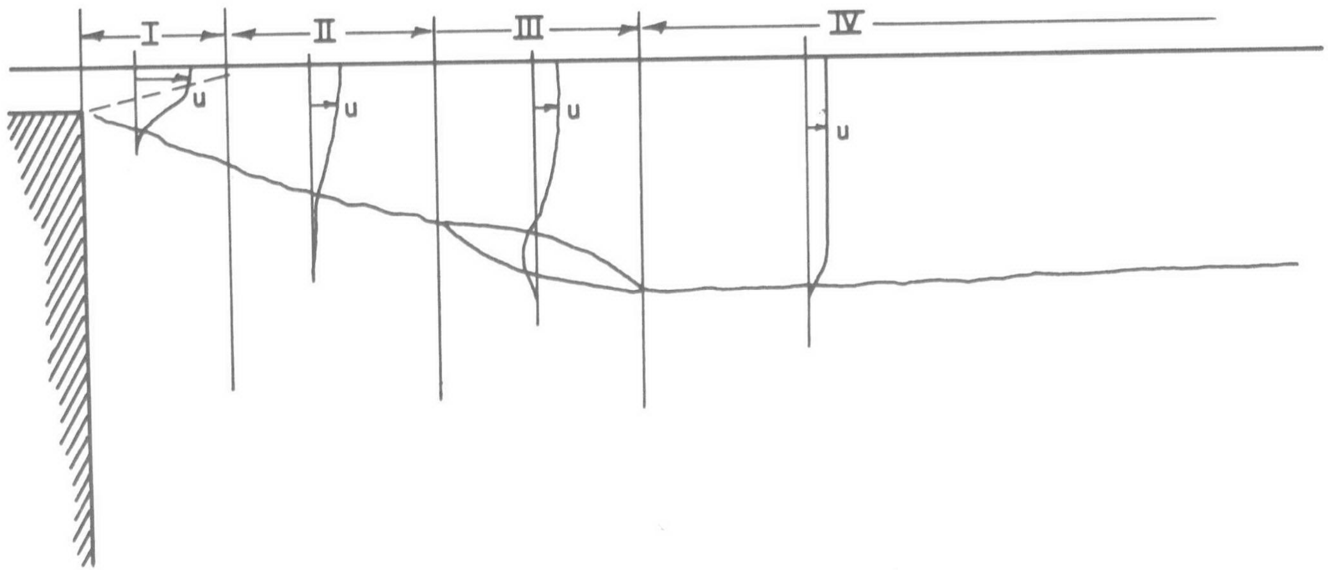

Figure 4.4 The zones in a surface horizontal buoyant jet .

The matching of the zones and the conditions under which some zones are absent will also be discussed. However, no discussion will be given on Zone I, the zone of flow establishment, since it is similar to the corresponding zone in an ordinary jet which is well documented in the available literature.

4.2.1 Derivation of Equations

In this section, the governing equations will be derived for the two-dimensional surface horizontal buoyant jet. In the formulation presented in this section, it will be assumed that

a) the velocity and density deficiency profiles in the vertical direction are similar in shape

b) a steady state solution exists

c) Boussineq approximation: density differences are only important in modifying the gravity term.

d) the flow is primarily horizontal (boundary layer assumption)

It should be pointed out that the similarity profiles to be used in Zones II and IV may be different.

Under these assumptions, the equations of motion are as follows:

Continuity:

$$\frac{\partial u}{\partial x} + \frac{\partial v}{\partial y} = 0 \tag{4.1}$$

Momentum:

$$\frac{\partial}{\partial x}(u^2) + \frac{\partial}{\partial y}(uv) = -\frac{1}{\rho}\frac{\partial p}{\partial x} + \frac{\partial \tau}{\partial y} \tag{4.2}$$

$$0 = -\frac{\partial p}{\partial y} - \rho g \tag{4.3}$$

Conservation of density deficiency:

$$\frac{\partial(\rho u)}{\partial x} + \frac{\partial(\rho v)}{\partial y} = \frac{\partial}{\partial y}\left(D \frac{\partial \rho}{\partial y}\right) \tag{4.4}$$

where x, y are the horizontal and vertical coordinates

u, v are the velocity components in the horizontal and vertical directions

p is the pressure

τ is the kinematic shear stress = shear stress/density

ρ is the density

ρ_o is the density of the ambient fluid

D is the diffusivity

We shall now utilize the assumption of similarity and further specify that

$$u(x,y) = U(x)\ f\left(\frac{y-\eta}{h}\right)$$

$$\rho(x,y) = \rho_o - T(x)\ f\left(\frac{y-\eta}{h}\right)$$

where $\eta(x)$ is the free surface elevation and $h(x)$ a characteristic thickness of the spreading layer. The function $f(\zeta)$ specifying the shape of the similarity profile will be left arbitrary. Examples may be $f(\zeta) = e^{-\zeta^2}$ (near the source) or $f(\zeta) = \begin{cases} 1 & |\zeta| < 1 \\ 0 & |\zeta| > 1 \end{cases}$ (far from the source).

We now integrate the Eqs. (4.1) through (4.4) from $y = -\infty$ to $y = \eta$. Integration of the continuity equation gives

$$\alpha \frac{d}{dx}(Uh) = U \frac{d\eta}{dx} - v(\eta) + v(-\infty)$$

where

$$\alpha \equiv \int_{-\infty}^{0} f(\xi)\, d\xi$$

Now the kinematic free surface boundary condition is $\frac{D}{Dt}(y-\eta)=0$ on $y = \eta(x)$, i.e.,

$$-U\frac{d\eta}{dx} + v(\eta) = 0$$

Thus,

$$\frac{d}{dx}(Uh) = \frac{v(-\infty)}{\alpha}$$

It is generally assumed that $v(-\infty)$ (the entrainment velocity), is related to U, the characteristic velocity, by an entrainment coefficient e which can be a function of the Richardson number (Ellison and Turner 1959)

$$e = e(Ri) \quad , \qquad Ri = \frac{g\ Th}{\rho_o\ U^2}$$

Thus

$$\frac{d}{dx}(Uh) = \frac{e}{\alpha}U \tag{4.5}$$

In a similar fashion, the other Eqs. (4.2), (4.3) and (4.4) can be integrated. The only term requiring some explanation is the pressure integral. From Eq. (4.3),

$$p(x,y) = -g\int_{\eta}^{y} \rho(x,\xi)\,d\xi$$

Letting $\rho = \rho_o - \theta(x,y)$, and using the similarity profile

$$\theta(x,\xi) = T(x)\ f\left(\frac{\xi-\eta}{h}\right)$$

we obtain,

$$-\frac{p}{g} = \rho_o(y-\eta) - T\int_{\eta}^{y} f\left(\frac{\xi-\eta}{h}\right)d\xi = \rho_o(y-\eta) - Th\int_{0}^{\frac{y-\eta}{h}} f(\zeta)d\zeta$$

from which

$$-\frac{1}{g}\frac{\partial p}{\partial x} = -\rho_o\frac{d\eta}{dx} - \frac{d}{dx}(Th)\cdot\int_0^{\frac{y-\eta}{h}} f(\zeta)d\zeta - Th\, f\left(\frac{y-\eta}{h}\right)\frac{d}{dx}\left\{\frac{y-\eta}{h}\right\}.$$

As $y \to -\infty$, we expect $\frac{\partial p}{\partial x} \to 0$ since there is no motion horizontally. Thus

$$\frac{d\eta}{dx} = \frac{\alpha}{\rho_o}\frac{d}{dx}(Th)$$

We now calculate

$$-\int_{-\infty}^{\eta}\frac{1}{g}\frac{\partial p}{\partial x}dy = \int_{-\infty}^{\eta}\left\{-(Th)'\alpha - (Th)'\cdot\int_0^{\frac{y-\eta}{h}} f(\zeta)d\zeta + Th\, f\left(\frac{y-\eta}{h}\right)\left[\frac{y-\eta}{h^2}h' + \frac{1}{h}\frac{d\eta}{dx}\right]\right\}dy$$

$$= -(Th)'\int_{-\infty}^{\eta}dy\int_{-\infty}^{\frac{y-\eta}{h}} f(\zeta)d\zeta + Th\int_{-\infty}^{\eta} f\left(\frac{y-\eta}{h}\right)\frac{y-\eta}{h}\frac{h'}{h}dy + Th\int_{-\infty}^{\eta} f\left(\frac{y-\eta}{h}\right)\frac{d\eta}{dx}\frac{dy}{h}$$

After interchanging the order of integration for the double integral, and carrying out one of the integrals, we get

$$-\frac{1}{g}\int_{-\infty}^{\eta}\frac{\partial p}{\partial x}dy = \frac{d}{dx}(Th^2)\cdot\int_{-\infty}^{0}\zeta f(\zeta)d\zeta + \frac{(Th)\cdot(Th)'}{\rho_o}\alpha^2$$

Note that $\frac{T}{\rho_o} << 1$ so that the second term on the right can be neglected compared with the first.

Returning now to Eq. (4.2), and integrating with respect to y from $-\infty$ to η, and using the kinematic free surface boundary condition, we get

$$\frac{d}{dx}(U^2h) = \alpha_1\frac{d}{dx}(Th^2) + (\tau_s - \tau_i)\alpha_2$$

where

$$\alpha_1 = \frac{g}{\rho_o}\int_{-\infty}^{0}\zeta f(\zeta)d\zeta \Big/ \int_{-\infty}^{0} f^2(\zeta)d\zeta \;;\quad \alpha_2 = \frac{1}{\int_{-\infty}^{0} f^2(\zeta)d\zeta}$$

τ_s and τ_i are the shear on the free surface and the interface respectively.

Equation (4. 4), when integrated with respect to y from $-\infty$ to η gives

$$\frac{d}{dx}(ThU) = \alpha_2 D \frac{\partial\theta}{\partial y}\Big|_{\eta} = -\alpha_2 H$$

where H is proportional to the rate of heat loss at the free surface.

To summarize, under the assumptions made, the equations governing the surface spreading are

Continuity:

$$\frac{d}{dx}(Uh) = \frac{e}{\alpha} U \tag{4. 6}$$

Momentum:

$$\frac{d}{dx}(U^2 h) = \alpha_1 \frac{d}{dx}(Th^2) + \alpha_2 (\tau_s - \tau_i) \tag{4. 7}$$

Heat balance:

$$\frac{d}{dx}(ThU) = -\alpha_2 H \tag{4. 8}$$

The Eqs. (4. 6), (4. 7) and (4. 8) constitutes a set of three ordinary differential equations for the unknowns U, T, and h subject to the given conditions $U = U_o$, $T = T_o$, $h = h_o$ at $x = 0$. They are derived from the Navier-Stokes equations by making the assumptions stated in the beginning of this section.

Before these equations can be solved, it is necessary to specify the functions H, τ_i and τ_s as functions of the other unknowns. We shall neglect τ_s, the shear at the free surface.

For τ_i, we shall assume

$$\tau_i = \varepsilon \frac{U}{h}$$

where ε is an effective viscosity coefficient. In the analyses to be presented in the following sections, ε is taken to be constant. However, the general features of the solutions, as well as the method of solution, are equally applicable when ε is not constant but depends on, say, U. The critical relations to be derived in the following sections will be different when ε is not constant. However, the procedure for finding them will be similar.

For the quantity H, we shall assume

$$H = -KT$$

where K is an effective heat exchange coefficient. In this investigation K will also be assumed constant. Again the general features of the solution and the method of solution are also applicable when K is not constant but depends on, say, the temperature.

4.2.2 General Discussion of the Equations and Solutions

Before analyzing quantitatively the flow field in the several zones, it is instructive to examine some of the properties of Eqs. (4.6), (4.7) and (4.8).

It will be shown that for some combinations of input parameters, a continuous solution cannot be found. In this section, the region in parameter space where a continuous solution can be obtained will be delineated. In the event the parameters fall outside the region, then the solution is either non-existent, or discontinuous or not source governed. These cases will be discussed in detail in later sections.

Normalizing the variables by the source conditions U_o, h_o, T_o,

$$u^* = \frac{U}{U_o}, \qquad h^* = \frac{h}{h_o}, \qquad T^* = \frac{T}{T_o}, \qquad x^* = \frac{x}{\alpha h_o}$$

and defining $F_o = \frac{-U_o^2}{2\alpha_1 T_o h_o}$, $R = \frac{h_o U_o}{\varepsilon \alpha \alpha_2}$, $k = \frac{\alpha \alpha_2 K}{U_o}$,

equations (4.6), (4.7) and (4.8) become, after dropping the *'s,

$$\frac{d(uh)}{dx} = eu \tag{4.6a}$$

$$\frac{d}{dx}(u^2 h) = -\frac{1}{2F_o}\frac{d}{dx}(Th^2) - \frac{1}{R}\frac{u}{h} \tag{4.7a}$$

$$\frac{d}{dx}(uhT) = -kT \tag{4.8a}$$

For application to practical situations, it is necessary to obtain the numerical values of the α's based on assumed form of f (ζ). For example, if $f(\zeta) = \begin{cases} 1 & -1 < \zeta < o \\ o & \zeta < -1 \end{cases}$, then $\alpha = 1$, $\alpha_1 = -\frac{g}{2\rho_o}$, $\alpha_2 = 1$.

If, $f(\zeta) = e^{-\zeta^2}$, then $\alpha = \sqrt{\pi/2}$, $\alpha_1 = \sqrt{\frac{2}{\pi}}\,\frac{g}{\rho_o}$, $\alpha_2 = 2\sqrt{2/\pi}$

It is seen that the dependence of the α's on the choice of f(ζ) is rather weak. In any event, the basic features of the solution will not change with a change in the choice of f (ζ). The proper basis of choosing f (ζ) is a detailed set of experiments. Since this is lacking at present, we shall choose the simplest form of f(ζ), namely the first choice mentioned above for our subsequent discussion. Choice of other forms of f(ζ) will not change the argument or method of solution or the basic features of the solutions which follow although the numerical values will change slightly. When experimental evidence accumulates to allow a more accurate choice of f(ζ), the analysis may easily be repeated to obtain the solutions based on the new f(ζ).

Equations (4.6a), (4.7a) and (4.8a) constitute three nonlinear ordinary differential equations to be solved for the three unknowns u, h, and T subject to the conditions $u = h = T = 1$ at $x = 0$. The system of equations depends also on three parameters F_o, R and k. It will be shown later that the character of the solutions are strongly dependent on the relative magnitudes of these three paramters. Thus it is important to first inquire into the typical orders of magnitude of these parameters.

Typical values of the parameters K and ε are very small. One expects K to be of order 10^{-5} or 10^{-4} ft/sec while ε to be of order 10^{-4} to 10^{-2} ft^2/sec. Thus for U_o, h_o of order unity, $k \sim 0\,(10^{-4})$, and $R \sim 0\,(10^3)$. F_o, however, can vary over a wide range. Since T_o is small, F_o can be expected to be relatively large. We are, therefore, primarily interested in the case k very small and R large.

It can be readily shown that Eqs. (4.6a), (4.7a) and (4.8a) may be put into the following form:

$$\frac{dT}{dx} = -\frac{kT}{uh} - e\frac{T}{h} \tag{4.6b}$$

$$\frac{dh}{dx} = \frac{-2e + \frac{e}{2F_o}\frac{hT}{u^2} + \frac{k}{2F_o}\frac{hT}{u^3} - \frac{1}{R}\frac{1}{hu}}{\frac{1}{F_o}\frac{hT}{u^2} - 1} \tag{4.7b}$$

$$\frac{du}{dx} = \frac{u}{h}\left[e - \frac{dh}{dx}\right] \tag{4.8b}$$

It can be readily seen that the denominator in Eq. (4.7b) is simply $\frac{1}{F} - 1$ where F is the local Froude number which is the inverse of the Richardson number. It now becomes obvious that for the existence of a continuous solution, it is necessary that if $F \to 1$, the numerator in 4.7b must also tend to zero. It will be seen in the following discussion that this necessary condition is not satisfied except possibly fortuitously. On the other hand, for some combinations of the parameters F_o, k, R, the local Froude number never approaches one so that a continuous solution does exist.

It is convenient to rewrite Eq. (4.7b) in the form

$$\frac{dh}{dx} = \frac{e\left\{2 - \frac{1}{2F}\right\} - \frac{k}{2Fu} + \frac{1}{R}\frac{1}{hu}}{1 - \frac{1}{F}} \tag{4.9}$$

We further note that

$$ThF = F_o u^2$$

Hence

$$\frac{dT}{T} + \frac{dh}{h} + \frac{dF}{F} = 2\,\frac{du}{u}$$

therefore,

$$\frac{dF}{F} = 2\,\frac{du}{u} - \frac{dT}{T} - \frac{dh}{h}$$

Thus, F would increase or decrease according to whether

$$2\,\frac{u'}{u} - \frac{T'}{T} - \frac{h'}{h}$$

is positive or negative. From (4.8a) we have

$$\frac{T'}{T} + \frac{h'}{h} + \frac{u'}{h} = -\frac{k}{uh}$$

and from Eq. (4.6a) we have

$$\frac{u'}{u} = \frac{e}{h} - \frac{h'}{h}$$

therefore,

$$\frac{F'}{F} = 3\left[\frac{e}{h} - \frac{h'}{h}\right] + \frac{k}{uh}$$

Since h is always positive, F would increase or decrease according to whether

$$3(e - h') + \frac{k}{u}$$

is positive or negative. In particular, for F to increase, we need

$$\frac{k}{u} > 3(h' - e)$$

Using Eq. (4. 9), this condition becomes

$$\frac{k}{u} > 3e + \frac{6F}{2F+1} \frac{1}{Rhu}$$

Thus,

$$\frac{dF}{dx} > 0 \qquad \text{if} \qquad \frac{k}{u} > 3e + \frac{6F}{2F+1} \frac{1}{Rhu} \tag{4. 10a}$$

and $$\frac{dF}{dx} = 0 \qquad \text{if} \qquad \frac{k}{u} = \qquad '' \tag{4. 10b}$$

and $$\frac{dF}{dx} < 0 \qquad \text{if} \qquad \frac{k}{u} < \qquad '' \tag{4. 10c}$$

With the help of Eqs. (4. 9) and (4. 10), we can now discuss the influences of the parameters k, R, and F_o on the characteristics of the solution. As was mentioned in the beginning of this section, we shall be concerned only with the case when F_o is fairly large, while k and 1/R are both very small, since this is the case of practical interest. Note that h, u, F, and e are all positive quantities for a valid solution.

If $k = 1/R = 0$, then Eq. (4. 10c) is satisfied at $x = 0$ and F would decrease and asymptotically approach the critical value F_{cr} at which $e = 0$ (see Fig. 4. 2 .

If $k = 0$ and $R \neq 0$, then condition (4. 10c) is always satisfied. F would continue to decrease past F_{cr} and reach $F = 1$ at which point $\frac{dh}{dx} \to \infty$ leading to the non-existence of a continuous solution.

If $\frac{1}{R} = 0$ but $k \neq 0$, then we may have Eq. (4. 10c) satisfied at $x = 0$. Thus F decreases which implies e decreases. When it decreases sufficiently so that $k = 3eu$, then F would increase again. Thus, F never decreases below the value F_{cr} since if it does, e would be zero and F would increase since (4. 10c) would be satisfied.

Finally, we shall consider the most interesting case physically when both $\frac{1}{R}$ and k are not zero. Suppose first that k is very large. In particular, suppose $k > 3e_o + \frac{3}{R}$. Then (4.10a) is always satisfied and we would have F increasing all the time. When F becomes larger and larger, the solution becomes more and more nearly that of an ordinary jet. On the other hand, if k is very small, we would expect F to decrease initially. In that case, u decreases, h increases and hu increases with x so that (4.10a) becomes more likely to be satisfied as x becomes larger. For sufficiently small k, however, F would decreases to $F_{cr} = 1/Ri_{cr}$ at which point e = 0 and hu becomes constant. The right hand side of condition (4.10) then becomes,

$$\frac{6F_{cr}}{2F_{cr}+1} \quad \frac{1}{R(hu)}$$

It is clear that this may still be larger than $\frac{k}{u}$. The question then becomes whether condition (4.10c) is satisfied all the way to F = 1. If so, we expect no continuous solution. Since both k and $\frac{1}{R}$ are small in practice a good estimate can be derived for the critical value of k such that below that, no continuous solution exists as follows: since e = 0 for $F < F_{cr}$, the critical value for k must be such that

$$k = \frac{2}{Rh_1}$$

where h_1 is the value of h at the critical point. For k and $\frac{1}{R}$ small, this value of h_1 can be assumed to be approximately equal to the asymptotic value of h as $x \to \infty$ in the solution for $k = \frac{1}{R} = 0$. These solutions are exhibited in Fig. 4.5 in Sec. 4.2.3. When this is done, it is found that the critical relation may be approximate by

$$(kR) \cong 2.9\,[F_o]^{-0.655} \tag{4.11}$$

Thus for

$$(kR) < 2.9\,[F_o]^{-0.655} \tag{4.11a}$$

we would encounter a discontinuous solution, while for

$$(kR) > 2.9\,[F_o]^{-0.655} \qquad (4.11b)$$

we would have a jet type solution. However it should be pointed out that even though we have called it a jet type solution, the flow field may appear quite different from that in an ordinary jet. In fact, even if condition (4.11b) is satisfied, F, the local Froude number may first decrease and then increase. The ordinary jet is characterized by a local Froude number of infinity. Thus the jet region may behave somewhat differently until F becomes quite large.

From the above discussion, it is seen that the flow field in a horizontal buoyant jet at the surface can be very different from that in either an ordinary non-buoyant jet or a submerged buoyant jet. For the case when no heat loss occurs at the water surface, no steady state solution is possible. The source will, sooner or later, be inundated. For non-zero heat exchange, a steady state can be found as will be demonstrated in the following sections. Moreover, given all the other parameters, a critical value of k, the surface exchange coefficient exists such that for values of k larger than this,jet type solution may be found while for k less than this critical value, the solution may be discontinuous. For k and $\frac{1}{R}$ very small, this critical relation is given approximately by Eq. (4.11). In practical situations, k is expected to be very small and the condition of (4.11a) is likely to be satisfied. In the following sections, this case will be considered in detail, since it is the case of practical interest. It is also the case which results in the most complicated flow pattern.

4.2.3 Solution of the Equations

In the beginning of Sec. 4.2, it was deduced from physical reasoning that the flow field induced by a surface horizontal warm jet can be divided into four zones as shown in Fig.4.4. In the general discussion in Sec. 4.2.2, it was found that a jet type solution may be expected if condition (4.11b) is satisfied. In that case, Zone II, the jet region extends all the way to infinity. If condition (4.11a) is satisfied, we expect Zone II to extend at most up to some distance from the source. It will be shown later in Sec. 4.2.4 that there exists another critical relation between the parameters such that if satisfied, Zone II is absent entirely and Zone IV extends all the way to the source, inundating it. In this section, we shall examine the flow field in the Zones II, III and IV separately.

(A) Zone II

Since k and $\frac{1}{R}$ are usually very small, we shall first investigate the case when both are zero. In that case, Eqs. (4.6), (4.7) and (4.8) become

$$\frac{d}{dx}(Uh) = \frac{e}{\alpha}U$$

$$\frac{d}{dx}(UhT) = 0$$

$$\frac{d}{dx}(U^2h) = \alpha_1 \frac{d}{dx}(Th^2)$$

We shall consider U, h, T as mean quantities over the vertical and specify $f(\zeta) = \begin{cases} 1, & -1 < \zeta < 0 \\ 0 & \zeta \leq -1 \end{cases}$ so that $\alpha = 1$ and $\alpha_1 = -\frac{g}{2\rho_o}$. It can be readily seen that choice of $f(\zeta)$ to be some other profile will only change the coefficients α and α_1 slightly without affecting the essence of the solution.

Let U_o, h_o, T_o be the source conditions at x = 0 and define dimensionless quantities u, h*, T*, x* as

$$\left.\begin{aligned} u &= U/U_o \\ h^* &= h/h_o \\ T^* &= T/T_o \end{aligned}\right\} \qquad (4.12)$$

$$x^* = x/h_o$$

Substituting into the equations and dropping *'s, the problem then becomes

$$\frac{d}{dx}(uh) = eu \tag{4.13}$$

$$\frac{d}{dx}(uhT) = 0 \tag{4.14}$$

$$\frac{d}{dx}(u^2 h) = \frac{-1}{2F_o} \frac{d}{dx}(T h^2) \tag{4.15}$$

$$F_o = \frac{U_o^2 \rho_o}{g T_o h_o} \tag{4.16}$$

with $u = h = T = 1$ at $x = 0$ (4.17)

From Ellison and Turner (1959, (see Fig.4.2), the quantity e is a function of the local Richardson number which is the reciprocal of the local Froude number

$$Ri = \frac{1}{F} = \frac{Th}{u^2 F_o}$$

It can be approximated by the function

$$e(Ri) = \begin{cases} e_o \left\{ \dfrac{2}{1 + \dfrac{Ri}{Ri_{cr}}} - 1 \right\}^n , & Ri < Ri_{cr} \\ 0 , & Ri > Ri_{cr} \end{cases} \tag{4.18}$$

where e_o is the value of e at $Ri = 0$, Ri_{cr} is the critical Richardson number beyond which $e = 0$, and n is an exponent. From the data, we may deduce the following values for the parameters.

$$\begin{aligned} e_o &\approx 0.075 \\ Ri_{cr} &\approx 0.85 \\ n &\approx 7/4 \end{aligned} \tag{4.19}$$

Equations (4.13), (4.14) and (4.15), with e given by Eqs. (4.18) and (4.19), subject to the condition of Eq. (4.17) constitutes an initial value problem with only one parameter F_o. The solutions have been affected by using a fourth order Runge-Kutta numerical scheme and are shown in Fig. 4.5a. for a variety of F_o's.

In the case k and $\frac{1}{R}$ are not zero, the Eqs. (4.6), (4.7) and (4.8) can also be solved if condition (4.11b) is satisfied giving rise to a jet type solution. A computer program SBJ2 written in Fortran IV language is included in Appendix B with which this solution mav be obtained. A few examples are shown in Fig. 4.5b. In the event k and $\frac{1}{R}$ are not zero but condition (4.11b) is not satisfied then it can be expected that an internal hydraulic jump would occur either away from or inundating the source. The method of finding the solution is to use the program SBJ2 twice, first to solve the jet portion to the point of the jump and then to continue the solution by re-initializing the program SBJ2 with the parameters just after the jump. The method of matching the solutions and locating the jump will be discussed in Sec. 4.2.5 after we have investigated the flow fields in Zones III and IV. The case when the source is inundated will also be discussed in Sec. 4.2.5.

It should be remarked that if k and $\frac{1}{R}$ are such that condition (4.11b) is not satisfied, the solutions obtained herein for $k = \frac{1}{R} = 0$ may be used to match with the flow in Zone IV to within a good approximation.

(B) Zone III

From the general discussion, it is seen that an internal hydraulic jump is a possibility in the development of a surface layer. The conditions across the jump will now be obtained. Consider an abrupt internal hydraulic jump with upstream conditions ρ_1, u_1, h_1 and downstream conditions ρ_2, u_2, h_2 as shown in Fig. 4.6.

Conservation of mass requires

$$\rho_1 u_1 h_1 + \rho_o \overline{E} = \rho_2 u_2 h_2 \qquad (4.20)$$

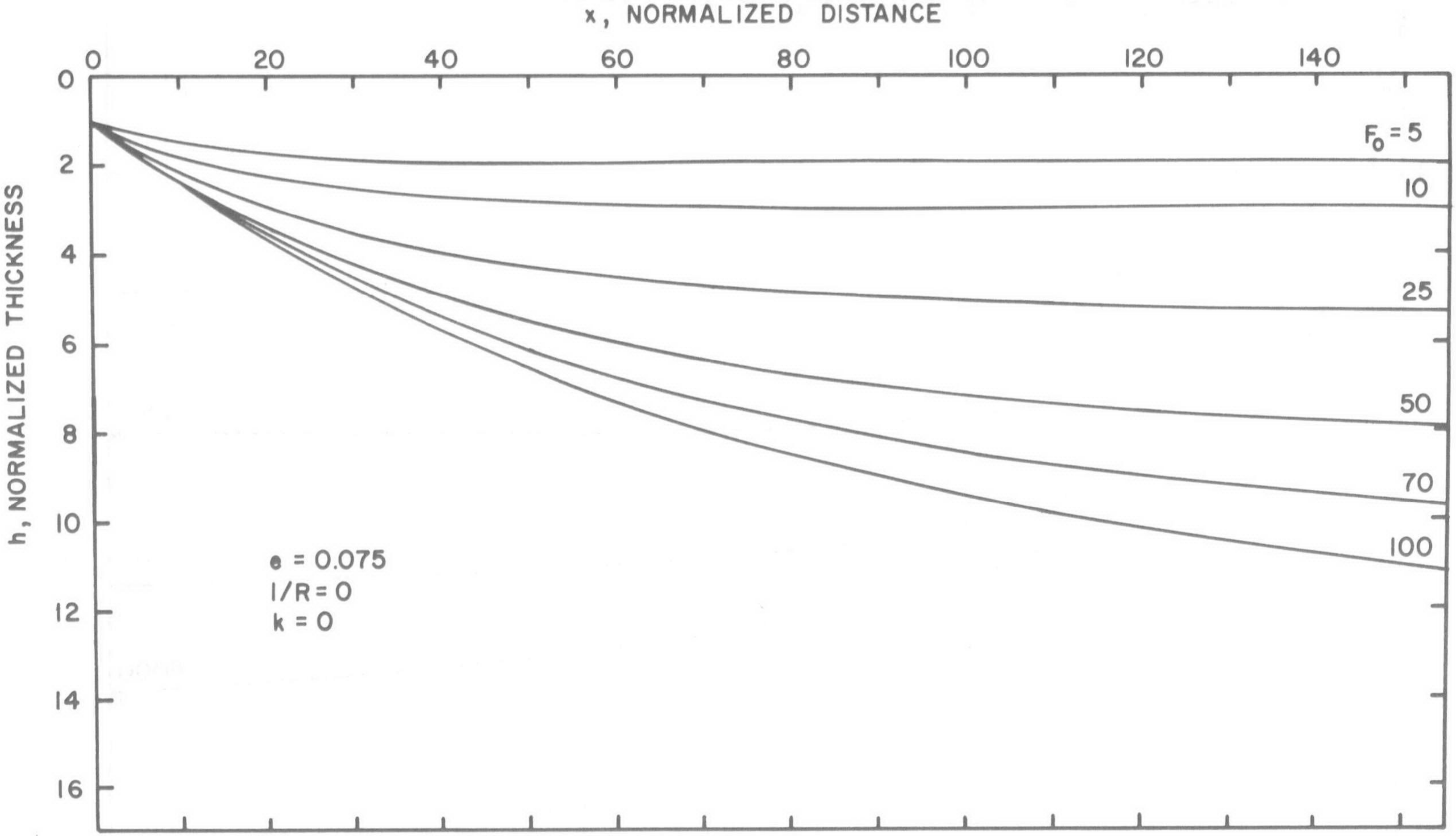

Figure 4.5a Predicted jet thickness and density deficiency in a surface horizontal buoyant jet for k = l/R = 0 (two dimensional case).

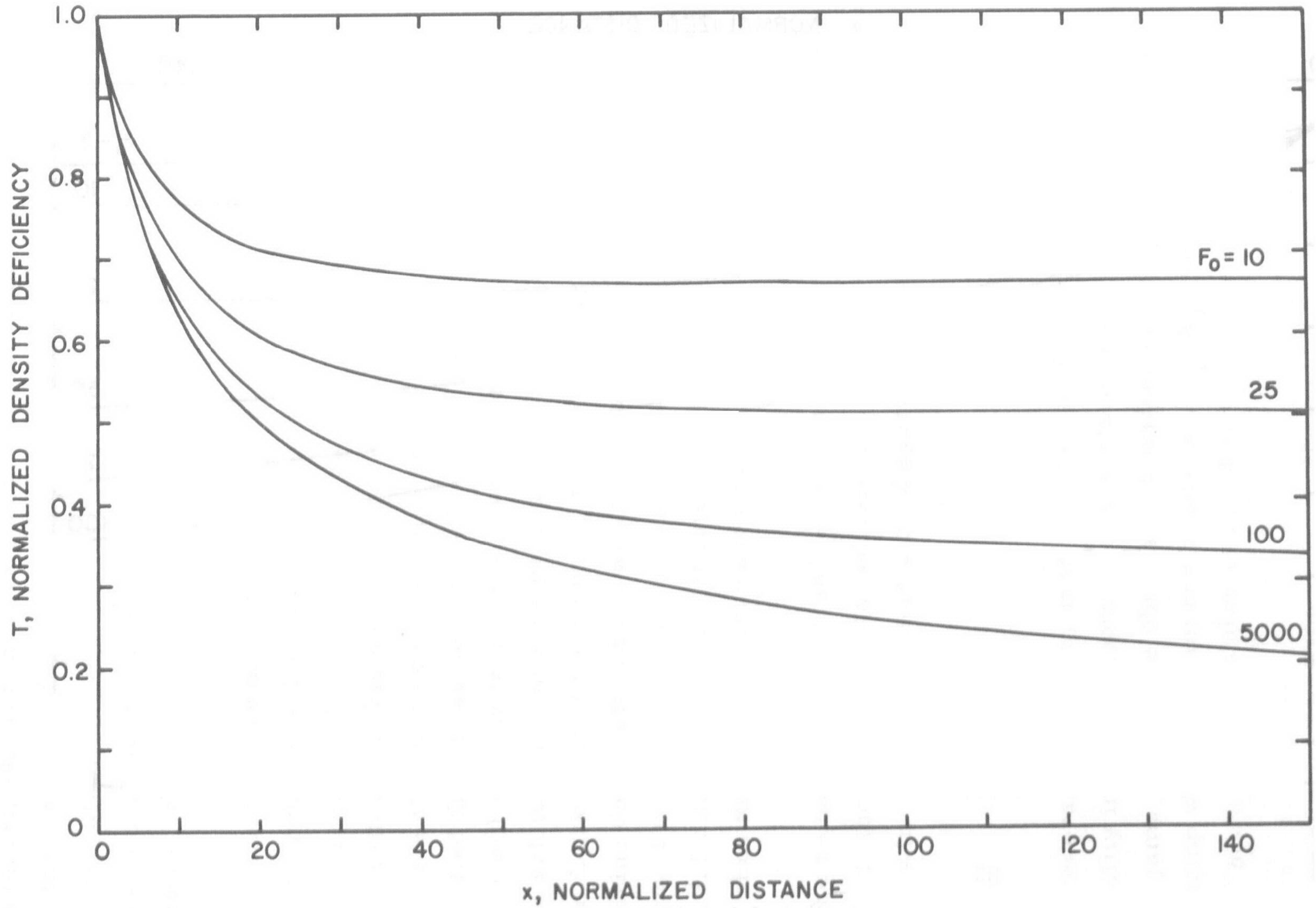

Figure 4.5a Continued.

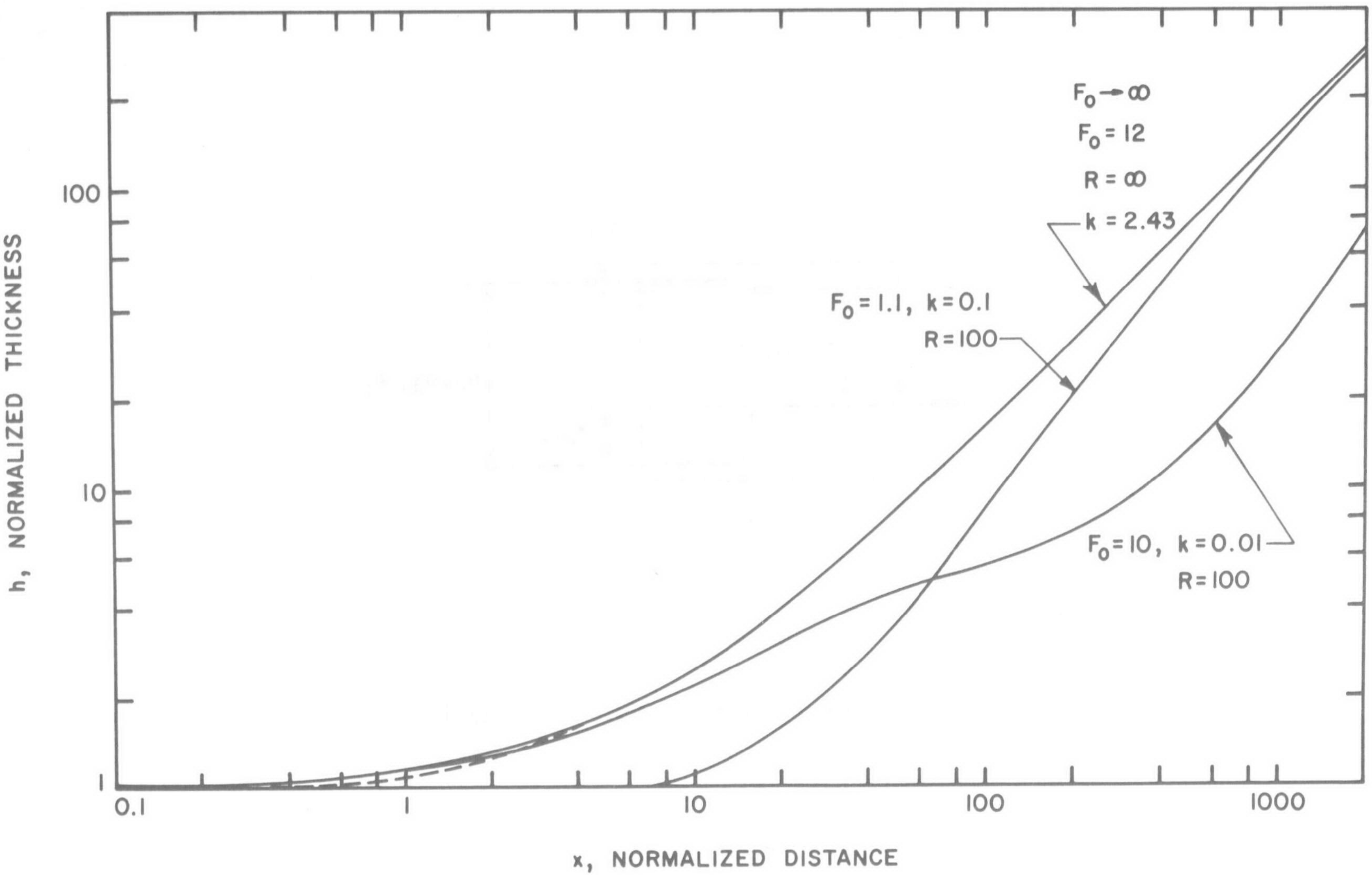

Figure 4.5b Predicted jet thickness in a surface horizontal buoyant jet for the case when $k > k_{cr+}$ (two dimensional case).

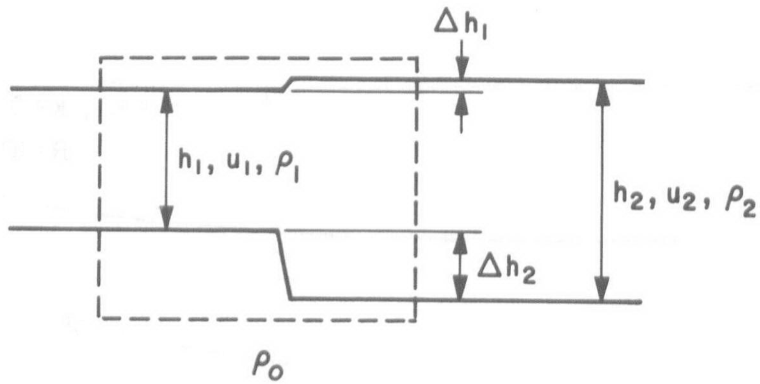

Figure 4.6 Definition sketch.

where $\overline{E}$ = the volume of fluid entrained in the jump.

Conservation of momentum requires

$$-\rho_1 u_1^2 h_1 + \rho_2 u_2^2 h_2 = \int (p_1 - p_2)\, dy$$

where the integral extends over the vertical sides of the control surface dotted in Fig. 4.6. We note that

$$\rho_2 h_2 = \rho_1 h_1 + \rho_o (\Delta h)_2$$

where $(\Delta h)_2$ is the jump of the interface.

The integral $\int (p_1 - p_2)\, dy$ is thus

$$\frac{\rho_2 g h_2^2}{2} - \left[\frac{\rho_1 g h_1^2}{2} + \frac{\rho_1 g h_1 + \rho_2 g h_2}{2} (\Delta h)_2\right]$$

Since

$$(\Delta h)_2 = \frac{\rho_2 h_2 - \rho_1 h_1}{\rho_o}$$

the momentum conservation equation gives

$$\rho_2 u_2^2 h_2 - \rho_1 u_1^2 h_1 = \frac{g}{2}\left[\rho_1 h_1^2 - \rho_2 h_2^2\right] + \frac{g}{2\rho_o}\left[\rho_2^2 h_2^2 - \rho_1^2 h_1^2\right] \qquad (4.21)$$

In addition to the conservation equations for mass and momentum, there is also the conservation equation for buoyancy. Thus

$$(\rho_o - \rho_1)\, u_1 h_1 = (\rho_o - \rho_2)\, u_2 h_2 \qquad (4.22)$$

The three conservation Eqs. (4.20), (4.21) and (4.22) now allow the jump conditions to be determined. For our purposes here, we will assume $\overline{E} = 0$, i.e., no significant entrainment occurs in the jump. Invoking the Boussinesq approximation, we get

$$u_1 h_1 = u_2 h_2$$

and

$$\rho_1 = \rho_2 \equiv \rho$$

The momentum equation, (4.21) then gives

$$\frac{u_1}{u_2} = \frac{h_2}{h_1} = \frac{1}{2}\left[\sqrt{1+8F_1} - 1\right] \quad \text{where} \quad F_1 = \frac{u_1^2}{g\left(\frac{\rho_o - \rho}{\rho_o}\right) h_1} \tag{4.23}$$

Thus the velocity ratio and the thickness ratio are expressed in terms of the upstream densimetric Froude number. We note that if $F_1 < 1$, $\frac{h_2}{h_1} < 1$ while for $F_1 > 1$, $\frac{h_2}{h_1} > 1$. To find if either or both are admissible, we note that the total head H upstream of the jump is

$$H_1 = \frac{u_1^2}{2g}$$

while that downstream is

$$H_2 = \frac{u_2^2}{2g} + \frac{\Delta\rho}{\rho}(h_2 - h_1)$$

where zero head has been referred to the free surface upstream of the jump. The difference of head $\Delta = H_1 - H_2$ is therefore

$$\Delta = \left(1 + \frac{1}{2}\frac{h_2}{h_1}\right)\left(\frac{h_2}{h_1} - 1\right)h_1 \frac{\Delta\rho}{\rho}$$

Thus, Δ is positive if $h_2/h_1 > 1$ and negative if $h_2/h_1 < 1$. But Δ being negative implies a gain in total head in going across the jump which is clearly impossible. Hence a jump can only occur if $F_1 > 1$. The jump considered herein is very simple. A more detailed theory of internal hydraulic jumps in discrete layered fluids can be found in Yih (1965).

(C) Zone IV

Having found the solutions for Zones II and III in the previous subsections, we must now consider Zone IV. It should be remarked here that the solution obtained in Zone IV would determine where the jump (Zone III) would occur. In fact, it is possible that Zone II and III are completely absent if the source becomes inundated.

In Zone IV, we have $F < 1$. Thus the entrainment is zero. The Eqs. (4.6), (4.7) and (4.8) then become

$$\frac{d}{dx}(Uh) = 0$$

$$\frac{d}{dx}(UhT) = -KT$$

$$\frac{d}{dx}(U^2h) = -\frac{g}{2\rho_o}\frac{d}{dx}(Th^2) - \epsilon\frac{U}{h}$$

Normalizing U, h, T with respect to the conditions at the beginning of Zone IV, U_o, h_o, T_o and dropping $*$'s as before, we get

$$\frac{d}{dx}(uh) = 0 \tag{4.24}$$

$$\frac{d}{dx}(Thu) = -kT \tag{4.25}$$

$$\frac{d}{dx}(u^2h) = -\frac{1}{2F_o}\frac{d}{dx}(Th^2) - \frac{u}{h}\frac{1}{R} \tag{4.26}$$

where $x = 0$ corresponds to the beginning of Zone IV, $k = \frac{K}{U_o}$, and $R = \frac{U_o h_o}{\epsilon}$.

Although Eqs. (4.24) and (4.25) are easily integrated, Eq. (4.26) does not allow closed form solutions. To gain some physical insight into the situation, we note that since in Zone IV, we have $F_o < 1$, the momentum flux is very small. Thus we shall first examine analytically the solutions by neglecting the inertia term. In that case Eq. (4.26) becomes

$$\frac{1}{2F_o}\frac{d}{dx}(Th^2) = -\frac{u}{hR}$$

The Eqs. (4.23) and (4.24) readily integrate to

$$uh = 1$$
$$T = e^{-kx}$$

so that we have

$$\frac{d}{dx}(e^{-kx}h^2) = -\frac{2F_o}{Rh^2} \equiv -\frac{\gamma}{h^2} \tag{4.27}$$

where $\gamma \equiv \frac{2F_o}{R}$ is a ratio of the source Froude number to source Reynolds number. It can be readily shown that the solution to Eq. (4.27) is

$$h^4 = e^{2kx}\left[1 - \frac{2\gamma}{k} + \frac{2\gamma}{k}e^{-kx}\right] \tag{4.28}$$

Note that if $\frac{2\gamma}{k} > 1$, then for sufficiently large x, h^4 becomes negative. This implies there is no steady state solution. Since

$$\frac{2\gamma}{k} = \frac{4F_o}{kR}$$

this condition is the same as

$$h_o^4 < \frac{4\varepsilon q_o^2 \rho_o}{gT_oK} \tag{4.29}$$

If condition (4.29) obtains, no steady state solution exists. This means that the internal hydraulic jump must occur so that the parameters following the jump are such that

$$h_2^4 \geq \frac{4\varepsilon q_2^2 \rho_o}{g\,T_2K} \tag{4.30}$$

where the subscript 2 in Eq. (4.30) has been inserted to stress the fact that these are the downstream conditions after the jump (and the initial conditions for Zone IV). If the solution in Zone II (jet region) is such that condition (4.30) cannot be met at all by an internal hydraulic jump, then the source will be inundated to satisfy (4.30).

The considerations given on the previous page lead to the condition given by Eq. (4.30) which involves the assumption that the inertia or momentum flux of the flow is negligible compared with the pressure induced forces and the viscous forces. This assumption may not be adequate under all conditions. Return now to Eqs. (4.24) through (4.26). We first integrate Eqs. (4.24) and (4.25) to get

$$uh = 1$$
$$T = e^{-kx}$$

Substituting these into Eq. (4.26), letting $\xi = kx$, $s = \frac{1}{Rk}$, and rearranging we get

$$\frac{dh}{d\xi} = \frac{\frac{1}{2F_o} h^4 e^{-\xi} - s}{\frac{1}{F_o} h^3 e^{-\xi} - 1} \tag{4.31}$$

This is a first order equation with two parameters F_o and ε. Moreover, since we are discussing Zone IV, $F_o < 1$. It should be realized that for a physically realizable solution, h must be bounded for all finite ξ. We now note that if $\frac{1}{2F_o} \leq s$, then Eq. (4.31) does not possess any physically realizable solution since $\frac{dh}{d\xi}$ at $\xi = 0$ is not positive. If $\frac{dh}{d\xi}$ is negative at some ξ, say at $\xi = 0$, (i.e., $\frac{1}{2F_o} < s$) then $\frac{dh}{d\xi}$ will stay negative until the denominator changes sign since the numerator will never change sign as long as $\frac{dh}{d\xi} < 0$. But the denominator changing sign implies it becomes zero for some ξ which leads to an infinite $\frac{dh}{d\xi}$. Thus $\frac{dh}{d\xi} > 0$ everywhere for proper solution. For proper solution, it is necessary (though not sufficient) that $F_o < \frac{1}{2s}$. The larger the s, the smaller can be the value F_o. Given the numerical value of s, there is then a critical value of F_o say $F_{o\,cr}$ such that proper solution can exist only if $F_o < F_{o\,cr}$. This value, $F_{o\,cr}$ corresponds to the case when the energy lost in the internal hydraulic jump is minimum. We now proceed to find the critical relation between F_o and s.

For purposes of discussion, it will be convenient to use the local densimetric Froude number

$$F = F_o \frac{u^2}{Th} = \frac{F_o}{h^3} e^{\xi}$$

Equation (4.31) can then be written in its alternate form

$$\frac{dh}{d\xi} = \frac{\frac{h}{2F} - s}{\frac{1}{F} - 1} \tag{4.32}$$

We note that for proper solution $\frac{1}{F} > 1$ and $\frac{dh}{d\xi} > 0$ always. Hence $\frac{h}{2F} > s$ always. Since $h' > 0$, h is monotically increasing with ξ. However, $\frac{1}{F}$ may decrease to nearly 1 and then increase again. If this occurs $\frac{dh}{d\xi}$ would become large unless the numerator also approaches zero. Thus we expect that as $F \to 1$, $\frac{h}{2} \to s$. In particular, if F_o is nearly 1 we must have s nearly $\frac{1}{2}$. Thus we have found that one point on the critical relation

$$F_o = F_{o\,cr}(s)$$

is

$$1 = F_{o\,cr}(\tfrac{1}{2})$$

To obtain the critical Froude number for other $F_o < 1$, we note that given that we have the correct F_o for the given s, then integration of Eq. (4.31) would continue with F increasing such that at $\xi = \xi_1$ F becomes almost 1 and from ξ_1 on, F decreases again. We note that we can solve the problem from $\xi = \xi_1$ backwards in ξ and thus obtain $F_{o\,cr}(s)$. Let h_1, F_1, ξ_1 be the values at ξ_1 when $\frac{dF}{d\xi} = 0$ and $F_1 = 1 - \delta$ where $\delta > 0$. We now define new variables h^*, η by

$$h^* = \frac{h}{h_1}, \quad \eta = -\xi + \xi_1,$$

Eq. (4.31) then becomes

$$\frac{dh^*}{d\eta} = \frac{\frac{s}{h_1} - \frac{1}{2F_1} h^{*4} e^{\eta}}{\frac{1}{F_1} h^{*3} e^{\eta} - 1}$$

Moreover, $\frac{s}{h_1} \approx \frac{1}{2}$ from previous considerations. This equation subject to $\frac{s}{h_1} = \frac{1}{2}$, $F_1 = 1 - \delta$ has been solved and from the solution the critical relation $F_{o\,cr}(s)$ is deduced and plotted in Fig. 4.7.

It must be pointed out that F is never equal to 1 anywhere in the flow field. The critical Froude number $F_{o\,cr}$ is just an upper bound for the existance of a proper solution. In a practical situation, it can be expected that the internal hydraulic jump would occur in such a location that the critical relation is nearly satisfied, i.e., $F_o = F_{o\,cr} - \delta$ where δ is a very small quantity.

It is interesting to note that the critical relation derived herein is very nearly the same as condition (4.30) for F_o smaller than about 0.04.

The critical relation can be checked by attempting to solve the problem with several values of F_o in the neighborhood of $F_{o\,cr}$. This was done for $s = 1, 2, 5$ and 10. The results confirm the critical relation obtained.

Thus, we have found that the solution in Zone IV (after an internal hydraulic jump) is characterized by a) h is always increasing, b) F, the local Froude number is always less than 1. Moreover, there exists a critical relation between the Froude number F_o at the beginning of Zone IV to the quantity $s = \frac{\varepsilon}{kh_o}$ where h_o is the thickness of the buoyant layer at the beginning of Zone IV. This critical relation is shown in Fig. 4.7. For a proper solution, the value of F_o must be smaller than $F_{o\,cr}(s)$.

4.2.4 Matching of Solutions

The solutions obtained in the previous section for Zones II, and IV must be matched by the conditions in Zone III to give the overall quantitative description of the phenomenon. We note that as the solution in Zone II proceeds, we have the following quantities at each step of integration: h, the jet thickness, T, the density difference, u, the velocity from which we can obtain the local Froude number F. Let the subscript 1 be applied

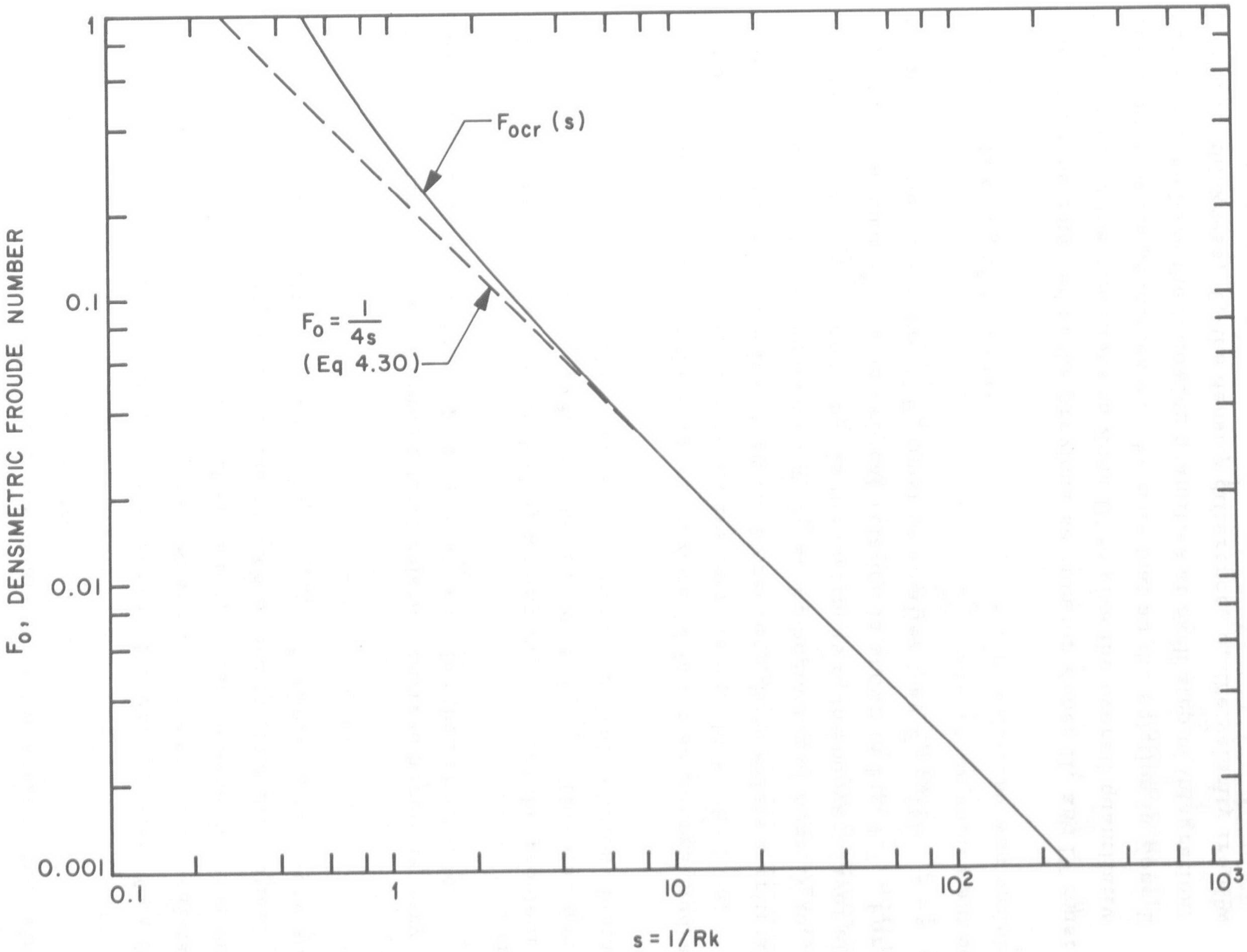

Figure 4.7 Critical relation $F_o = F_{ocr}(s)$.

to all these quantities to denote the fact that they are upstream of the internal hydraulic jump. If the jump occurred at station x_1 where the solution variables are h_1, u_1, T_1 and F_1 then from Eq. (4.23), Sec. 4.2.3, the variables just downstream of the jump would assume the values

$$h_2 = \frac{h_1}{2}\left[\sqrt{1 + 8F_1} - 1\right]$$

$$u_2 = \frac{2u_1}{\sqrt{1 + 8F_1} - 1}$$

$$F_2 = \frac{8F_1}{\left[\sqrt{1 + 8F_1} - 1\right]^3}$$

These quantities (immediately after the jump) must satisfy the critical relation (Fig. 4.7) given by

$$F_2 \le F_{o\,cr}(s)$$

where $s = \frac{\varepsilon}{kh_2}$ and $F_2 = F_o \frac{u_2^2}{T_2\ h_2}$

Note that, in general, it is expected that as x increases, h_2 decreases while F_2 increases. Thus s increases while $F_{o\,cr}$ decreases. The condition $F_2 \le F_{o\,cr}$, if satisfied at $x = x_1$, would therefore also be satisfied for $x \le x_1$. Thus the analyses given in the previous sections do not give a unique location for the internal hydraulic jump. In order to specify the location of the jump, it may be postulated that it will occur at the farthest possible location from the source. This would correspond to the smallest possible jump. However, this is only an assumption and must be verified by experiments before it can be applied to a practical problem.

It should also be pointed out that there may be no location where the condition $F_2 \le F_{o\,cr}$ is satisfied. In such a case, the implication is that

F_2 is too large or $F_{o\,cr}$ too small (or $s = \frac{\varepsilon}{kh_2}$ too large). The physical interpretation of this situation is that the jump should have occurred even before the source. In other words, the shear is too large and k too small for the available source momentum to push the jump away. One expects in this case that the source will be inundated.

The critical condition for which this occurs can be deduced if we note that this critical state corresponds to the case when the jump occurs just at the source. F_2 at the source can be obtained by the relation

$$F_2 = \frac{8F_o}{\left[\sqrt{1 + 8F_o} - 1\right]^3}$$

Thus

$$F_2 = F_{o\,cr}(s)$$

where

$$s = \frac{\varepsilon}{kh_2}$$

and

$$h_2 = h_o\left[\tfrac{1}{2}\{\sqrt{1+8F_o} - 1\}\right]$$

Thus given F_o, these relations together with the relation in Fig. 4.7 allows the determination of the critical condition for inundation. This has been done and is shown in Fig. 4.8.

At the other extreme, it is possible that the condition $F_2 < F_{o\,cr}$ is always satisfied but $F_2 = F_{o\,cr}$ is not satisfied. This would be the case when k is large compared with ε represented approximately by condition (4.11b). As was discussed in Sec. 4.2.2, in this case the local Froude number would actually increase with x. Thus F_2 would be a decreasing function of x and h_2 would be an increasing function of x. This implies s is a decreasing function of x and hence $F_{o\,cr}$ would increase with x.

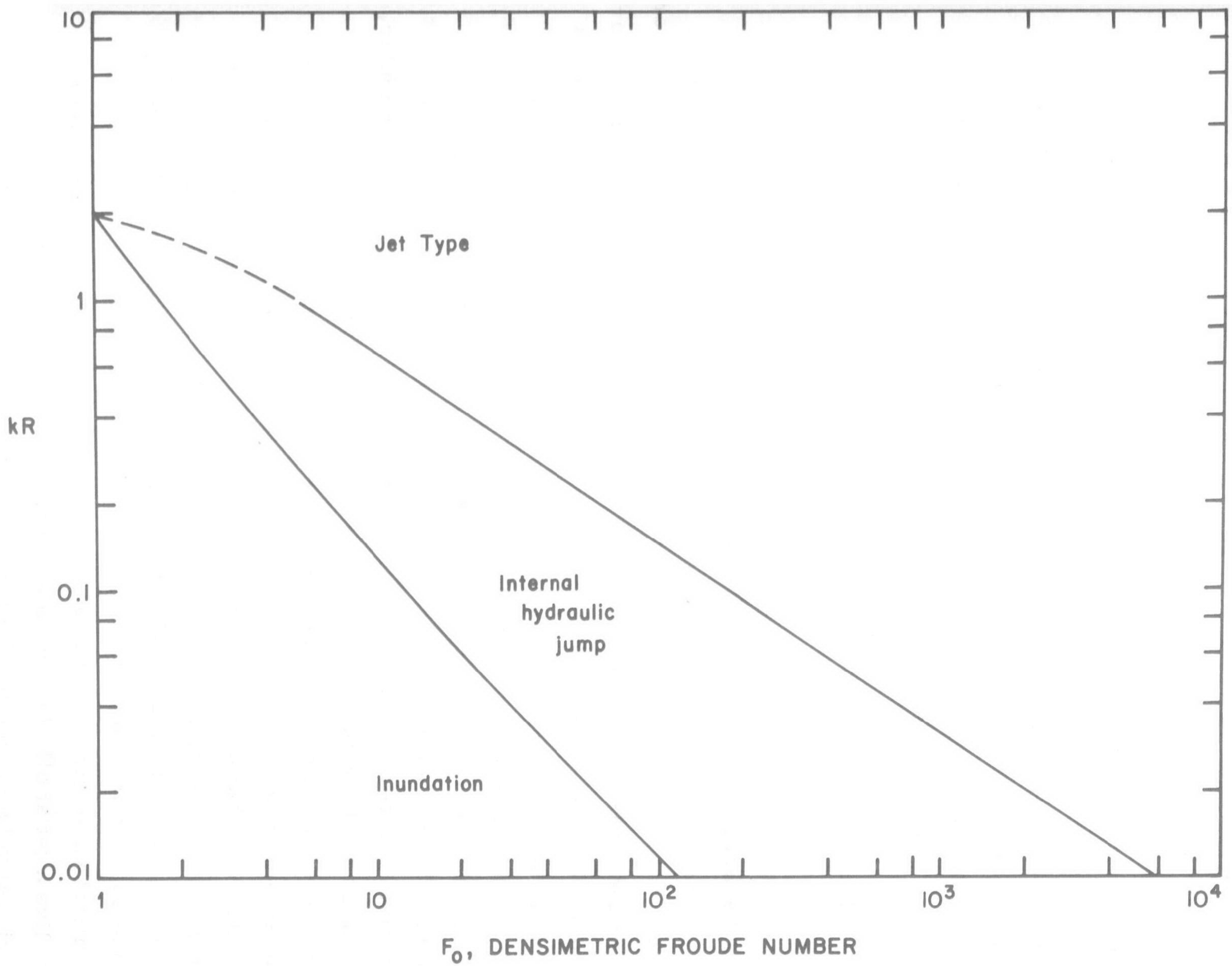

Figure 4.8 Division of parameter space into regions of different flow pattern.

Thus if $F_2 < F_{o\,cr}$ initially, it would remain so all the time for this case. Physically this case corresponds to one when an internal hydraulic jump is unnecessary. The flow is internally supercritical all the time and when F becomes large, the flow field resembles an ordinary submerged jet. However, it is envisioned that this situation would not be likely to obtain in any physical case since k is usually very small.

Condition (4.11) is also shown in Fig. 4.8. With this figure, it is now possible to determine, before hand, from just the source conditions and the environmental conditions, whether the solution is of jet type, includes an internal hydraulic jump or the source is inundated.

4.2.5 Summary and Discussion

In the previous sections, the dispersion of heat resulting from the horizontal discharge of a two-dimensional warm jet at the surface into a quiescent cooler ambient is investigated. The effects of source momentum, source buoyancy, entrainment, surface heat exchange, and interfacial shear are all included. It is found that, unlike the case of submerged buoyant jets or surface nonbuoyant jets, the source characteristics are not the only parameters governing the flow. Downstream conditions can play an important role in influencing the entire flow field possibly all the way to the source, inundating the orifice. In this investigation, the case of an infinite ambient fluid is examined and it is found that the surface heat exchange mechanism can replace the necessary downstream conditions. In particular, it is found that the relative magnitudes of the source Froude number F_o, source Reynolds number R, and the dimensionless heat exchange coefficient k play an important role not only in the detailed quantitative description of the flow field but also in determining the type of flow field. For example, referring to Fig. 4.8, it is found that for given F_o, if kR is larger than the critical value given approximately by Eq. (4.11) (topline in Fig. 4.8), then the solution is of jet type. On the other hand, if kR is smaller than the critical value given by the lower line in Fig. 4.8, then the flow field is not like a jet at all. In fact, the source is inundated. For kR between these two critical values, then the flow field consists of a jet type region near the source and a two-layered stratified flow region farther from the source with an internal hydraulic jump between these two regions.

The analysis presented herein allows the determination of the flow field given the source characteristics and the ambient heat exchange. A computer program is given in Appendix B to solve the problem numerically. First, the values k, R and F_o are determined from the given source conditions and heat exchange coefficient. Figure 4.8 should then be used to determine the type of solution to be expected. If it is found that kR is larger than the upper critical value, the program will give the solution. If it is found that an internal hydraulic jump should occur, then it is necessary to first run the program until the local Froude number becomes nearly unity. Then the output of the program is examined to determine the location where the condition

$$F_2 = F_{o\,cr}(s)$$

is just satisfied. This is then the location of the jump. The subsequent flow field may now be obtained by a second run of the program with $F_o = F_2$, $k = \frac{k}{u_2} = \frac{k}{u_1}\frac{h_2}{h_1}$, and $R = u_1 h_1 R$ where u_1, h_1, h_2 are the values of u, h and h_2 at the location of the jump according to the first solution. Finally, if it is found that kR is less than the lower critical value, then the source will be inundated. Although the flow field in this case cannot strictly be analyzed using the present technique especially near the source, still, it is possible to obtain an approximate solution using this method by requiring that inundation occurs to the extent such that h_2, the dimensional depth of inundation satisfies the condition

$$F_2 = \frac{q^2}{g\frac{T_o}{\rho_o}h^3_2} = F_{o\,cr}\left(\frac{\varepsilon}{kh_2}\right)$$

where q is the unit discharge. With this new value of $F_o = F_2$, $k = \frac{Kh_2}{q}$, $R = \frac{q}{\varepsilon}$, the program will give the solution.

It must be remarked here that the investigation described in the previous sections are based on several assumptions. For example, the shear law adopted here is given by the relation

$$\tau = \epsilon \frac{u}{h}$$

where ϵ is a constant, and cannot be justified rigorously. It seems reasonable to assume that the shear should be an increasing function of u and a decreasing function of h. The relation chosen clearly satisfies these requirements.

The region where τ may be of import is in Zone IV where it may influence the solution in such a way as to lead to either an internal hydraulic jump or inundation of the source. In Zone IV there is no entrainment so that uh = constant and thus the shear law chosen is equivalent to

$$\tau = \text{constant } u^2$$

This is equivalent to saying that the skin friction coefficient is a constant. The skin friction coefficient in pipes and channels are generally found to be a function of Reynolds number and surface roughness. Since there is no entrainment, the Reynolds number in Zone IV is constant. Thus the shear law adopted seems to be a reasonable choice.

The numerical value of ϵ to be chosen in a specific case is difficult to assess since there is little data on the subject, although there are some (e. g. Lofquist (1960)). On the other hand, there is an abundance of data on the shear coefficient in pipes and channels (e. g. , see Schlicting 1960, Chapter 20). In addition, it has been found by Keulegan (1944) that in the laminar case, the interfacial shear between two fluids for the case when the upper and lower fluids are both of infinite extent can be given by

$$\tau = 0.196 \ \rho u^2 \left(\frac{ux}{\nu} \right)^{-\frac{1}{2}}$$

where u is the relative freestream velocity between the two fluids, ρ is the density, ν the kinematic viscosity and x the distance downstream.

The corresponding shear law for the laminar boundary layer on a flat plate according to the well known solution by Blasius is

$$\tau = 0.332 \ \rho u^2 \left(\frac{ux}{\nu}\right)^{-\frac{1}{2}}$$

Thus the shear at an interface is approximately one-half that at a solid surface. Until adequate data on interfacial shear are available, it may be proposed that the shear coefficient be taken to be half the corresponding value for the case of a fluid-solid surface. If that is done, it is found that the shear coefficient is of order 10^{-3} or 10^{-2} ft^2/sec.

The surface heat exchange law chosen in this investigation is

$$H = - KT$$

The rate of heat transfer is taken to be proportional to the temperature excess above the ambient which is assumed to be at the equilibrium temperature. This is an often used approximation to a very complicated phenomenon. Typical values of the measured rate of heat exchange, for example, is Lake Hefner and Lake Colorado City indicate that K is not a constant but depends on the equilibrium temperature and wind speed. This is certainly not surprising. Typical values of K are of the order 10^{-5} ft/sec or 10^{-4} ft/sec (Edington and Geyer, 1955).

In order to obtain the quantitative description of the flow field, it is necessary not only to have the source characteristics but also the interfacial shear coefficient ϵ, the heat exchange coefficient K and the entrainment coefficient e as a function of the local Richardson number. The formulation in this chapter assumes that the coefficients ϵ, K are constants and the coefficient e(Ri) is as given by the experimental findings of Ellison and Turner (1959). As data becomes more plentiful it may be found that ϵ and K are not constants and e(Ri) is not as given by Ellison and Turner. For example, ϵ may be a function of u, h while K may be a function of T. In that case, the formulation can be readily modified to incorporate them. It is believed however, that the basic features of the findings are valid and once adequate data is established to fully define the coefficients, this model will provide a good quantitative description of the flow field.

4.3 Axisymmetric Surface Buoyant Jet

In this section, we shall investigate the axisymmetric analog of the surface buoyant jet. A schematic diagram of this phenomenon is shown in Fig. 4.9. It can be expected that since the only difference is one of geometry, the general physical nature of the phenomenon is the same as the two-dimensional case. Thus for K, the surface heat exchange coefficient large, we expect a jet type solution. For smaller K, there would be an internal hydraulic jump. For K sufficiently small, the source may be inundated. For $K = 0$, no steady state solution may exist.

The analysis to be presented in the following has not been carried out to the same detail as in the two-dimensional case. The critical relations between the parameters which divide the parameter space have not been derived for this case. These critical relations are more involved because there are now four parameters F_o, R, E and k to be defined later. Moreover, they are all independent whereas in the two-dimensional case E was absent and the parameters k and R were found to occur approximately as a group kR for small k and 1/R. Thus the parameter space for the axisymmetric case is basically four-dimensional, and the critical relations are two three-dimensional surfaces in the parameter space. These critical relations, however, can be found and should be done in the future. In the following, the governing equations will be derived and solutions will be found for some special cases.

We shall make the same basic assumptions as in the two-dimensional case. The equations of motion are then as follows:

Continuity:

$$\frac{\partial u}{\partial r} + \frac{u}{r} + \frac{\partial w}{\partial z} = 0 \qquad (4.33)$$

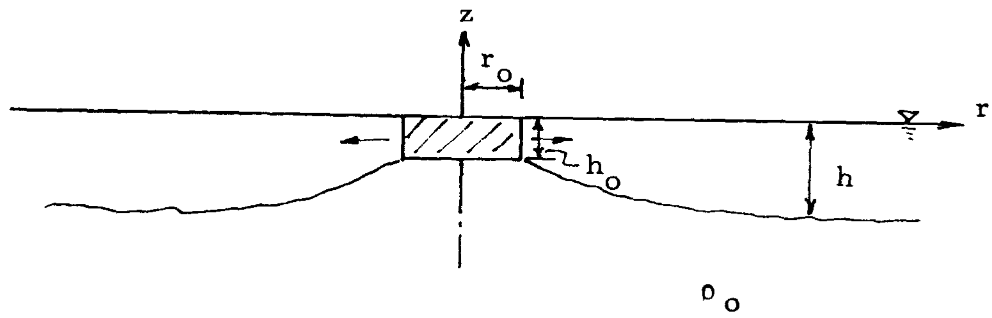

Figure 4.9 Definition sketch.

Momentum:

$$u \frac{\partial u}{\partial r} + w \frac{\partial u}{\partial z} = -\frac{1}{\rho}\frac{\partial p}{\partial r} + \frac{\partial \tau}{\partial z} \tag{4.34}$$

$$\frac{\partial p}{\partial z} = -\rho g \tag{4.35}$$

$$u\frac{\partial \rho}{\partial r} + w\frac{\partial \rho}{\partial z} = D\frac{\partial^2 \rho}{\partial z^2} \tag{4.36}$$

The assumption of similarity implies

$$u(r,z) = U(r)\, f\left(\frac{z-\eta}{h}\right) \tag{4.37}$$

$$\rho_o - \rho = T(r)\, f\left(\frac{z-\eta}{h}\right) \tag{4.38}$$

where $\eta(r)$ is the free surface profile and $h(r)$ is the characteristic depth of the spreading layer. Integration of Eq. (4.35) with respect to z from $-\infty$ to η using (4.38) gives, as in the two-dimensional case,

$$p = -\rho_o g(z-\eta) + g\, Th \int_o^{\frac{z-\eta}{h}} f(\zeta)\, d\zeta$$

so that

$$-\frac{1}{\rho_o}\frac{\partial p}{\partial r} = -g\frac{d\eta}{dr} - \frac{g}{\rho_o} Th\, f\left(\frac{z-\eta}{h}\right)\frac{\partial}{\partial r}\left(\frac{z-\eta}{h}\right) \tag{4.39}$$

We now integrate the Eqs. (4.33), (4.34) and (4.36) with respect to z from $-\infty$ to η. Equation (4.33) gives

$$\frac{1}{r}\frac{d}{dr}(Urh)\left(\int_{-\infty}^{0} f(\zeta)d\zeta\right) + w(\eta) - U\frac{d\eta}{dr} = w_{-\infty}$$

The S_f boundary condition is $\frac{d}{dt}(z-\eta) = 0$, which implies $-U\frac{d\eta}{dr} + w = 0$ on $z = \eta$. Therefore,

$$\frac{1}{r}\frac{d}{dr}(Uhr) = \frac{w_{-\infty}}{\alpha} \qquad \text{where } \alpha = \int_{-\infty}^{0} f(\zeta)\, d\zeta$$

Introducing the entrainment coefficient e, we have

$$\frac{1}{r}\frac{d}{dr}(Uhr) = \frac{e}{\alpha}U \tag{4.40}$$

Integration of Eq. (4.34) yields

$$\int_{-\infty}^{\eta}\left\{\frac{\partial}{\partial r}(u^2) + \frac{\partial}{\partial z}(wu) + \frac{u^2}{r}\right\}dz = \int_{-\infty}^{\eta}\frac{1}{\rho_o}\frac{\partial p}{\partial r}dz + \tau_S - \tau_i$$

which gives

$$\frac{1}{r}\frac{d}{dr}(U^2hr)\cdot\int_{-\infty}^{0}f^2(\zeta)d\zeta = \frac{g}{\rho_o}\frac{d}{dr}(Th^2)\cdot\int_{-\infty}^{0}\zeta f(\zeta)d\zeta + \frac{g}{2\rho_o^{\,2}}\frac{d}{dr}(T^2h^2)\left[\int_{-\infty}^{0}f(\zeta)d\zeta\right]^2$$

$$+ \tau_S - \tau_i$$

Letting

$$1/\int_{-\infty}^{0}f^2(\zeta)d\zeta = \alpha_2, \quad \frac{g}{\rho_o}\int_{-\infty}^{0}\zeta f(\zeta)d\zeta \Big/ \int_{-\infty}^{0}f^2(\zeta)d\zeta = \alpha_1,$$

we have

$$\frac{1}{r}\frac{d}{dr}(U^2hr) = \alpha_1\frac{d}{dr}(Th^2) + \alpha_2(\tau_S - \tau_i) \tag{4.41}$$

Equation (4.36) can be written

$$\frac{\partial}{\partial r}(\theta u) + \frac{\partial}{\partial z}(\theta w) + \frac{\theta u}{r} = D\frac{\partial^2\theta}{\partial z^2}$$

where $\theta = \rho_o - \rho$

Integrating with respect to z from $-\infty$ to η gives

$$\frac{d}{dr}\left\{\int_{-\infty}^{\eta}\theta u\, dz\right\} + \frac{1}{r}\int_{-\infty}^{\eta}\theta u\, dz = D\frac{\partial\theta}{\partial z}\Big|_{-\infty}^{\eta}$$

Now $D\frac{\partial\theta}{\partial z}$ at η is the surface loss which we will assume to be, as before, $-KT$. Hence

$$\frac{1}{r}\frac{d}{dr}(TUhr) = -K\alpha_2 T \tag{4.42}$$

Equations (4.40), (4.41) and (4.42) are the three equations for U, T and h and are entirely analogous to Eqs. (4.6), (4.7) and (4.8) of the last section for the two-dimensional case. It can be expected that the character of the solutions are similar. Just as in the two-dimensional case, the relative magnitudes of the parameters would influence the character of the solutions. Rather than discussing the general problem, we shall first examine some special cases. As in the two-dimensional case, we shall assume $\tau_S = 0$.

<u>Case 1) T = 0</u>

For the case when the surface jet consists of the same fluid as the ambient, then $T = 0$ and Eq. (4.42) is absent. The entrainment coefficient may be taken constant and τ_i is negligible. Then the equations are

$$\frac{d}{dr}(Uhr) = \frac{e}{\alpha}Ur$$

$$\frac{d}{dr}(U^2hr) = 0$$

It can be readily shown that

$$h = \frac{e}{\alpha}r$$

and

$$U \propto \left(\frac{u_o^2 h_o}{e}\alpha\right)^{\frac{1}{2}} \frac{1}{r}$$

Thus the jet boundary grows linearly with r while the surface velocity decreases as $1/r$.

It should be remarked that if K is very large, then this should represent an approximate solution to the problem for large r.

Case 2) Surface Plume; $e = K = 0$

We next consider the case when the initial momentum at the source is very small. This can only be the case if the velocity is very small. Let U_o be the efflux velocity, h_o be the thickness at the source radius r_o, then we are assuming

$$2\pi r_o h_o U_o = Q_o$$

$$r_o h_o U_o^2 \cong 0$$

Under the assumption that $e = 0$ and $K = 0$, the equations become

$$\frac{d}{dr}(Uhr) = 0$$

$$\frac{d}{dr}(TUhr) = 0$$

$$\frac{d}{dr}(Th^2) = \frac{\tau_i}{\alpha_1}$$

Just as in the two-dimensional case, we assume that $\tau_i = \varepsilon \frac{U}{h}$ where ε is an effective viscosity coefficient. We further take

$$f(\zeta) = \begin{cases} 0 & -\infty < \zeta < -1 \\ 1 & -1 \le \zeta \le 0 \end{cases}$$

so that $\alpha_1 = -\frac{g}{2\rho_o}$. The equations then reduce to

$$\frac{d}{dr}(Uhr) = \frac{d}{dr}(UhrT) = 0$$

$$\frac{d(Th^2)}{dr} = \frac{-2\varepsilon\rho_o}{g}\frac{U}{h}$$

With the conditions $U = U_o$, $h = h_o$, $T = T_o$ at $r = r_o$, we get

$$Uhr = U_o h_o r_o, \quad T = T_o$$

and

$$2hT_o \frac{dh}{dr} = -\frac{2\varepsilon\rho_o}{g} \frac{U_o h_o r_o}{h^2 r}$$

which integrates to

$$h = \left\{ h_o^{\,4} - \frac{\varepsilon\rho_o U_o h_o r_o}{gT_o} \ell n \frac{r}{r_o} \right\}^{\frac{1}{4}}$$

we note that at $r = r_{max} = r_o \exp \left\{ \frac{h_o^{\,4} g\, T_o}{\varepsilon\rho_o U_o h_o r_o} \right\}$, $h = 0$. Thus, this solution is at best a quasi-steady solution. If we accept this quasi-steady solution as a time dependent solution, we find that the amount of fluid contained in the spreading layer is

$$V = \int_0^{r_{max}} h 2\pi r\, dr = h_o \int_o^{r_{max}} \frac{h}{h_o} 2\pi r\, dr$$

But

$$\frac{h}{h_o} = \left(\ell n \frac{r_o}{r_{max}}\right)^{\frac{1}{4}} \left[\ell n \frac{r_{max}}{r}\right]^{\frac{1}{4}}$$

so that

$$V = 2\pi h_o r_{max}^{\;2} \left(\ell n \frac{r_o}{r_{max}}\right)^{\frac{1}{4}} \int_{\frac{r_o}{r_{max}}}^{1} \left[\ell n \left(\frac{1}{x}\right)\right]^{\frac{1}{4}} x dx$$

For $r_{max} >> r_o$,

$$V \propto h_o r_{max}^{\;2} \left(\ell n \frac{r_o}{r_{max}}\right)^{\frac{1}{4}}$$

We observe that

$$h_o = \left[\frac{\varepsilon\rho_o U_o h_o r_o}{gT_o} \ell n \frac{r_{max}}{r_o}\right]^{\frac{1}{4}}$$

As the pool spreads or as r_{max} increases the thickness h_o increases. As $r_{max} \to \infty$ so does h_o. However we note that h_o increases extremely slowly with r_{max}. For example, let

$$h_o = A\left(\log \frac{r_{max}}{r_o}\right)^{\frac{1}{4}} \quad \text{where } A = \left[\frac{2.3\ \varepsilon\rho_o U_o h_o r_o}{gT_o}\right]^{\frac{1}{4}}$$

then for

$$r_{max} = 10\ r_o,\ h_o = A$$

while for

$$r_{max} = 10^{16} r_o,\ h_o = 2A$$

If r_o is but one foot, $10^{16} r_o$ is 2×10^{12} miles which is eighty million times the circumference of the earth! Thus for all practical purposes, the thickness can be assumed constant at say 1.5A. In practice, the uncertainty in the value of the coefficient ε and the many assumptions involved in the formulation certainty justifies this replacement.

Case 3) Surface Plume, $e = 0$, $K \neq 0$

We next examine the case where $K \neq 0$. The governing equations are

$$\frac{d}{dr}(Uhr) = 0$$

$$\frac{d}{dr}(UhrT) = -KTr$$

$$\frac{d}{dr}(Th^2) = -\frac{2\varepsilon\rho_o}{g}\frac{U}{h}$$

We again let $U = U_o$, $h = h_o$, $T = T_o$ at $r = r_o$. Then the first two equations give

$$Uhr = U_o h_o r_o = Q_o$$

$$T = T_o e^{-\frac{K(r^2-1)}{2Q_o}}$$

Substituting into the third equation and assuming $e^{K/2Q_o} \approx 1$, we get

$$\frac{d}{dr}\left\{e^{-\frac{K}{2Q}r^2} h^2\right\} = -\frac{2\varepsilon\rho_o Q_o}{gT_o}\frac{1}{h^2 r}$$

Let

$$k = \frac{K}{2Q_o}, \quad \gamma = \frac{2\varepsilon\rho_o Q_o}{gT_o},$$

then $\frac{d}{dr}[e^{-kr^2}h^2] = -\gamma\frac{1}{h^2 r}$

with solution

$$h^4 = e^{2kr^2}\left\{h_o^4 e^{-2kr_o^2} - 2\gamma\int_{r_o}^{r} e^{-kr^2}\frac{dr}{r}\right\}.$$

We note that the function $I(r) \equiv \int_{r_o}^{r} e^{-kr^2}\frac{dr}{r}$ is a monotonically increasing function of r. Thus for given h_o, r_o, and k, there may be a value of r such that I is larger than $h_o^4 e^{-2kr_o^2}/2\gamma$. In that case h^4 becomes negative and the solution needs interpretation; one expects inundation to a new value of h_o.

We now note that by letting $x = (r/r_o)^2$, then

$$I = \tfrac{1}{2}\int_{kr_o^2}^{kr^2} e^{-x}\frac{dx}{x} = \tfrac{1}{2}[E_1(kr_o^2) - E_1(kr^2)]$$

As $r \to \infty$,

$$I(\infty) = \frac{1}{2}\int_{kr_o^2}^{\infty} e^{-x}\,\frac{dx}{x} = \frac{1}{2}\,E_1(kr_o^2)$$

where E_1 is the exponential integral which is tabulated.

Thus for **legitimate solution,** we need $h_o^4 e^{-2kr_o^2} \geq \gamma E_1(kr_o^2)$, i.e.,

$$h_o \geq \left[\gamma\, e^{2kr_o^2}\, E_1(kr_o^2)\right]^{\frac{1}{4}}$$

Thus for $h_o > \left[\gamma\, e^{2kr_o^2}\, E_1(kr_o^2)\right]^{\frac{1}{4}}$, we have

$$h^4 = h_o^4 e^{-2kr_o^2} - 2\gamma \int_{r_o}^{r} e^{-kr^2}\,\frac{dr}{r}\,.$$

For $h_o < \left[\gamma\, e^{2kr_o^2}\, E_1(kr_o^2)\right]^{\frac{1}{4}}$, we expect the source to be inundated to the level $\left[\gamma\, e^{2kr_o^2}\, E_1(kr_o^2)\right]^{\frac{1}{4}}$.

Case 4) Discussion of the General Case

From these special cases, it is seen that the features of the phenomenon is analogous to the two-dimensional case. Rather than considering further special cases, we shall discuss the general case. The insight gained in examining the two-dimensional case and in the special cases treated in this section will be utilized.

We recall the governing equations

$$\frac{1}{r}\,\frac{d}{dr}(Uhr) = \frac{e}{\alpha}\,U \tag{4.40}$$

$$\frac{1}{r}\frac{d}{dr}(U^2hr) = \alpha_1\frac{d}{dr}(Th^2) - \alpha_2(\tau_i) \tag{4.41}$$

$$\frac{1}{r}\frac{d}{dr}(TUhr) = -K\alpha_2 T \tag{4.42}$$

Let the conditions at the source be: at $r = r_o$, $U = U_o$, $h = h_o$, $T = T_o$. We now normalize the variables by these characteristic values. Thus define $u^* = U/U_o$; $T^* = T/T_o$; $h^* = h/h_o$; $r^* = r/r_o$. We get, dropping $*$'s,

$$\frac{1}{r}\frac{d}{dr}(uhr) = Eu \tag{4.43}$$

$$\frac{1}{r}\frac{d}{dr}(u^2hr) = -\frac{1}{F_o}\frac{d}{dr}(Th^2) - \frac{1}{R}\frac{u}{h} \tag{4.44}$$

$$\frac{1}{r}\frac{d}{dr}(Tuhr) = -kT \tag{4.45}$$

where

$$E = \frac{er_o}{h_o\alpha}, \quad F_o = \frac{-U_o^2}{\alpha_1 T_o h_o}, \quad R = \frac{U_o h_o^2}{\epsilon\alpha_2 r_o}, \quad k = \frac{K\alpha_2 r_o}{U_o h_o}$$

Thus the system depends on four parameters E, F_o, R, and k. The parameter space is therefore four-dimensional. The critical relations delineating the type of flow field are therefore three-dimensional surfaces in the four-dimensional space.

The critical relations would divide the parameter space into three regions such that given all other quantities, there are two critical values of k, k_{cr+} and k_{cr-}. For $k > k_{cr+}$, a continuous solution may be expected. This solution would become, for large r, nearly the same as the one discussed in Case 1. For $k < k_{cr-}$, one expects the source to be inundated and the solution should resemble that discussed in Case 3. For k between these critical values, a circular hydraulic jump would be encountered. The detailed solutions would be more complicated than the two-dimensional case because the location of the jump is not only influenced by the four parameters but also by the radial coordinate r.

It should be pointed out that although the assumptions made in deriving these equations in the axisymmetric case, are basically the same as in the two-dimensional case, there is a lack of experimental data on the entrainment and shear coefficients. In the two-dimensional case, there has at least been some experiments. Thus any results obtained herein must be viewed with great caution. The system of equations 4. 43 through 4. 45 can be solved numerically for $k > k_{cr+}$. Some example solutions are presented in Figures 4. 10 and 4. 11.

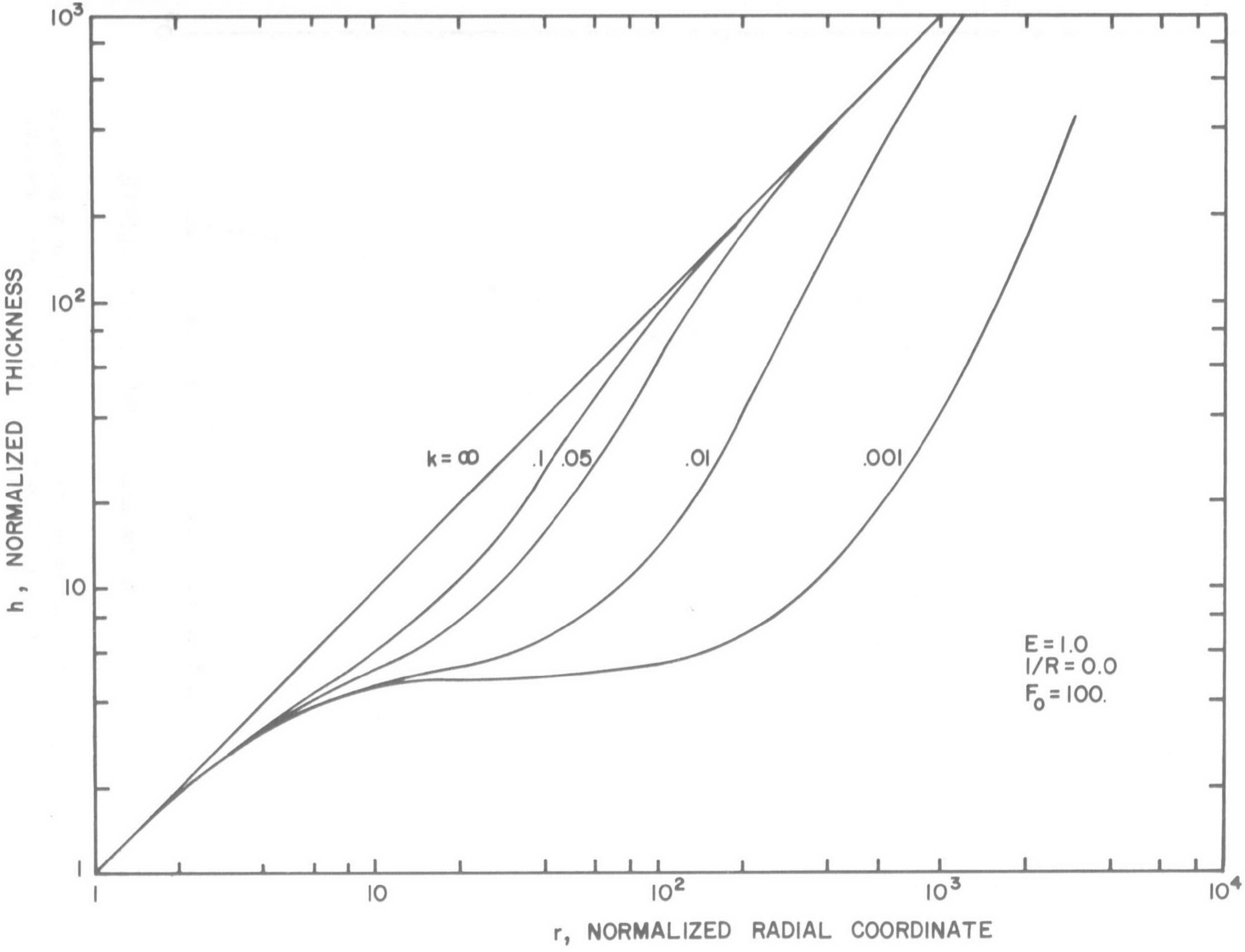

Figure 4.10 Predicted jet thickness in a surface horizontal buoyant jet (axisymmetric case).

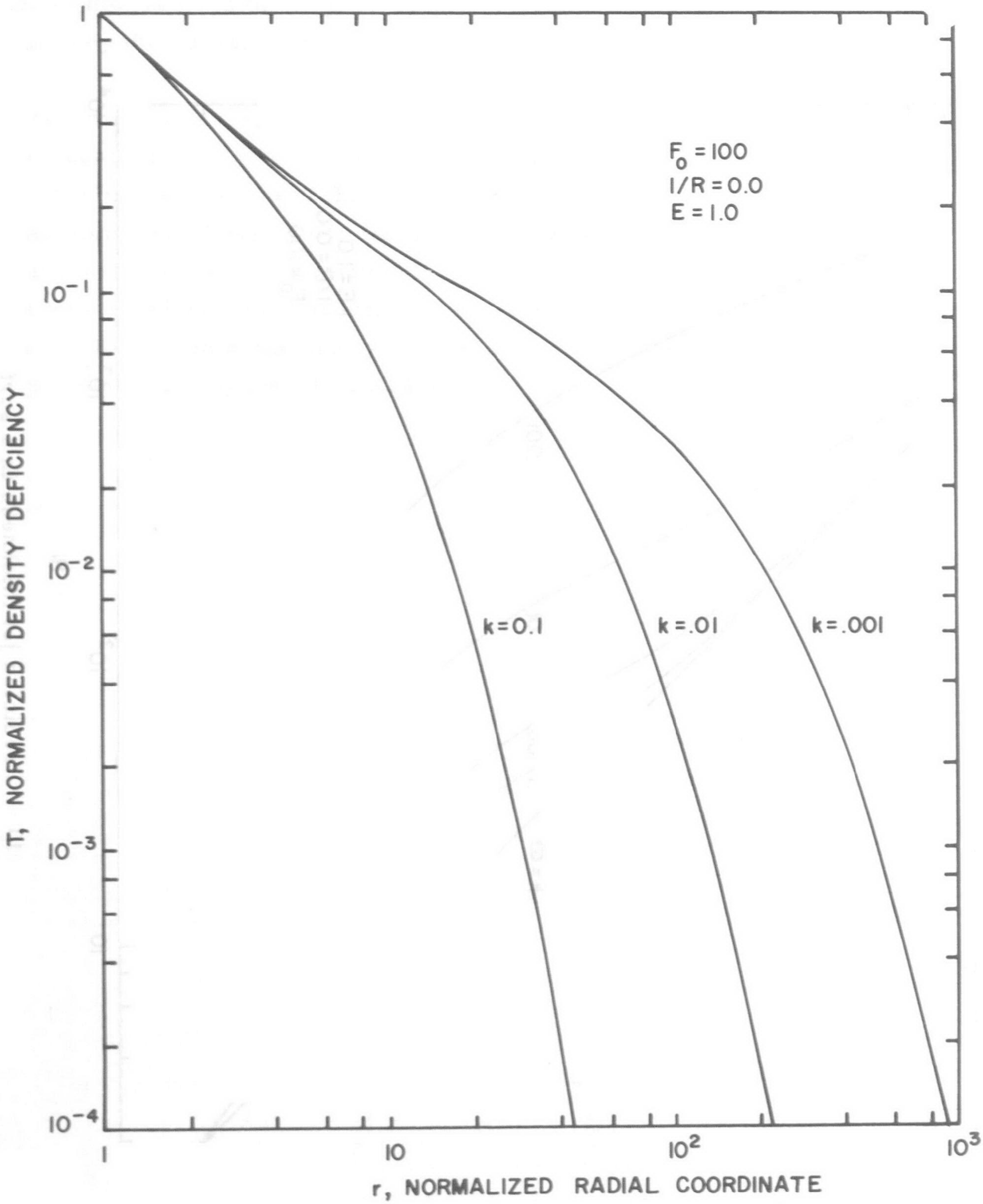

Figure 4.11 Predicted jet density deficiency in a surface horizontal buoyant jet (axisymmetric case).

4.4 Example Applications

We conclude this chapter by presenting some examples on the two-dimensional problem.

Example 1

Given
$$h_o = 1 \text{ ft.}$$
$$U_o = 10^{-1} \text{ ft/sec.}$$
$$g\frac{T_o}{\rho_o} = 10^{-3} \text{ ft/sec}^2$$
$$\varepsilon = 10^{-3} \text{ ft}^2/\text{sec}$$
$$K = 10^{-3} \text{ ft/sec}$$

hence,

$$F_o = \frac{U_o^{\,2}}{g\,T_o h_o} = 10, \qquad k = \frac{K}{U_o} = 10^{-2}, \qquad 1/R = \frac{\varepsilon}{U_o h_o} = 10^{-2}$$

Thus $kR = 1$. Examination of Fig. 4.8 shows that we are in the region of parameter space where the solution is of jet type. Thus the program SBJ2 would simply give the solution with input $F_o = 10$, $k = 10^{-2}$, $1/R = 10^{-2}$, $e_o = 0.075$. This particular solution was obtained and the quantity h/h_o is shown plotted in Fig. 4.5b.

Example 2

Given
$$h_o = 10 \text{ ft.}$$
$$U_o = 0.1 \text{ ft/sec}$$
$$g\frac{T_o}{\rho_o} = 10^{-4} \text{ ft/sec}^2$$
$$\varepsilon = 10^{-3} \text{ ft}^2/\text{sec}$$
$$K = 10^{-5} \text{ ft/sec}$$

then,

$$k = \frac{K}{U_o} = 10^{-4}, \qquad \frac{1}{R} = \frac{\varepsilon}{U_o h_o} = 10^{-3}, \qquad F_o = \frac{U_o^2}{\frac{T_o}{g \frac{}{\rho_o} h_o}} = 10$$

Thus $kR = 10^{-1}$. From Fig. 4.8, we expect inundation. The inundation would occur until a depth h_2, such that the following condition is just satisfied.

$$\frac{(U_o h_o)^2}{(g \frac{T_o}{\rho_o}) h_2^3} < F_{ocr} \left(\frac{\varepsilon}{K h_2} \right)$$

Thus

$$F_2 = \frac{1}{10^{-4} h_2^3} < F_{ocr} \left(\frac{10^{-3}}{10^{-5} h_2} \right)$$

$$F_2 = \frac{10^4}{h_2^3} < F_{ocr} \left(\frac{100}{h_2} \right)$$

The following table may be readily constructed:

h_2	$F_2 = 10^4/h_2^3$	$s = 100/h_2$
30	0.37	3.33
40	0.156	2.5
50	0.08	2
45	0.110	2.22
44	0.118	2.27

Comparing the values of F_2 and s with those on Fig. 4.7 reveals that h_2 should be 44 ft. Thus the source will be inundated to a depth of 44 ft.
To obtain the characteristics of the flow field and temperature distribution, we simply use the program SBJ2 with $F_0 = 0.118$, $k = \frac{Kh_2}{h_o U_o} = 4.4 \times 10^{-4}$,

and $1/R = \frac{\varepsilon}{q} = 10^{-3}$.

Example 3

Given $h_o = 10$ ft

$U_o = 0.1$ ft/sec

$$g\frac{T_o}{\rho_o} = 10^{-4} \text{ ft/sec}^2$$

$\varepsilon = 10^{-3}$ ft^2/sec

$K = 2 \times 10^{-5}$ ft/sec

This case differs from example 2 only in that the value of K is doubled. We first calculate

$$F_o = \frac{U_o^{\ 2}}{g\frac{T_o}{\rho_o} h_o} = 10, \quad k = \frac{K}{U_o} = 2\times10^{-4}, \quad 1/R = \frac{\varepsilon}{U_o h_o} = 10^{-3}$$

Thus $kR = 0.2$. Referring to Fig. 4.8, we see that an internal hydraulic jump would develop. The program SBJ2 is thus first used with $F_o = 10$, $k = 2 \times 10^{-4}$, and $1/R = 10^{-3}$. Portions of the output is tabulated as follows. Also the quantity $s = \frac{\varepsilon}{Kh_2}$ is calculated and inserted as the last column.

x/h_o	h_2/h_o	F_2	s
1.0	4.03	0.175	1.24
6.0	4.08	0.262	1.22
7.0	4.07	0.278	1.23
8.0	4.07	0.294	1.23

The values of F_2 and s when referred to Fig. 4.7 shows that the jump would occur at about $x/h_o = 7$ or about 70 feet from the source. At that point, the excess temperature is about 80% of that at the source and the flow rate about 25% more than that at the source. Thus we deduce that after the jump, $F_2 \cong 0.278$, $h_2 = 41$ ft, $U_2 = \frac{1.25}{41} \cong 0.03$ ft/sec. To obtain the flow field after the jump, we may use SBJ2 again with $F_o = 0.278$, $k \approx \frac{2 \times 10^{-5}}{0.03} \approx 6.7 \times 10^{-4}$, $1/R = \frac{10^{-3}}{1.25} = 8 \times 10^{-4}$ where now the output quantities are normalized to the values just after the jump and x is now measured from the jump location.

CHAPTER 5 PASSIVE TURBULENT DIFFUSION FROM A CONTINUOUS SOURCE IN A STEADY SHEAR CURRENT OR AN UNSTEADY UNIFORM CURRENT WITH UNSTEADY SURFACE EXCHANGE

5.1 Introduction

The mixing process undergone by the cooling water discharged from a power plant can be divided into three stages, as discussed in Chapter 3. In the case when the discharge is from a submerged outfall, these three stages are (Fig. 5.1):

1. An initial mixing stage governed by the momentum and buoyancy of the discharge.
2. An intermediate stage of dynamic spreading governed by the buoyancy and the density stratification.
3. A final stage of essentially passive turbulent diffusion.

In this chapter we shall treat the third stage of passive turbulent dispersion when the dilution and dispersion are primarily governed by ambient turbulence and currents. This phenomenon is very similar to the case of the mixing of sewage effluent from a submerged ocean outfall.

Two mathematical models will be established in this chapter for the calculation of the distribution of excess temperature (or dilution of the effluent) due to the effects of ambient turbulence and current, and surface heat exchange. The first model is for the case of the steady state passive turbulent diffusion from a continuous source in a steady shear current as shown in Fig. 5.2a. The second model is for an unsteady case where the current and surface exchange coefficients are time-varying as shown in Fig. 5.2b. However, in the second model the current is taken to be uniform with depth.

Note that the location of the source can be below the water surface such as in the case of an effluent field trapped by ambient density stratification.

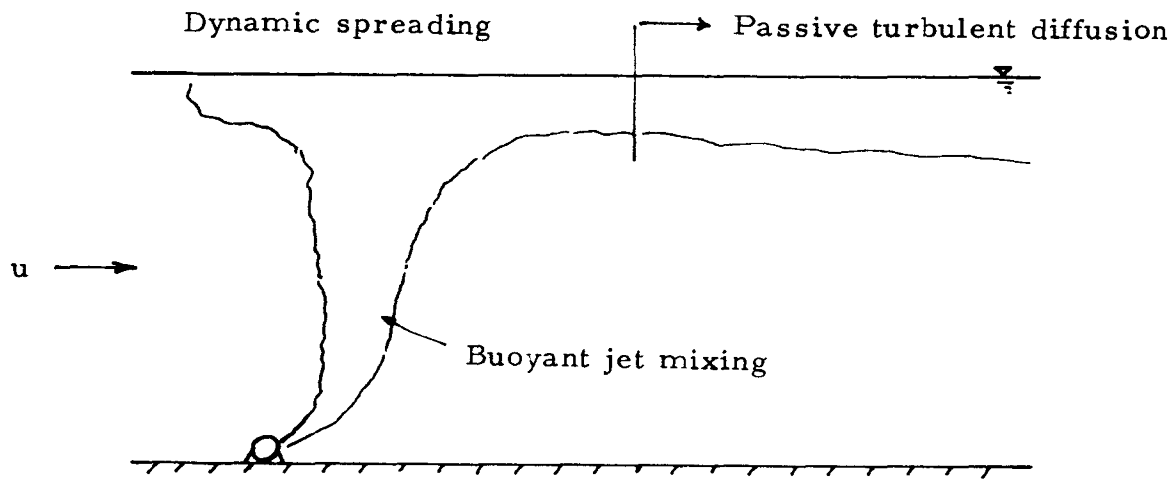

a) Effluent field established at water surface.

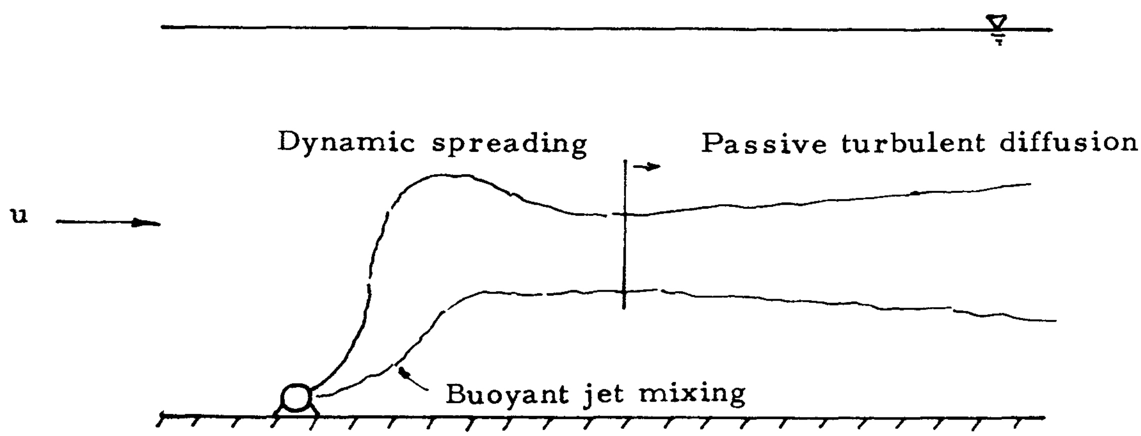

b) Effluent field trapped below water surface .

Figure 5.1 Various stages of mixing of submerged cooling water discharges. Effluent field established at water surface.

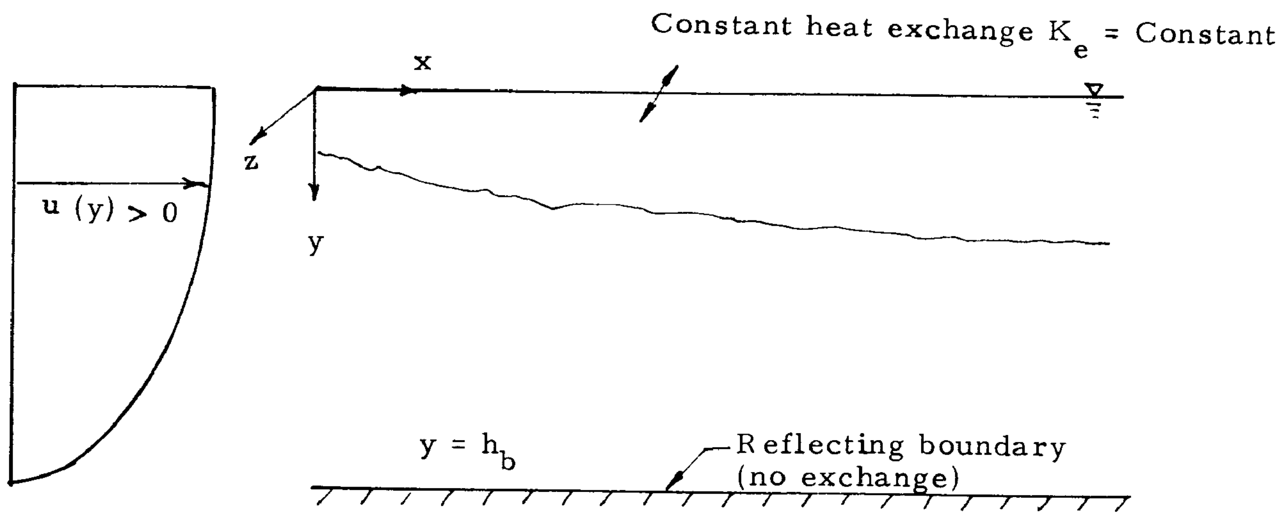

a) A steady continuous source in a steady shear current with constant surface heat exchange.

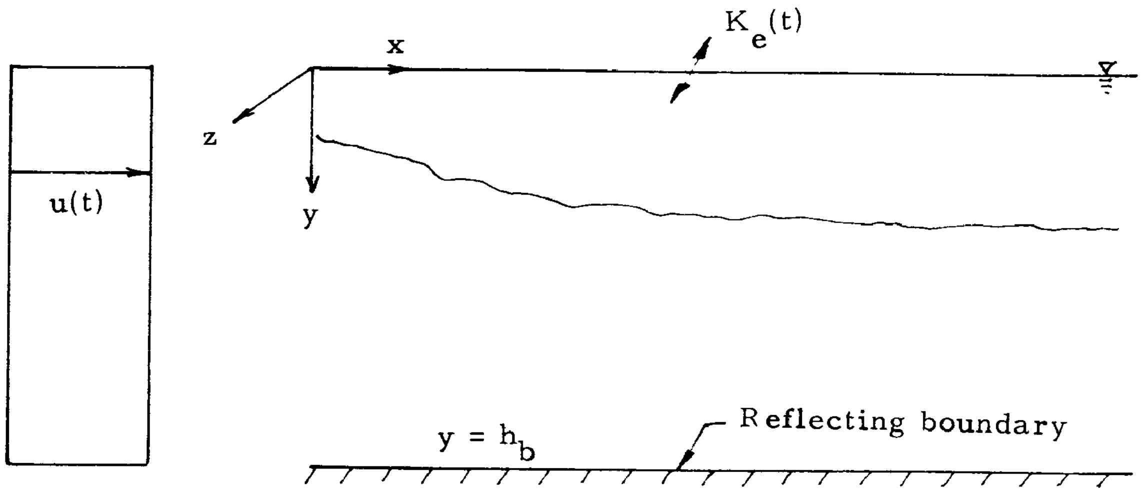

b) An unsteady continuous source in a uniform unsteady current with time varying surface heat exchange .

Figure 5. 2 Passive turbulent diffusion cases studied.

If this is the case then the excess temperature over the ambient will be practically zero unless there is salinity difference. Since the models to be developed are applicable not only to the prediction of excess temperature distribution, but also to other water quality indicators, the case of submerged source is also of practical interest.

5.2 Derivation of Basic Equations

The basic relation governing turbulent passive diffusion is a conservation equation for the diffusant: either heat content or a tracer concentration. The mixing is assumed to be completely dominated by the ambient current and turbulence characteristics. Thus, before the problem can be solved, the environmental conditions must be known.

The models to be developed in this chapter are equally applicable to the dispersion of heat or any other tracer (such as the concentration of coliform bacteria). However, there are some differences and therefore they will be discussed separately.

5.2.1 The Problem for Excess Heat

The equation of conservation of heat content without internal heat source is:

$$\frac{\partial H_t}{\partial t} + u\frac{\partial H_t}{\partial x} + v\frac{\partial H_t}{\partial y} + w\frac{\partial H_t}{\partial z}$$

$$= \frac{\partial}{\partial x}(K_x \frac{\partial H_t}{\partial x}) + \frac{\partial}{\partial y}(K_y \frac{\partial H_t}{\partial y}) + \frac{\partial}{\partial z}(K_z \frac{\partial H_t}{\partial z}) \qquad (5.1)$$

where H_t = the total heat content above a given reference heat content;

t = time;

x, y, z = coordinates in longitudinal, vertical and transverse directions (see Fig. 5.2);

u, v, w = velocities in (x, y, z) directions;

K_x, K_y, K_z = exchange coefficients (eddy diffusivity plus molecular diffusivity) in (x, y, z) directions.

In a natural body of water, the vertical velocity v is usually small (except near zones of strong upwelling and sinking flow). In this model, v is taken to be zero. In addition, it is a reasonable assumption that the flow is predominantly in one direction, say x. Thus w is taken to be zero. Equation (5.1) then becomes

$$\frac{\partial H_t}{\partial t} + u\frac{\partial H_t}{\partial x} = \frac{\partial}{\partial x}(K_x \frac{\partial H_t}{\partial x}) + \frac{\partial}{\partial y}(K_y \frac{\partial H_t}{\partial y}) + \frac{\partial}{\partial z}(K_z \frac{\partial H_t}{\partial z}) \qquad (5.2)$$

The mechanism for surface heat exchange can be expressed as (Edinger and Geyer, 1965)

$$- K_y \frac{\partial H_t}{\partial y} = - K_E(T_p - E) \qquad (5.3)$$

at $y = 0$, i.e., the water surface; where

K_E = surface heat exchange coefficient;
T_p = surface water temperature;
E = equilibrium temperature.

At the bottom, the exchange of heat may be taken to be zero, i.e.,

$$K_y \frac{\partial H_t}{\partial y} = 0 \qquad (5.4)$$

at $y = h_b$, i.e., the bottom.

The equation governing heat exchange processes in the ambient without any waste heat addition is simply:

$$\frac{\partial H_a}{\partial t} + u\frac{\partial H_a}{\partial x} = \frac{\partial}{\partial y}(K_y \frac{\partial H_a}{\partial y}) \qquad (5.5)$$

where H_a = heat content of the ambient water.

Note that in Eq. (5.5) inhomogeneities in the horizontal directions are neglected. In general this is a good approximation for a body of water which is not too vast. The boundary conditions at the surface and bottom are similar to Eqs. (5.3) and (5.4), i.e.,

$$K_y \frac{\partial H_a}{\partial y} = K_E(T_a - E) \qquad \text{at } y = 0 \tag{5.6}$$

and

$$K_y \frac{\partial H_a}{\partial y} = 0 \qquad \text{at } y = h_b \tag{5.7}$$

where T_a is the surface temperature of ambient water.

To obtain the relation for excess heat distribution, we simply subtract Eq. (5.5) from (5.2) to obtain

$$\frac{\partial H}{\partial t} + u\frac{\partial H}{\partial x} = \frac{\partial}{\partial x}(K_x \frac{\partial H}{\partial x}) + \frac{\partial}{\partial y}(K_y \frac{\partial H}{\partial y}) + \frac{\partial}{\partial z}(K_z \frac{\partial H}{\partial z}) \tag{5.8}$$

where $H = H_t - H_a$ is the excess heat content due to waste heat addition. The surface and bottom boundary conditions are then:

$$K_y \frac{\partial H}{\partial y} = K_E(T_p - T_a) \qquad \text{at } y = 0 \tag{5.9}$$

and

$$K_y \frac{\partial H}{\partial y} = 0 \qquad \text{at } y = h_b \tag{5.10}$$

Note that K_E and E are assumed to be the same in Eqs. (5.3) and (5.6). For the temperature range encountered in the passive turbulent diffusion stage, this is believed to be an adequate assumption.

Defining the excess temperature to be T, and assuming a constant specific heat C_h over the temperature range of interest, Eqs. (5.8) to (5.10) become :

$$\frac{\partial T}{\partial t} + u\frac{\partial T}{\partial x} = \frac{\partial}{\partial x}(K_x \frac{\partial T}{\partial x}) + \frac{\partial}{\partial y}(K_y \frac{\partial T}{\partial y}) + \frac{\partial}{\partial z}(K_z \frac{\partial T}{\partial z}) \tag{5.11}$$

$$K_y \frac{\partial T}{\partial y} = \frac{K_E}{\rho C_h} T = K_e T \qquad \text{at } y = 0 \tag{5.12}$$

and

$$K_y \frac{\partial T}{\partial y} = 0 \qquad \text{at } y = h_b \tag{5.13}$$

where $K_e = K_E/(\rho\, C_h)$

ρ = density of water

5.2.2 The Problem for a Tracer

We now consider the corresponding problem where the dispersing substance is a tracer which is otherwise not present in the ambient water. The conservation relation is:

$$\frac{\partial c}{\partial t} + u\frac{\partial c}{\partial x} + v\frac{\partial c}{\partial y} + w\frac{\partial c}{\partial z} = \frac{\partial}{\partial x}(K_x\frac{\partial c}{\partial x}) + \frac{\partial}{\partial y}(K_y\frac{\partial c}{\partial y}) + \frac{\partial}{\partial z}(K_z\frac{\partial c}{\partial z}) - K_d c \tag{5.14}$$

where c = the concentration of the tracer

K_d = the decay coefficient of the tracer or the die-off rate. (Clearly, $K_d = 0$ for conservative tracers such as dye.)

Again, we assume $v = w = 0$. Equation (5.14) becomes

$$\frac{\partial c}{\partial t} + u\frac{\partial c}{\partial x} = \frac{\partial}{\partial x}(K_x\frac{\partial c}{\partial x}) + \frac{\partial}{\partial y}(K_y\frac{\partial c}{\partial y}) + \frac{\partial}{\partial z}(K_z\frac{\partial c}{\partial z}) - K_d c \tag{5.15}$$

For tracers, such as dye, salt or radioactivity, there is no surface or bottom exchange; hence

$$\frac{\partial c}{\partial y} = 0 \qquad \text{at } y = 0 \text{ and } y = h_b \tag{5.16}$$

The basic equations and boundary conditions are very similar between the cases for excess heat and for a tracer. In fact, both problems can be included in a single more general mathematical model. This is discussed in the next section.

5.2.3 The General Problem

The general equation governing either excess temperature or a tracer substance (based upon Eqs. (5.11) and (5.15)) can be written

$$\frac{\partial c}{\partial t} + u\frac{\partial c}{\partial x} = \frac{\partial}{\partial x}(K_x\frac{\partial c}{\partial x}) + \frac{\partial}{\partial y}(K_y\frac{\partial c}{\partial y}) + \frac{\partial}{\partial z}(K_z\frac{\partial c}{\partial z}) - K_d c \qquad (5.17)$$

The general boundary conditions can be written

$$K_y\frac{\partial c}{\partial y} = K_e c \qquad \text{at } y = 0$$

$$\frac{\partial c}{\partial y} = 0 \qquad \text{at } y = h_b \qquad (5.18)$$

In these equations, c is either the excess temperature or the tracer concentration. For a tracer without surface exchange, then $K_e = 0$; while for the case of excess temperature or a non-decaying tracer $K_d = 0$.

Note that the problem is not yet posed completely. To fully define the problem, the initial condition, and the source condition must be specified along with the environmental characteristics such as u, K_x, K_y and K_z. These will be discussed as we treat the two models separately in the following sections.

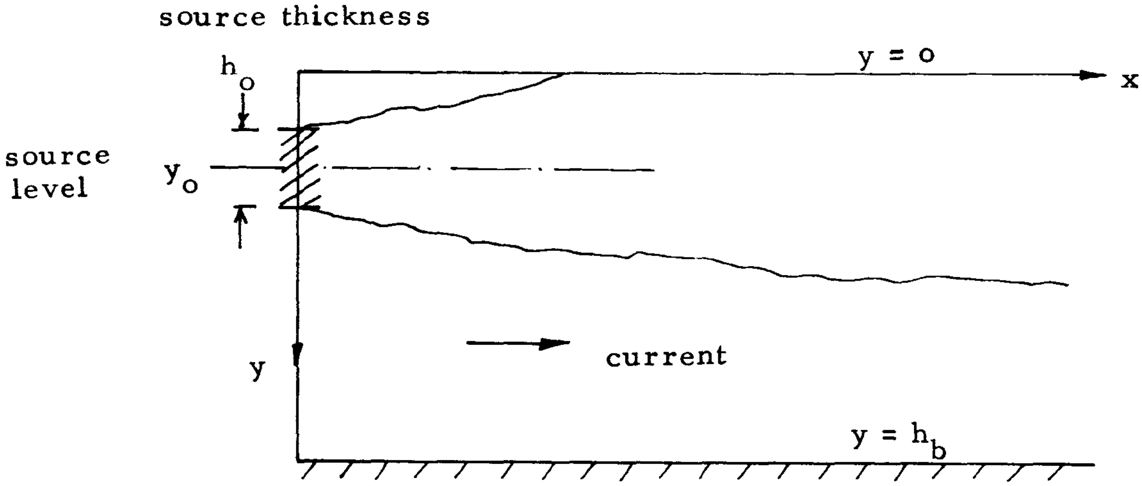

Elevation

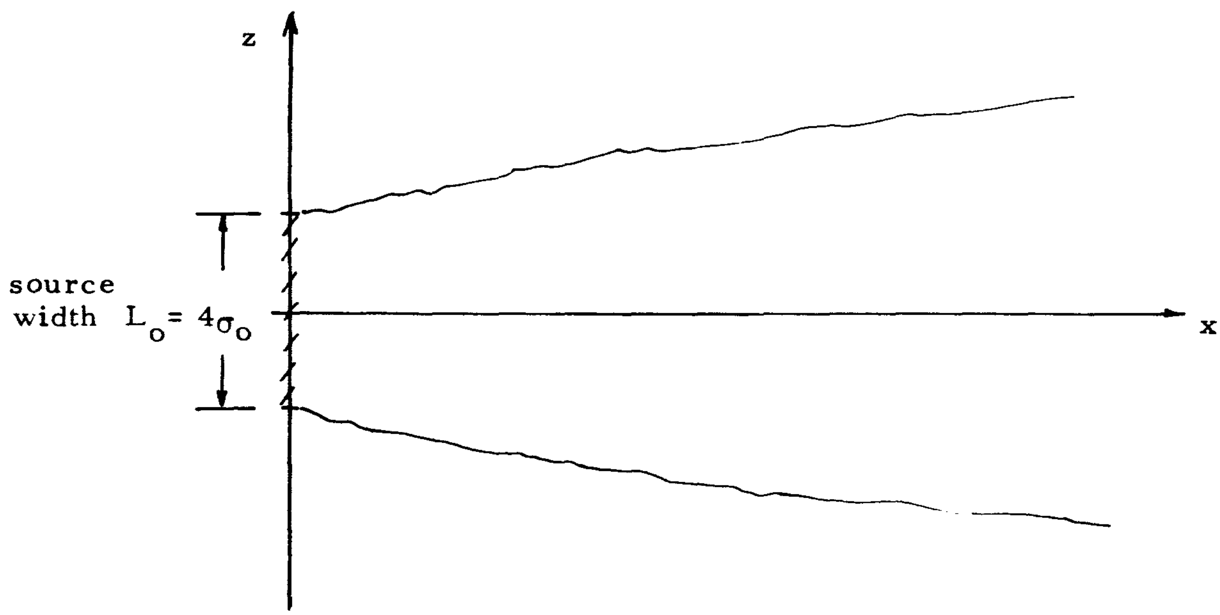

Plan

Figure 5.3 Flow configurations in cases with steady releases.

a) Submerged release.

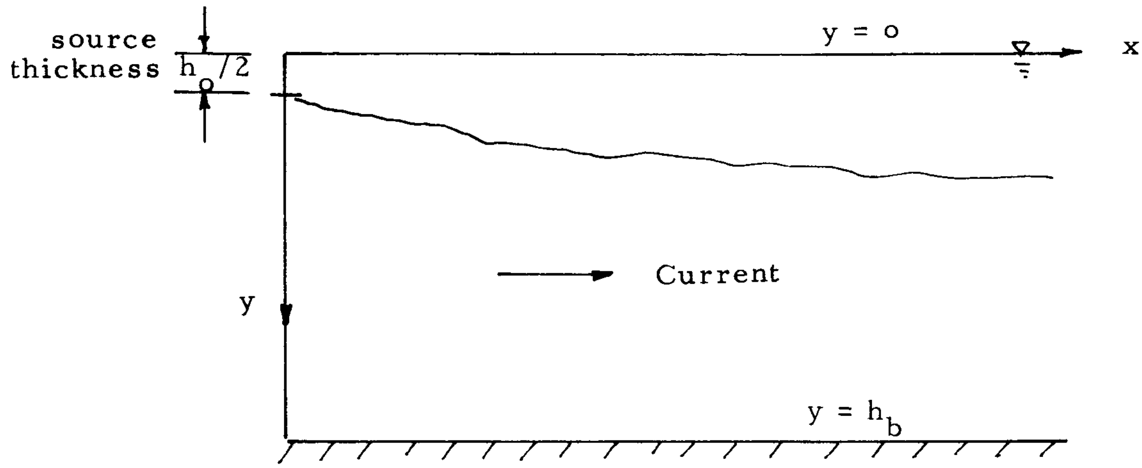

Elevation

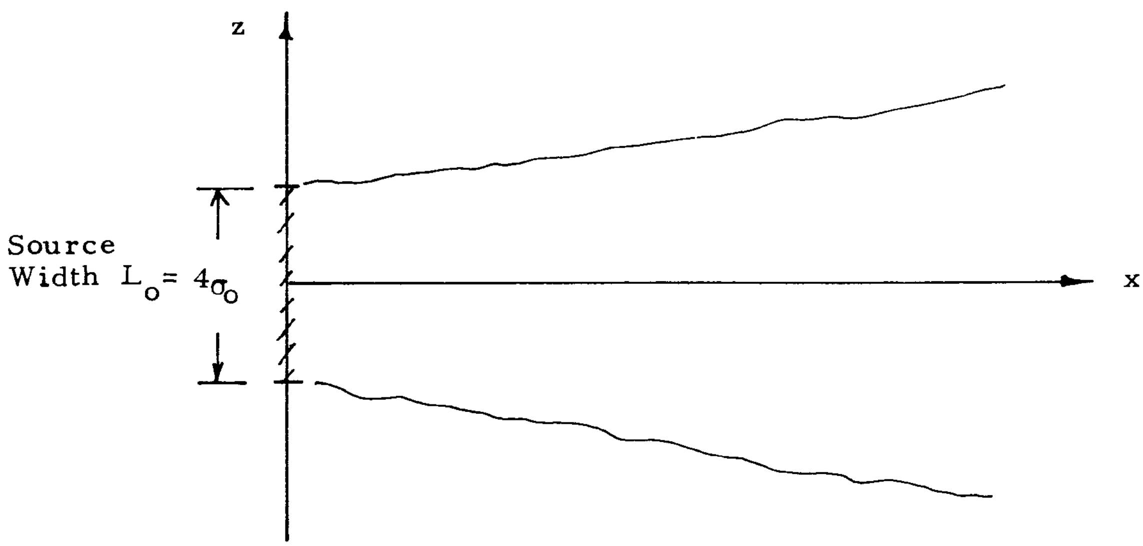

Plan

Figure 5. 3 Flow configurations in cases with steady releases.

b) Surface release.

5.3 Steady Release in a Steady Environment

5.3.1 Formulation

For the case of steady release of waste heat or a tracer substance into a steady environment, the governing equation (5.17) becomes:

$$u\frac{\partial c}{\partial x} = \frac{\partial}{\partial x}(K_x\frac{\partial c}{\partial x}) + \frac{\partial}{\partial y}(K_y\frac{\partial c}{\partial y}) + \frac{\partial}{\partial z}(K_z\frac{\partial c}{\partial z}) - K_d c \qquad (5.19)$$

In general, the term representing the longitudinal transport $\frac{\partial}{\partial x}(K_x\frac{\partial c}{\partial x})$ is small in comparison with the transverse transport term $\frac{\partial}{\partial z}(K_z\frac{\partial c}{\partial z})$. Thus the longitudinal transport is neglected. Equation (5.19) can then be written as:

$$u\frac{\partial c}{\partial x} = \frac{\partial}{\partial y}(K_y\frac{\partial c}{\partial y}) + \frac{\partial}{\partial z}(K_z\frac{\partial c}{\partial z}) - K_d c \qquad (5.20)$$

The boundary conditions are of course, still given by Eq. (5.18).

5.3.1.1 Source Conditions

The source will be taken to be located at $x = 0$, at a depth $y = y_o$ with thickness h_o and width L_o as shown in Fig. 5.3a. For the case of surface release, $y = y_o = 0$ and the thickness is $h_o/2$ as shown in Fig. 5.3b. The distribution of c at the source is taken to be:

$$c(o, y, z) = c_{max}(o, y_o) \exp\left\{ - \frac{z^2}{\sigma_o^2\left[1 - \left\{\frac{2(y-y_o)}{h_o}\right\}^2\right]^{\frac{1}{2}}} \right\} \qquad (5.21)$$

where $c_{max}(o, y_o) = c(o, y_o, o)$ (Note: $c_{max}(x, y) = c(x, y, o)$.)

Equation (5.21) defines the source distribution to be Gaussian in the z-direction, and resembles an ellipse in the y-direction. This is the assumed distribution used in the examples in developing the model. The actual distribution, if known, should replace Eq. (5.21) in a practical application.

5.3.1.2 Environmental Characteristics

The environmental conditions relevant to the passive turbulent diffusion phase as formulated above include the ambient turbulence characteristics, represented by values of the eddy diffusivities K_z and K_y; the ambient current structure, represented by u(y); and the surface exchange coefficient K_E. The current is a directly measurable quantity. Given the general locale of the discharge, field data on u(y) can be gathered and used in the prediction model. The other quantities, namely K_z, K_y and K_E are more difficult to measure. In general, no direct measurements are made and the values are usually inferred from other observable phenomena.

It is not the intention of this study to develop a detailed method of estimating K_E accurately. Studies on the heat transfer between the water environment and the atmosphere have been initiated and are being extended by other investigators. Strictly speaking consideration of the heat exchange processes at the water surface is very complicated. Factors which are of importance include solar radiation, back radiation, conduction, convection and evaporation. The introduction of the coefficient K_E and the equilibrium temperature (see Edinger and Geyer, 1965), lumps the effects of all these mechanisms of heat transfer together. At present, this appears to be the most practical method available. As better relations become available, it should be possible to modify the models developed accordingly.

The eddy diffusivities K_z (horizontal) and K_y (vertical) are important in determining the dispersion of the heated effluent. Like the coefficient K_E, these diffusivities are also empirical coefficients which depend on more basic phenomena such as the turbulence structure in the fluid medium. In turn, it can be expected that the turbulence structure depends on the input of energy from the atmosphere through wind and waves, the density stratification or stability of the fluid medium and the current shear which can supply the energy in generating turbulence. These diffusivities will now be briefly discussed in the following subsections.

5.3.1.2a Horizontal Diffusion Coefficient K_z

In a large body of water, the horizontal diffusion coefficients are generally governed by the "4/3 power law", i.e., the horizontal diffusion coefficient is proportional to the 4/3 power of the length scale of the diffusing patch or plume:

$$K_z = A_L L^{4/3} \tag{5.22}$$

where A_L is a dissipation parameter ($cm^{2/3}$/sec or $ft^{2/3}$/sec.)
L is the width of the plume (usually taken to be $4\sigma_z$, σ_z being the standard deviation of the concentration distribution).

Equation (5.22) can be written in terms of σ_z

$$K_z = A \sigma_z^{4/3} \tag{5.23}$$

It should be noted that use of Eq. (5.23) results in a nonlinear governing equation.

In the ocean, numerous field experiments have been performed to estimate K_z. This is summarized in Fig. 5.4. It is seen that the value of A_L is in the neighborhood of 10^{-2} - 10^{-4} $ft^{2/3}$/sec. Thus the value of A is in the neighborhood of 10^{-3} - 6×10^{-2} $ft^{2/3}$/sec.

It should be pointed out that no effect of shear currents were removed in the field experiments so that direct use of the data requires some caution. It is believed that since the effects of shear is explicitly taken into account in the present model, the lower value of $A = 10^{-3}$ $ft^{2/3}$/sec might be more appropriate.

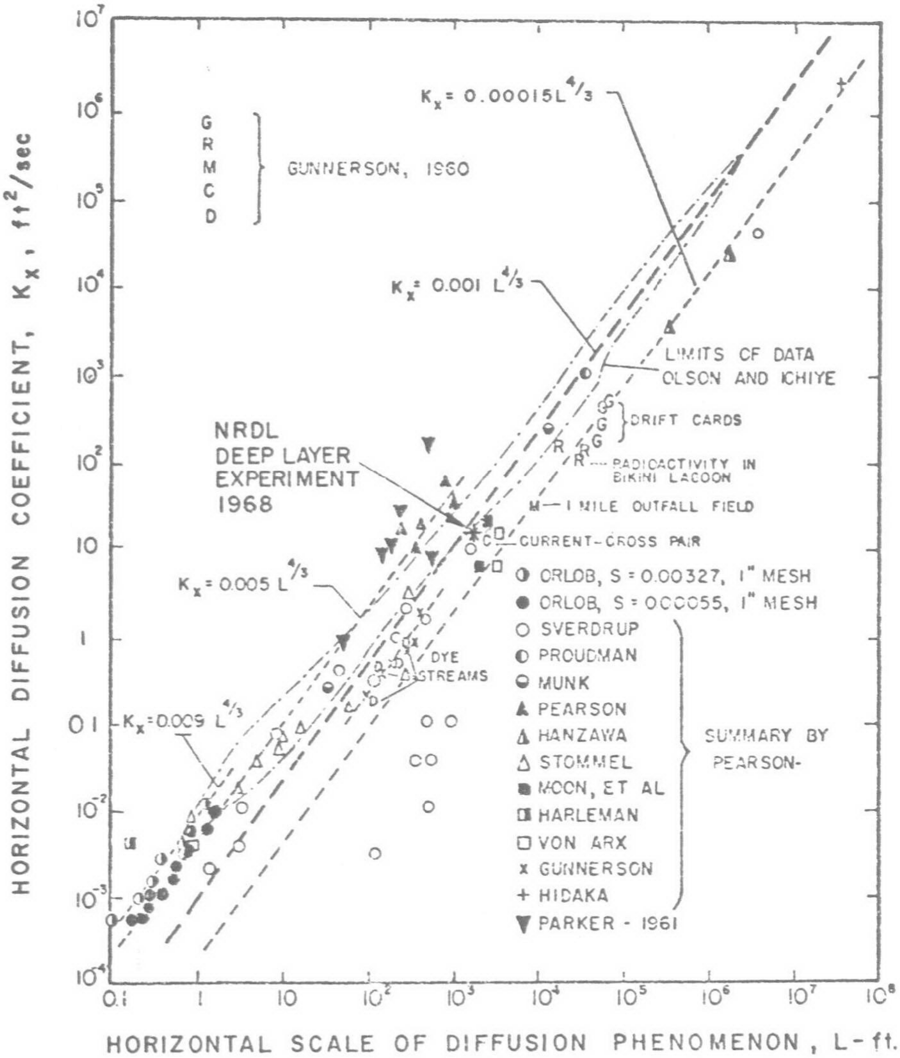

Figure 5.4 Horizontal diffusion coefficient as a function of horizontal scale (from Orlob (1959)).

It can also be observed that the data indicates A to be larger when the scale σ_z is smaller. This is reflected in somewhat larger K_z values for small L in Fig. 5.4 than those corresponding to $A = 10^{-3}$ $ft^{2/3}$/sec. For our purposes, it may be assumed that $A = 10^{-2}$ $ft^{2/3}$/sec. When more field data is available the model may be readily adapted to take advantage of them.

The experimental data summarized in Fig. 5.4 are all for the case when the diffusing pool is on the ocean surface. A few experiments have also been performed for the case when the diffusing pool is at depth (Parr 1936; Riley, 1951; Ozmidov, 1965; Munk, Ewing and Revelle, 1949; Kolesnikov, Panteleyev, and Pisarev, 1964; Snyder, 1967; and Schuert, 1969). The results generally indicate somewhat smaller values for the diffusivity. It is generally recognized that the presence of a stable density gradient damps out vertical turbulent fluctuations and hence vertical turbulent transport. However, conflicting views exist for the effect of stability on horizontal transport. The main difficulty is the lack of adequate field data.

On the one hand, Parr (1936), Riley (1951), and Ozmidov (1965) suggested that the horizontal diffusion coefficient increases with stability. Moreover, they attempted to verify the hypothesis: Parr by using data on the distribution of Atlantic Ocean waters flowing into the Caribbean Sea, while Riley by analyzing salinity and temperature distributions in the ocean. On the other hand, Munk, Ewing and Revelle (1949), Kolesnikov, Panteleyev, and Pisarev (1964), Snyder (1967), and Schuert (1969) suggest the opposite, i.e., the horizontal transport decreases with stability. Munk, et al. found that in Bikini Lagoon at 50 meter depth, the value of horizontal diffusion coefficient was only one-third of that near the surface. Kolesnikov found by direct measurements, A_L to be 0.01 $cm^{2/3}$/sec. at the surface and 0.0046 $cm^{2/3}$/sec. at 500 meter depth. Snyder found that at 9 foot depth, the value of A_L dropped to one-quarter of the value at the surface. Schuert found that at 300 meter depth, the value of A_L is about one order of magnitude smaller than in surface waters.

It can be seen from the above discussion that the dependence of K_z on stability is still controversial and unsettled. The diffusion model to be developed herein, however, can be modified to incorporate a K_z as a function of y, the vertical coordinate once a reliable relation is established.

5.3.1.2b Vertical Diffusion Coefficient

In contrast with the relative abundance of data for horizontal diffusion on the ocean surface, there is a scarcity of data for vertical diffusion. Evaluation of vertical diffusion coefficients have typically been implicit, e.g., based on the temperature and salinity distribution and their time and space variations. The matter is further complicated by the wide spread in the measured values, (from as low as 4×10^{-2} to as high as 200 cm^2/sec). Moreover, no obvious relations were available between the vertical diffusion coefficient and other readily measured parameters.

The presence of density stratification tends to supress vertical exchange. Therefore, one expects the vertical diffusivity to be a monotonic decreasing function of density stratification. The presence of shear tends to be destabilizing and increases vertical exchange. It can be expected that for similar flows the vertical diffusivity should be a monotonic non-increasing function of the Richardson number defined as

$$R_i = \left| \frac{\frac{g}{\rho} \frac{d\rho}{dy}}{\left(\frac{du}{dy}\right)^2} \right|$$

Numerous proposed relations between K_y and R_i are summarized in Table 5.1. Unfortunately, these cannot be checked and the constants (β) cannot be readily determined due to a scarcity of data on the shear.

Rather than relating K_y to R_i which is the physically more logical approach, it is also possible to attempt a correlation of K_y with

$$\epsilon = \left| \frac{1}{\rho_o} \frac{d\rho}{dy} \right|$$

the density gradient alone. Strictly speaking, one would not expect a one-to-one relationship to exist between K_y and ϵ.

TABLE 5.1

Summary of Formulas on Correlation of Vertical Diffusion Coefficient K_y with Richardson's Number R_i (or Density Gradient ϵ)

NOTE: K_{y0}: K_y at $R_i = 0$, i.e., the neutral case β: proportionalility constant varies from case to case

Rossby and Montgomery (1935)*	$K_y = K_{y0}\,(1 + \beta\, R_i)^{-1}$
Rossby and Montgomery (1935)*	$K_y = K_{y0}\,(1 + \beta\, R_i)^{-2}$
Holzman (1943)*	$K_y = K_{y0}\,(1 - \beta\, R_i)$ $\quad R_i \le \frac{1}{\beta}$
Yamamoto (1959)*	$K_y = K_{y0}\,(1 - \beta\, R_i)^{1/2}$ $\quad R_i \le \frac{1}{\beta}$
Mamayev (1958)*	$K_y = K_{y0}\, e^{-\beta R_i}$
Munk and Anderson (1948)**	$K_y = K_{y0}\,(1 + \beta\, R_i)^{-3/2}$ $\beta = 3.33$ based upon data by Jacobsen (1913) and Taylor (1931)
Harremoes (1968)	$K_y = 5 \times 10^{-3} \times \epsilon^{-2/3}$ cm^2/sec note: ϵ in m^{-1}; approximate experimental range $5x10^{-9} < \epsilon < 15 \times 10^{-5} m^{-1}$
Kolesnikov, et al (1961)***	$K_y = K_{y\,min} + \frac{\beta}{\epsilon}$ in cm^2/sec $K_{y\,min}$ and β are empirically determined to be: $K_{y\,min} = 12$, $\beta = 8.3 \times 10^{-5}$ (1958 and 1960 observations) $K_{y\,min} = 2$, $\beta = 10.0 \times 10^{-5}$ (1959 observations)

* As given by Okubo (1962)

** As given by Bowden (1962)

*** The formulas presented in the translated version are apparently erroneous.

All readily available data on K_y where ε is simultaneously measured are collected and plotted as shown in Fig. 5.5. It can be observed that almost all data fall within a factor of 10 of the empirical relation

$$K_y = \frac{10^{-4}}{\varepsilon} \quad (K_y \text{ in cm}^2/\text{sec}; \; \varepsilon \text{ in m}^{-1}) \tag{5.24}$$

$$4 \times 10^{-7}\text{m}^{-1} \leq \varepsilon \leq 10^{-2}\text{m}^{-1}$$

It should be noted that Fig. 5.5 contains only those available data where both K_y and ε are available.

The relation $K_y = 10^{-4}/\varepsilon$ can be deduced from the definition of the vertical diffusion coefficient provided some assumptions are made. We assume that diffusion occurs due to turbulence so that molecular diffusion may be ignored. With the assumption that the density variations are small in the ocean, the equation describing the variation of potential density is then

$$\frac{\partial \rho}{\partial t} + u\frac{\partial \rho}{\partial x} + v\frac{\partial \rho}{\partial y} + w\frac{\partial \rho}{\partial z} = \frac{\partial}{\partial x}(K_x\frac{\partial \rho}{\partial x}) + \frac{\partial}{\partial y}(K_y\frac{\partial \rho}{\partial y}) + \frac{\partial}{\partial z}(K_z\frac{\partial \rho}{\partial z})$$

where u, v, w are the mean currents in the x, y, z directions respectively.

Since horizontal variation of ρ are usually much smaller than vertical variations, we assume $\frac{\partial \rho}{\partial x} = \frac{\partial \rho}{\partial z} = 0$; also, we will assume $v = 0$. Then the equation becomes

$$\frac{\partial \rho}{\partial t} = \frac{\partial}{\partial y}(K_y\frac{\partial \rho}{\partial y})$$

The term $\frac{\partial \rho}{\partial t}$ is usually very small except for the near surface waters which may undergo some diurnal changes. Thus we assume steady state. Then

$$\frac{\partial}{\partial y}(K_y\frac{\partial \rho}{\partial y}) = 0$$

or

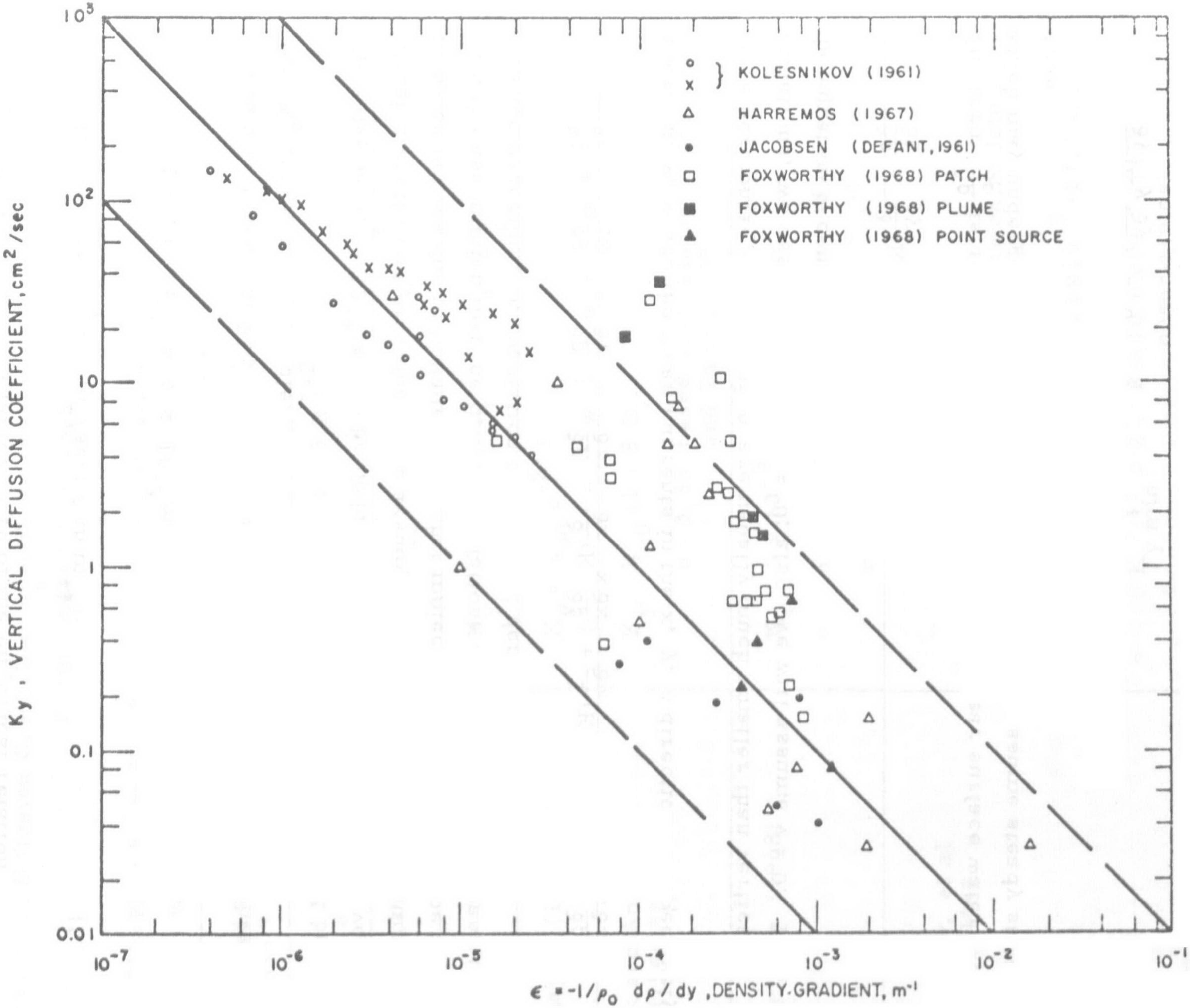

Figure 5.5 Correlation of Ky with density gradient.

A-2-1642

$$K_y \frac{\partial \rho}{\partial y} = \text{constant}$$

Hence

$$K_y = \frac{\text{Constant}}{\varepsilon}$$

This is exactly the form of the relation between K_y and ε found depicted in Fig. 5. 5.

It is proposed that unless independent field data is available, Eq. (5. 24) be used to estimate K_y for application of the present model. It is realized that this is approximate at best. However, it is, at present, the most rational method available. Future studies and measurements may alter this relation. The region of applicability of this relation is $10^{-6} < \varepsilon < 10^{-2}\ m^{-1}$.

In the surface mixed layer of the ocean, the density gradient is often zero. The empirical relation is certainly invalid since it implies an infinite K_y. In this case, the vertical transport is governed primarily by the vertical turbulence created by waves and wind. Relations between the vertical diffusion coefficient K_y in the mixed layer and the surface wave characteristics have been proposed by Golubeva (1963) and Isayeva and Isayev (1963). Their relations can be summarized by

$$K_{y1} = 0.02 \frac{H_w^{\,2}}{T_w}$$

where K_{y1} = vertical diffusivity at the surface

H_w = wave height

T_w = wave period

Thus given the sea state, K_{y1} can be estimated. Fig. 5. 6 shows the relation between K_{y1} and sea state.

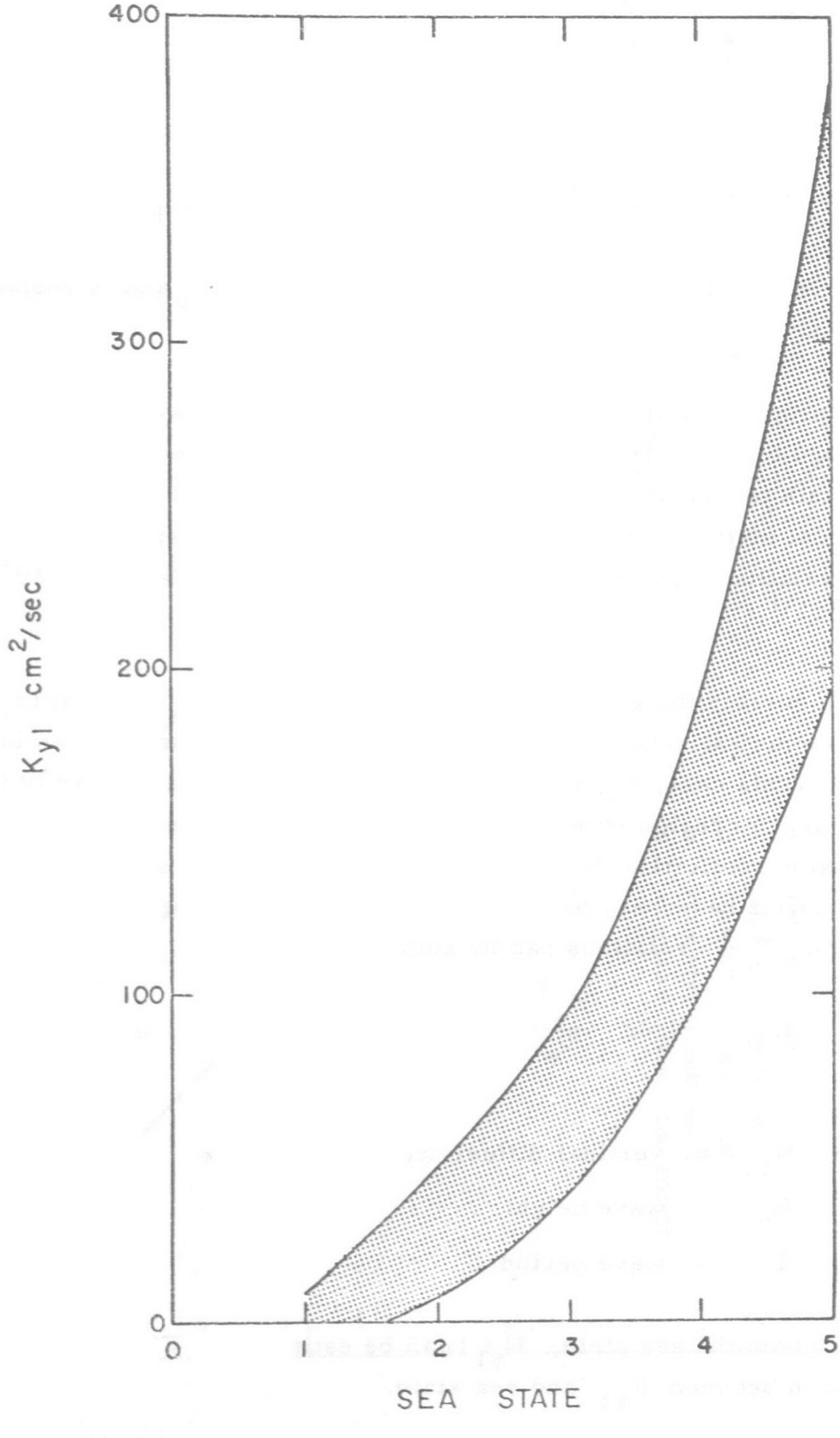

Figure 5.6 Dependence of Ky_1 on sea state .

In summary, data on vertical diffusivity are scarce. Although logically, K_y is expected to depend on Richardson number, for practical purposes, the empirical relation $K_y = 10^{-4}/\epsilon$ is proposed, subject to modification as better data become available.

In general, K_y has its maximum value in the surface layer: in the open ocean K_y at the surface varies between 10 - 200 $cm^2/sec.$; in coastal areas, 10 - 50 $cm^2/sec.$; in lakes, $\sim$ 10 $cm^2/sec.$ Below the surface mixed layer (or epiliminion) K_y drops to its minimum in the thermocline (of the order of 1 $cm^2/sec.$ in the open ocean; in lakes, K_y may drop to as low as 0.05 $cm^2/sec.$). Below the thermocline, K_y may increase again. Some typical values and K_y - profiles in lakes and reservoirs have been determined by Orlob and Selna (1970).

5.3.2 Method of Moments

The problem posed in Sec. 5.3.1 is complicated and cumbersome to solve due to the three independent variables and the complexity of the coefficient functions. This difficulty can be partially overcome by using the method of moments.

Define moments of the distribution by:

$$c_o(x, y) = \int_{-\infty}^{\infty} c(x, y, z)\, dz \tag{5.25}$$

$$c_1(x, y) = \int_{-\infty}^{\infty} zc(x, y, z)\, dz \tag{5.26}$$

$$c_2(x, y) = \int_{-\infty}^{\infty} z^2 c(x, y, z)\, dz \tag{5.27}$$

The zeroth moment c_o is the integrated amount of excess temperature or tracer in the z-direction. The first moment c_1 is related to the z-coordinate of the centroid of the c-distribution. In the present model, it is zero because of the symmetry of the distribution in the z-direction. The second moment c_2 defines the spread in the z-direction. The width of the effluent field is usually taken to be $4\sigma_z$ where $\sigma_z^2 = c_2/c_o$.

Multiplying Eq. (5.20) by z^o, z^2, and integrating over z, we obtain the equations governing the moments:

$$u \frac{\partial c_o}{\partial x} = \frac{\partial}{\partial y}(K_y \frac{\partial c_o}{\partial y}) - K_d c_o \tag{5.28}$$

$$u \frac{\partial c_2}{\partial x} = \frac{\partial}{\partial y}(K_y \frac{\partial c_2}{\partial y}) - K_d c_2 + 2K_z c_o \tag{5.29}$$

An alternate to Equation (5.29) can be written in terms of σ_z as:

$$u \frac{\partial \sigma_z^2}{\partial x} = \frac{\partial}{\partial y}(K_y \frac{\partial \sigma_z^2}{\partial y}) + 2K_y \frac{1}{c_o} \frac{\partial c_o}{\partial y} \frac{\partial \sigma_z^2}{\partial y} + 2K_z \tag{5.30}$$

The boundary conditions expressed in terms of the moments corresponding to Eq. (5.18) are:

$$\left.\begin{aligned} K_y \frac{\partial c_o}{\partial y} &= K_e c_o \\ K_y \frac{\partial c_2}{\partial y} &= K_e c_2 \end{aligned}\right\} \quad \text{at } y = 0 \tag{5.31}$$

or

$$K_y \frac{\partial \sigma_z^2}{\partial y} = 0 \qquad \text{at } y = 0$$

and

$$\frac{\partial c_o}{\partial y} = \frac{\partial c_2}{\partial y} = \frac{\partial \sigma_z^2}{\partial y} = 0 \qquad \text{at } y = h_b \tag{5.32}$$

The source condition expressed in terms of the moments corresponding to Eq. (5.21) are:

$$c_o(o, y) = c_o(o, y_o) \left\{1 - \left[\frac{2(y-y_o)}{h_o}\right]^2\right\}^{\frac{1}{4}} \tag{5.33}$$

$$c_2(o, y) = c_o(o, y_o)\, \sigma_z^{\,2}(o, y_o) \left\{1 - \left[\frac{2(y-y_o)}{h_o}\right]^2\right\}^{3/4} \tag{5.34}$$

or

$$\sigma_z^{\,2}(o, y) = \sigma_z^{\,2}(o, y_o) \left\{1 - \left[\frac{2(y-y_o)}{h_o}\right]^2\right\}^{\frac{1}{2}} \tag{5.35}$$

Thus by the moment method, the number of independent variables is reduced by one. Since the c-distribution in the z-direction is usually found to be of Gaussian form both from field and laboratory experiments, the diffusion process can be adequately described by knowing the zeroth and the second moments. In fact, if c is exactly Gaussian in the z-direction, then it is completely specified by its zeroth and second moments. Equations for higher moments can be formulated in a similar way. These are only necessary if the c-distribution is distinctly non-Gaussian in the z-direction In that case, for example, the third moment would indicate the skewness of the distribution.

5.3.3 Limiting Solution for Cases with Zero Vertical Transport

If the effluent field is trapped within a strong thermocline where vertical transport is small (for example, if K_y is close to the molecular value), a good approximation to the solution can be achieved by taking $K_y = 0$. The proper criterion for the validity of this approximation is that the vertical spreading over the distance of travel is small in comparison with the vertical dimension of the source, i.e.,:

$$\sqrt{K_y \frac{x_t}{u_o}} \ll h_o \tag{5.36}$$

where x_t is the horizontal distance of interest;
u_o is the characteristic velocity; and
h_o is the source thickness.

for $K_y = 0.1\ cm^2/sec.$, $u_o = 15\ cm/sec.$ (or 0.5 fps) and $x_t = 1{,}500$ meters, $\sqrt{K_y x_t / u_o} = 0.3$ m; therefore, for sources thicker than, say 10 meters, it will be sufficient to consider it as a case with zero vertical transport.

For cases with zero vertical transport, an analytical solution can be obtained as follows. Equation (5.28), when $K_y = 0$, becomes

$$u \frac{\partial c_o}{\partial x} = - K_d c_o \tag{5.37}$$

Integrate with respect to x, noting that u is only a function of y:

$$c_o(x, y) = c_o(o, y) \exp \left\{ - \frac{K_d}{u} x \right\} \tag{5.38}$$

Equation (5.30) becomes:

$$u \frac{\partial \sigma_z^2}{\partial x} = 2K_z \qquad \text{when } c_o \neq 0 \tag{5.39}$$

Applying the 4/3 power law for K_z:

$$K_z = A \sigma_z^{4/3}$$

Eq. (5.39) becomes

$$u \frac{\partial \sigma_z^2}{\partial x} = 2A\sigma_z^{4/3} \tag{5.40}$$

Integrating with respect to x, Eq. (5.40) gives:

$$\sigma_z^{2/3}(x, y) = \frac{2}{3} \frac{A}{u} x + \sigma_z^{2/3}(o, y) \tag{5.41}$$

For a given set of source conditions, i.e., $c_o(o, y)$ and $\sigma_z(o, y)$, environmental characteristics $u(y)$, A, and the decay coefficient K_d, solutions are given by Eqs. (5.38) and (5.41) if the vertical transport can be neglected. The maximum concentration or excess temperature (assuming c is Guassian in z) is given by

$$c_{max}(x, y) = c_{max}(o, y) \cdot \frac{c_o(x, y)}{c_o(o, y)} \cdot \frac{\sigma_z(o, y)}{\sigma_z(x, y)} \qquad (5.42)$$

5.3.4 Dimensionless Equations and Numerical Solutions

For general cases with non-zero vertical transport, it is necessary to resort to a numerical method of solution unless the environmental and source conditions are very simple.

Before the numerical solution is attempted, the governing equations, source conditions and environmental conditions will first be normalized by defining dimensionless variables (quantities with primes) as follows:

Coordinates:

$$x' = x/x_t \qquad (5.43)$$

$$y' = y/\sqrt{K_{yo}x_t/u_o} \qquad (5.44)$$

Velocity: $u' = u/u_o$ (5.45)

Vertical diffusion coefficient: $K'_y = K_y/K_{yo}$ (5.46)

Dissipation parameter: $\lambda' = Ax_t/\{\sigma_z^{2/3}(0, y_o)u_o\}$ (5.47)

Exchange coefficient: $K'_e = K_e\sqrt{x_t/K_{yo}u_o}$ (5.48)

Decay coefficient: $K'_d = K_d x_t/u_o$ (5.49)

Zeroth moment: $c'_o = c_o/c_o(o, y_o)$ (5.50)

Second moment: $c'_2 = c_2/[c_o(o, y_o)\ \sigma_z^2(o, y_o)]$ (5.51)

Lateral spreading: $\sigma'_z = \sigma_z/\sigma_z(o, y_o)$ (5. 52)

Maximum concentration: $c'_{max} = c_{max}/c_{max}(o, y_o)$ (5. 53)

NOTE: $c'_{max} = \dfrac{c'_o}{\sigma'_z}$

Here x_t is the terminal x value of interest;
K_{yo} is a characteristic vertical diffusion coefficient; and
u_o is a characteristic current speed

For example, the characteristic values K_{yo} and u_o can be taken to be their values at the free surface if the effluent is at the free surface.

The governing equations, (5. 28), (5. 29) and (5. 30), in dimensionless form becomes:

$$u' \frac{\partial c'_o}{\partial x'} = \frac{\partial}{\partial y'}\left(K'_y \frac{\partial c'_o}{\partial y'}\right) - K'_d c'_o \tag{5. 54}$$

$$u' \frac{\partial c'_2}{\partial x'} = \frac{\partial}{\partial y'}\left(K'_y \frac{\partial c'_2}{\partial y'}\right) + 2K'_z c'_o - K'_d c'_2 \tag{5. 55}$$

$$u' \frac{\partial \sigma'^2_z}{\partial x'} = \frac{\partial}{\partial y'}\left(K'_y \frac{\partial \sigma'^2_z}{\partial y'}\right) + 2K'_y \frac{1}{c'_o} \frac{\partial c'_o}{\partial y'} \frac{\partial \sigma'^2_z}{\partial y'} + 2K'_z \tag{5. 56}$$

The normalized boundary conditions corresponding to Eqs. (5. 31) and (5. 32) become

$$\left.\begin{aligned} K'_y \frac{\partial c'_o}{\partial y'} &= K'_e c'_o \\ K'_y \frac{\partial c'_2}{\partial y'} &= K'_e c'_2 \end{aligned}\right\} \quad \text{at } y = 0 \tag{5. 57}$$

or

$$K'_y \frac{\partial \sigma'^2_z}{\partial y'} = 0 \qquad y = 0$$

and

$$\frac{\partial c'_o}{\partial y'} = \frac{\partial c'_2}{\partial y'} = \frac{\partial \sigma'^2_z}{\partial y'} = 0 \qquad \text{at } y = h'_b \tag{5.58}$$

where

$$h'_b = h_b / \sqrt{K_{yo} x_t / u_o}$$

The normalized source conditions based upon Eqs. (5.33) to (5.35) are:

$$c'_o(o, y') = \left\{1 - \left[\frac{2(y' - y'_o)}{h'_o}\right]^2\right\}^{\frac{1}{4}} \tag{5.59}$$

$$c'_2(o, y') = \left\{1 - \left[\frac{2(y' - y'_o)}{h'_o}\right]^2\right\}^{3/4} \tag{5.60}$$

and

$$\sigma'^2_z(o, y') = \left\{1 - \left[\frac{2(y' - y'_o)}{h'_o}\right]^2\right\}^{\frac{1}{2}} \tag{5.61}$$

for $y' \geq 0$ and $y'_o - \frac{h'_o}{2} \leq y' \leq y'_o + h'_o/2$

where

$$y'_o = y_o / \sqrt{K_{yo} x_t / u_o} \quad , \quad h'_o = h_o / \sqrt{K_{yo} x_t / u_o}$$

Note that Eqs. (5.54) to (5.58) are identical in form to their corresponding dimensional equations. The main effects of this normalization are: 1) the region of interest in x is normalized to $0 \leq x' \leq 1$; 2) the source condition is normalized; and 3) the u- and K_y-profiles are normalized.

Thus, the problem of the steady state distribution of excess temperature (or tracer) resulting from a continuous source in a steady but non-uniform environment is formulated in dimensionless form. A computer program

(PTD) has been written based on the Crank-Nicolson Method and is included in Appendix C. Given the input conditions h'_o, y'_o, K_y- and u-profiles, K'_e, K'_d, h'_b, the problem can be solved by using the program.

Before discussing the example solutions obtained, we shall first choose the various parameters and parameter functions to specify the problem. The following values have been chosen as representative typical values:

$$A = 10^{-2}\ \text{ft}^{2/3}/\text{sec.}$$

$$x_t = 10,000\ \text{ft.}$$

$$K_{yo} = 10^{-2}\ \text{ft.}^2/\text{sec. (surface)}$$

$$u_o = 1\ \text{ft/sec. (surface)}$$

$$h_b = 100\ \text{ft.}$$

$$h_o = 20\ \text{ft.}$$

$$\sigma_z(o, y_o) = 30\ \text{ft.}$$

$$K_e = 10^{-5}\ \text{ft/sec.}$$

From these,

$$\lambda' = Ax_t/[\sigma_z^{2/3}(o, y_o)\ u_o] \cong 10$$

$$K'_e = K_e\sqrt{x_t/K_{yo}u_o} = 10^{-2}$$

$$h'_b = \frac{h_b}{\sqrt{K_{yo}x_t/u_o}} = 10$$

$$h'_o = \frac{h_o}{\sqrt{K_{yo}x_t/u_o}} = 2$$

In the following discussion, the primes will be dropped for simplicity.

The parameter functions $K_y(y)$ and $u(y)$ are chosen to be as shown schematically in Fig. 5.7. The constant parameters y_{K1}, y_{K2}, y_{K3}, y_{K4}, β_1, β_2 would specify the dimensionless Ky - profile while the constants y_e, u_o would specify the dimensionless u-profile. It should be pointed out here that x_t is more or less an arbitrary number. The program PTD can be run for x from 0 to any value, not necessarily 1. Also, by proper choice of y_o the source may be located at the surface ($y_o = 0$) or at any depth ($y_o > 0$).

Guided by the numerical values mentioned in the preceeding paragraphs, a total of 14 cases has been computed using the program PTD. The parameters and parameter functions chosen for each case are summarized in Table 5.2. As can be seen from the table, two different profiles were selected for Ky and u as functions of y. The first is when it is constant with depth. The second is when it takes on a shape judged typical of situations when the ambient is density stratified. The identification code is designated by two letters followed by three numbers. The first letter signifies whether the Ky-profile is constant (C) or not constant (S or T). In case it is not constant, S stands for the case when the source is at the surface and T the case when it is submerged (in the thermocline). The second letter signifies whether the velocity profile u(y) is constant (C) or not (N). The first number, n_1, refers to the value of λ: $\lambda = 1$ corresponds to $n_1 = 1$ and $\lambda = 10$ to $n_1 = 2$, thus, $\lambda = 10^{(n_1 - 1)}$. The second number n_2 refers to the value of K_e, by the relation $K_e = 10^{-n_2}$. The third number n_3 refers to the value of K_d by the relation $K_d = 10^{-n_3}$.

It should be noted that c_o, the zeroth moment of the distribution is independent of λ. Figures 5.8 a, b, and c show $c_o(y)$ plotted versus y for various values of x. Several different cases are shown on the same graph to delineate the effect of various parameters. Figure 5.8a is for the case when K_y is constant; Fig. 5.8b for the case when K_y is not constant and the source at the surface while Fig. 5.8c for K_y not constant and source submerged. The effects of K_e and K_d and the current profile can be observed by comparing the cases in each figure. The effect of

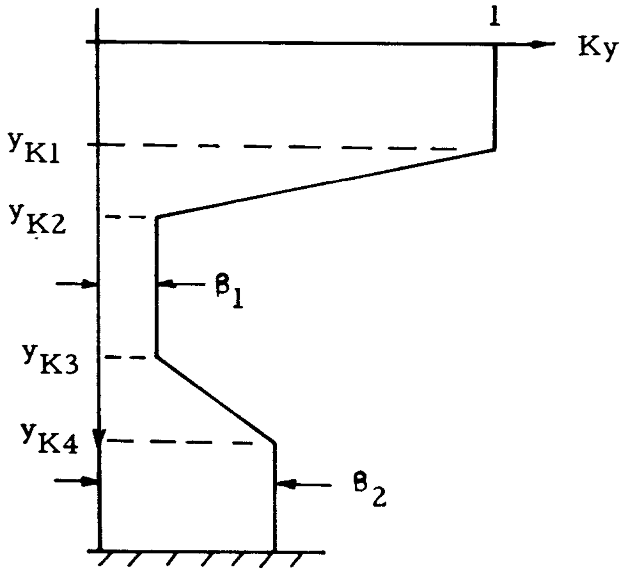

Ky-profile

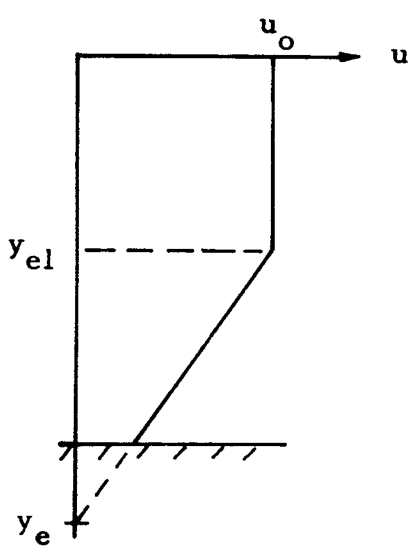

u-profile

Figure 5.7 Profiles of Ky and u used in study.

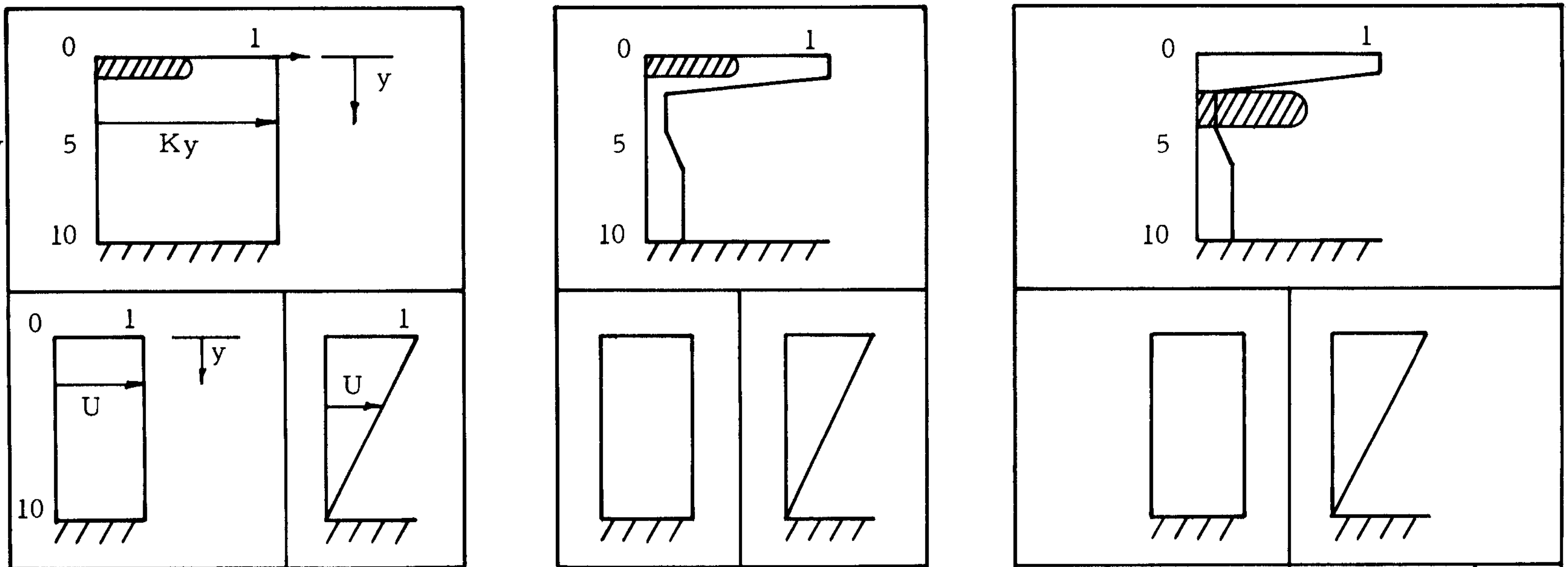

λ	1	10		10	1	10	10		1	10		1		10
K_e	0	0	10^{-2}	0	0	0	0	10^{-1}	0	0	0	0	10^{-2}	0
K_d	0	0	0	0	0	0	0	0	0	0	10^{-2}	0	0	0
ID	CC 100	CC 200	CC 220	CN 200	SC 100	SC 200	SN 200	SN 210	TC 100	TC 200	TC 202	TN 100	TN 120	TN 200

Table 5.2 Summary of PTD cases. (Ky = Vertical diffusivity; U = Current; λ = Dissipation parameter; K_e = Surface exchange coefficient; K_d = Decay coefficient) All quantities dimensionless.

K_y-profile can be seen by comparing Fig. 5.8a with 5.8b. As can be seen from these figures, the effects of the various parameters and parameter functions are as expected. For example, K_e tends to decrease c_o but primarily at the surface, and the current shear tends to promote somewhat higher dispersion.

The effect of λ on the solution is on the spread of the plume or in the value of the second moment c_2. Figures 5.9 a, b, and c show the solution $\sigma_z = \sqrt{c_2/c_o}$ plotted versus x for $y = y_o$. It is readily seen that when λ goes from 1 to 10, the spread at $x = 1$ increases about ten times. This is not surprising since λ is proportional to the horizontal diffusion coefficient. The effect of shear on σ_z can also be observed to promote a somewhat larger value of σ_z as would be expected. Comparison of Figs. 5.9 a and b with 5.9 c shows that the effect of shear is correspondingly larger when the source is submerged than when it is at the surface. This is because the value of the velocity at $y = 3$ for the TN - runs is only 0.7 times that for the TC-runs.

From the above discussion it is seen that the model developed did not yield any profoundly different results than what can be reasonably expected. In any practical situation, the parameters and parameter functions and the source conditions may be different from those chosen. The program can be readily modified to suit those conditions.

It should be reiterated here that the model which resulted in the program PTD is for the case of a steady discharge into a steady environment. In practice, the parameters K_e, u, and the source intensity are most probably not constant in time. In such a case, the program PTD should not be used. In the next section of this report, a limited unsteady case will be treated and discussed.

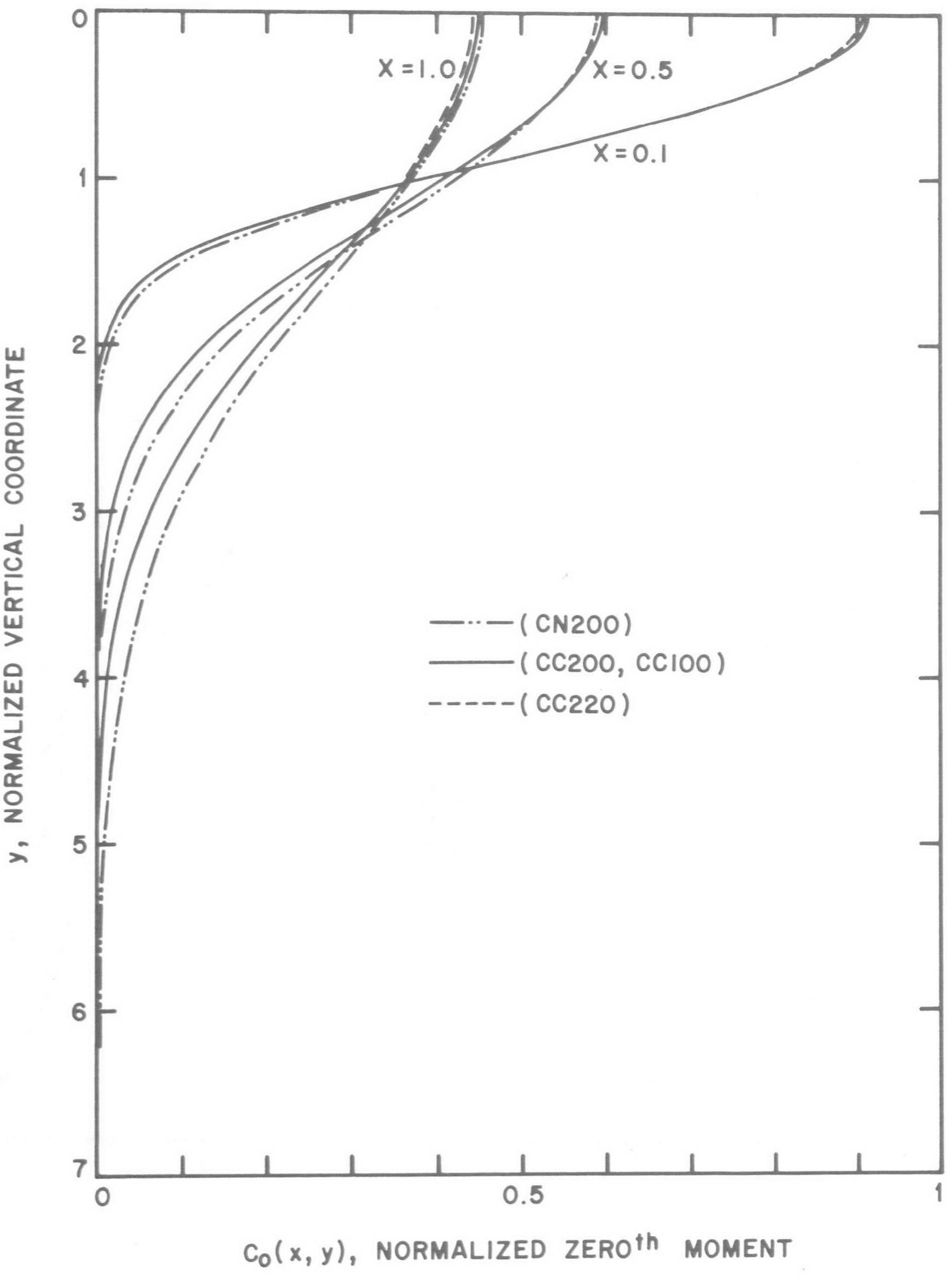

Figure 5.8a Vertical distribution of c_o (x, y) for PTD cases CN 200, CC 200, CC 100, CC 220 (Ky-profile uniform).

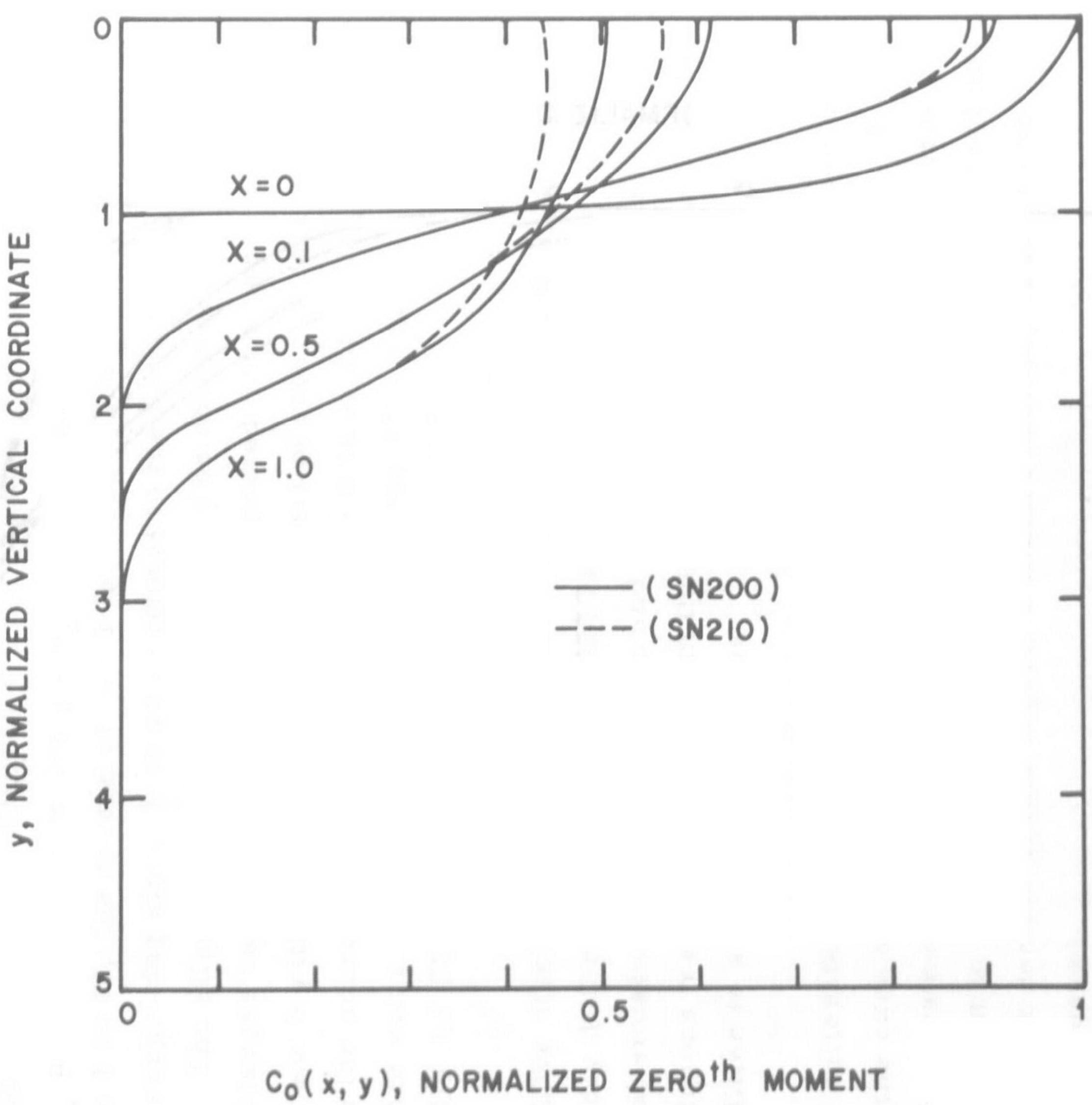

Figure 5.8b Vertical distribution of $c_o(x, y)$ for PTD cases SN 200, SN 210, SC 100, SC 200 (Ky-profile not uniform, surface release).

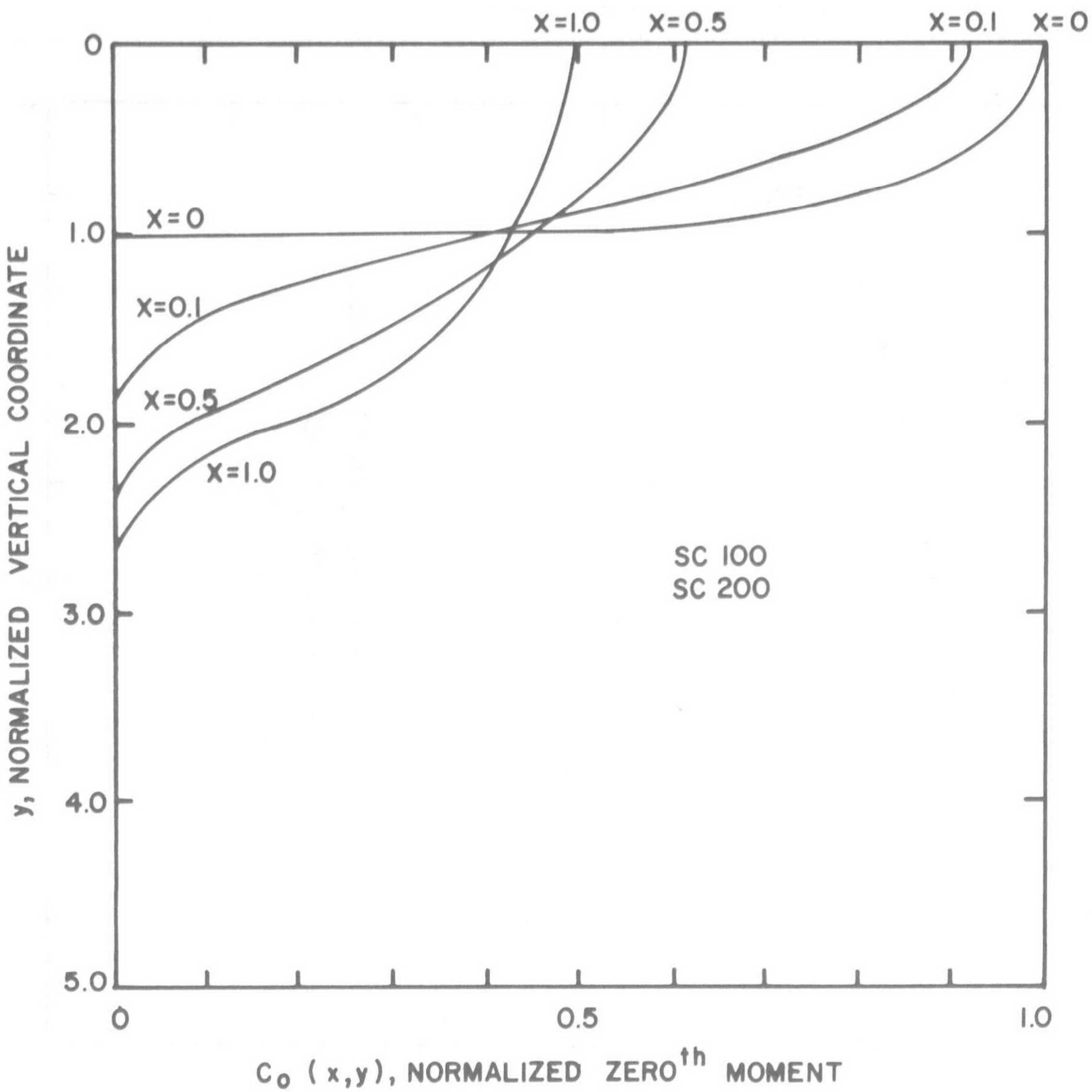

Figure 5. 8b Continued.

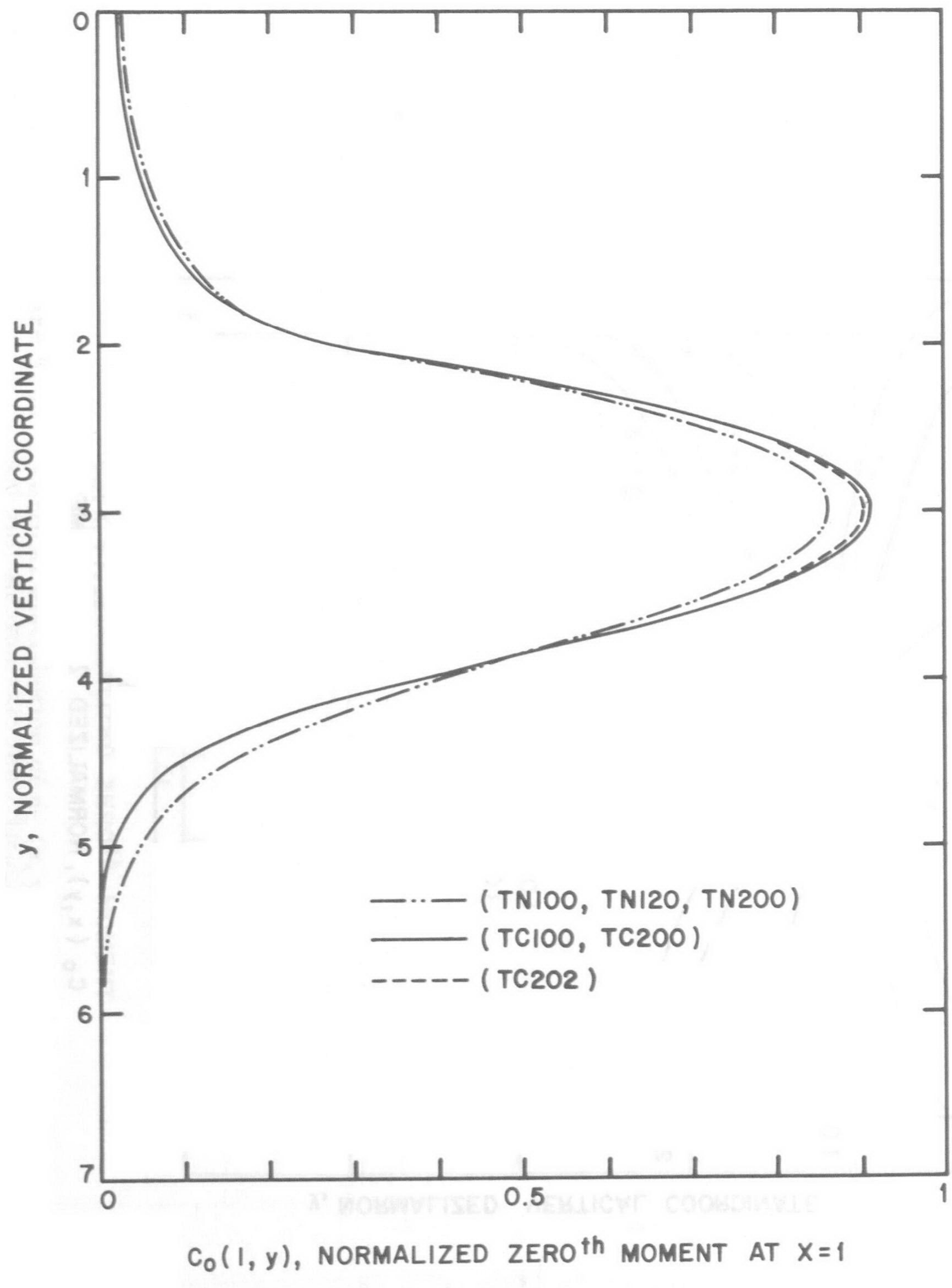

Figure 5.8c Vertical distribution of $c_o(x,y)$ for PTD cases TN 100, TN 120, TN 200, TC 100, TC 200, TC 202 (Ky-profile not uniform, subsurface release).

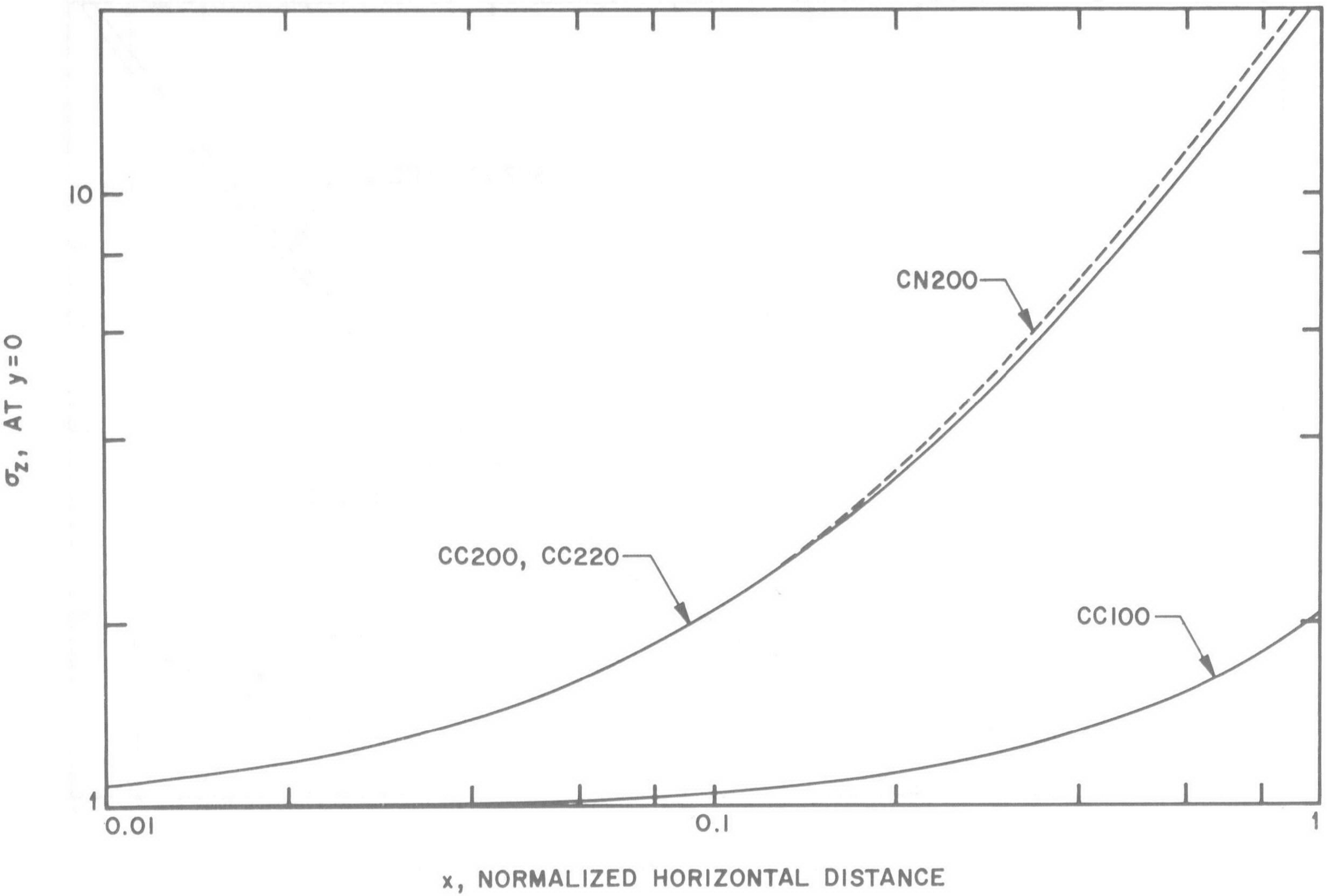

Figure 5.9a Width of diffusing plume for PTD cases CC 200, CN 200, CC 100, CC 220 (Ky-profile uniform).

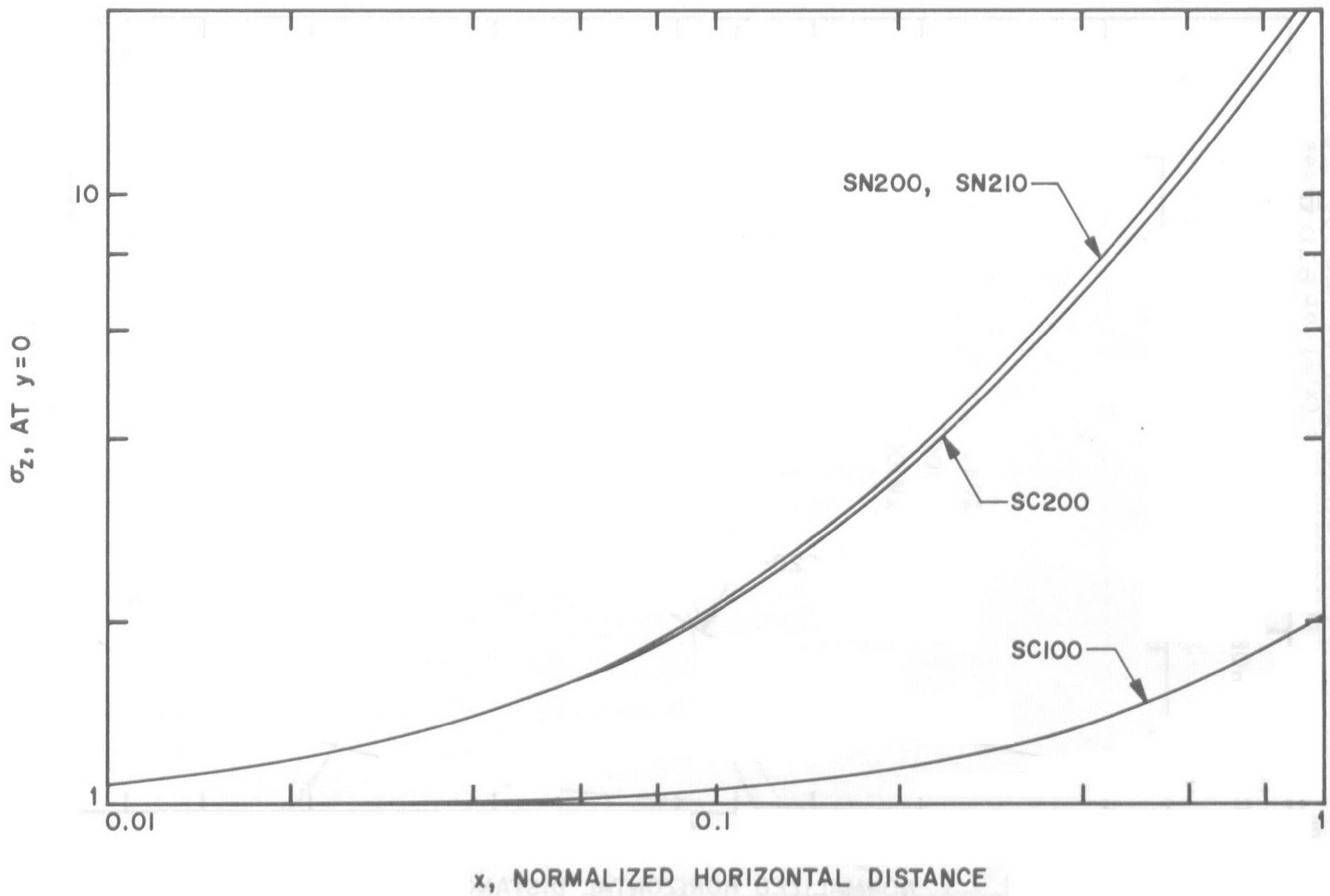

Figure 5.9b Width of diffusing plume for PTD cases SN 200, SN 210, SC 100, SC 200 (Ky-profile not uniform, surface release).

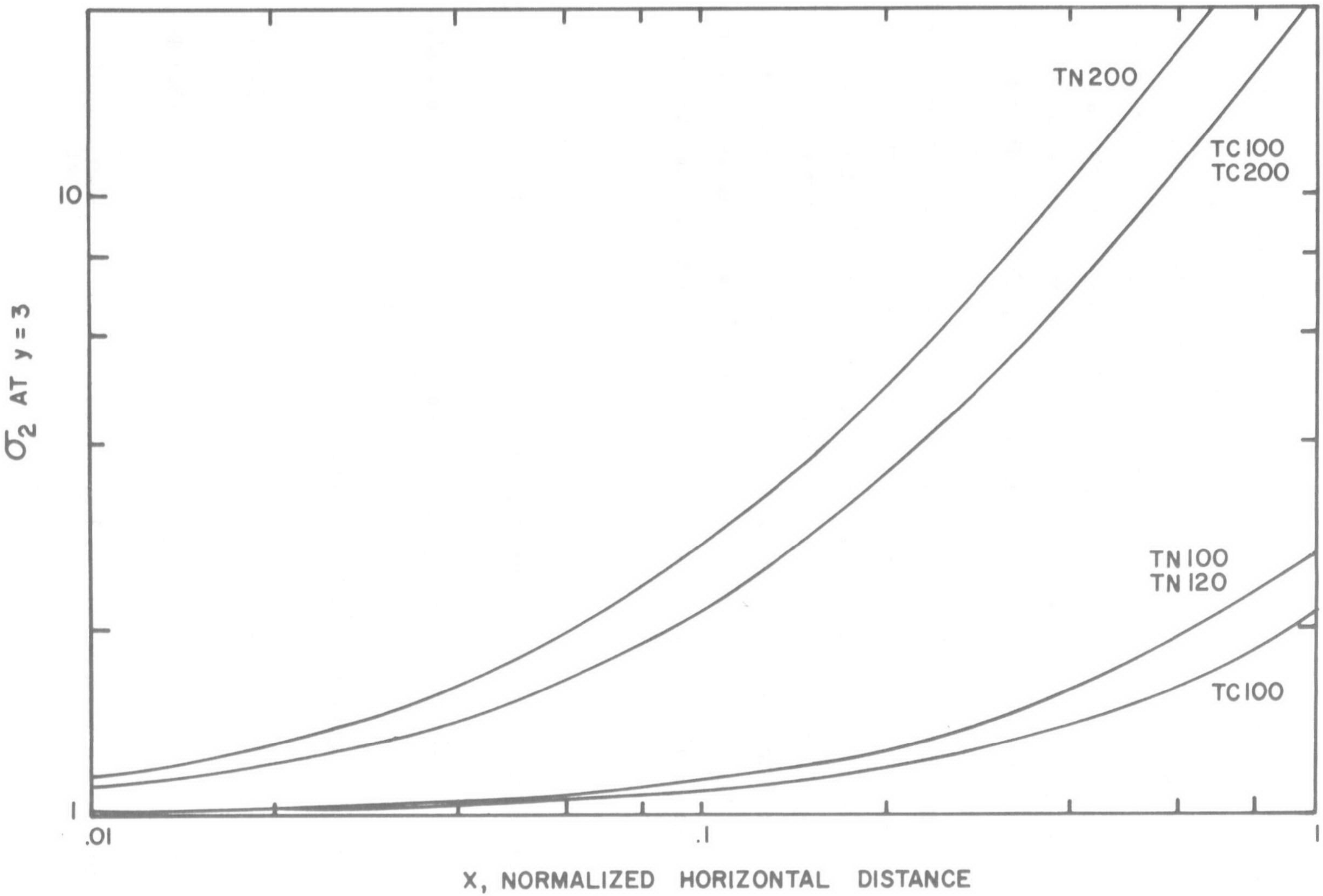

Figure 5.9c Width of diffusing plume for PTD cases TN 100, TN 120, TN 200, TC 100, TC 200, TC 202 (Ky-profile not uniform, subsurface release).

5.4 Continuous Release of Heat into a Uniform But Time-Varying Environment

In a natural water environment, the ambient current and the surface heat exchange are usually not constant but varies with time. Also, the rate of excess heat discharge may vary with time. Thus, the steady state problem formulated in the previous section should be generalized to allow for these variations in time. The general unsteady problem is very complex and will not be solved here. In this section, a somewhat simpler unsteady problem will be formulated and solved. In particular, the current and surface heat exchange are allowed to be time varying, but are assumed to be uniform in the space coordinates, i.e., no current shear will be considered. The rate of excess heat discharge is also allowed to be time varying. It is clear that this problem is substantially more complicated and cumbersome from a computational point of view. For example, the time history of variations of the input functions must be specified before the solution can be obtained. The method of approach to solve this problem is similar to the development in the previous section and will be summarized below.

5.4.1 Formulation

Neglecting longitudinal mixing as before, Eq. (5.17) becomes:

$$\frac{\partial c}{\partial t} + u\frac{\partial c}{\partial x} = \frac{\partial}{\partial y}(K_y\frac{\partial c}{\partial y}) + \frac{\partial}{\partial z}(K_z\frac{\partial c}{\partial z}) - K_d c \qquad (5.62)$$

The corresponding boundary conditions are:

$$K_y\frac{\partial c}{\partial y} = K_e c \qquad \text{at } y = 0 \qquad (5.63)$$

$$K_y\frac{\partial c}{\partial y} = 0 \qquad \text{at } y = h_b \qquad (5.64)$$

Note that u in Eq. (5.62) and K_e in Eq. (5.63) are known functions of time.

The source condition at x = 0 is taken to be:

$$c(o, y, z, t) = c(o, y_o, o, o) \cdot F_{co}(t) \exp\left\{ - \frac{z^2}{\sigma_{zo}^2 \left[1 - \left\{ \frac{2(y-y_o)}{h_o} \right\}^2 \right]^{\frac{1}{2}}} \right\} \qquad (5.65)$$

5.4.2 Method of Moments

Define moments as before (see Eqs. (5.25) to (5.27)) and integrate Eq. (5.62) with respect to z, we obtain:

$$\frac{\partial c_o}{\partial t} + u\frac{\partial c_o}{\partial x} = \frac{\partial}{\partial y}\left(K_y \frac{\partial c_o}{\partial y}\right) - K_d c_o \qquad (5.66)$$

$$\frac{\partial c_2}{\partial t} + u\frac{\partial c_2}{\partial x} = \frac{\partial}{\partial y}\left(K_y \frac{\partial c_2}{\partial y}\right) - K_d c_2 + 2K_z c_o \qquad (5.67)$$

The governing equation for the lateral spreading σ_z is:

$$\frac{\partial \sigma_z^2}{\partial t} + u\frac{\partial \sigma_z^2}{\partial x} = \frac{\partial}{\partial y}\left(K_y \frac{\partial \sigma_z^2}{\partial y}\right) + 2K_y \frac{1}{c_o}\frac{\partial c_o}{\partial y}\frac{\partial \sigma_z^2}{\partial y} + 2K_z \qquad (5.68)$$

The boundary conditions for the moments are:

$$\left.\begin{aligned} K_y \frac{\partial c_o}{\partial y} &= K_e c_o \\ K_y \frac{\partial c_2}{\partial y} &= K_e c_2 \end{aligned}\right\} \quad \text{at } y = 0 \qquad (5.69)$$

or

$$K_y \frac{\partial \sigma_z^2}{\partial y} \qquad \text{at } y = 0$$

and

$$\frac{\partial c_o}{\partial y} = \frac{\partial c_2}{\partial y} = \frac{\partial \sigma_z^2}{\partial y} = 0 \qquad \text{at } y = h_b \tag{5.70}$$

The source conditions expressed in terms of the moments are

$$c_o(o, y, t) = F_{co}(t) \left\{ 1 - \left[\frac{2(y-y_o)}{h_o} \right]^2 \right\}^{\frac{1}{4}} \tag{5.71}$$

$$c_2(o, y, t) = c_o(o, y_o, o) F_{co}(t)\, \sigma_{zo}^2 \left\{ 1 - \left[\frac{2(y-y_o)}{h_o} \right]^2 \right\}^{3/4} \tag{5.72}$$

$$\sigma_z^2(o, y) = \sigma_{zo}^2 \left\{ 1 - \left[\frac{2(y-y_o)}{h_o} \right]^2 \right\}^{\frac{1}{2}} \tag{5.73}$$

for $y \geq 0$ and $y_o - h_o/2 \leq y \leq y_o + h_o/2$

where $F_{co}(t)$ is a prescribed function of time and $\sigma_{zo} = \sigma_z(o, y_o, o)$.

Note that σ_{zo}, h_o and y_o are taken to be time independent. The time variation of the excess waste heat release is given by the function $F_{co}(t)$. The time-varying environmental conditions, K_e and u, are represented schematically as shown in Fig. 5.10.

Note that the front of the effluent field is at a value of x given by $\int_o^t u dt$ as shown in Fig. 5.10 since the longitudinal mixing is neglected here. Thus, the extent of the limit of the region of interest x_t is related to the limit of the time of interest t_t by

$$x_t = \int_o^{t_t} u(t)\, dt \tag{5.74}$$

The region of solution to be covered is therefore

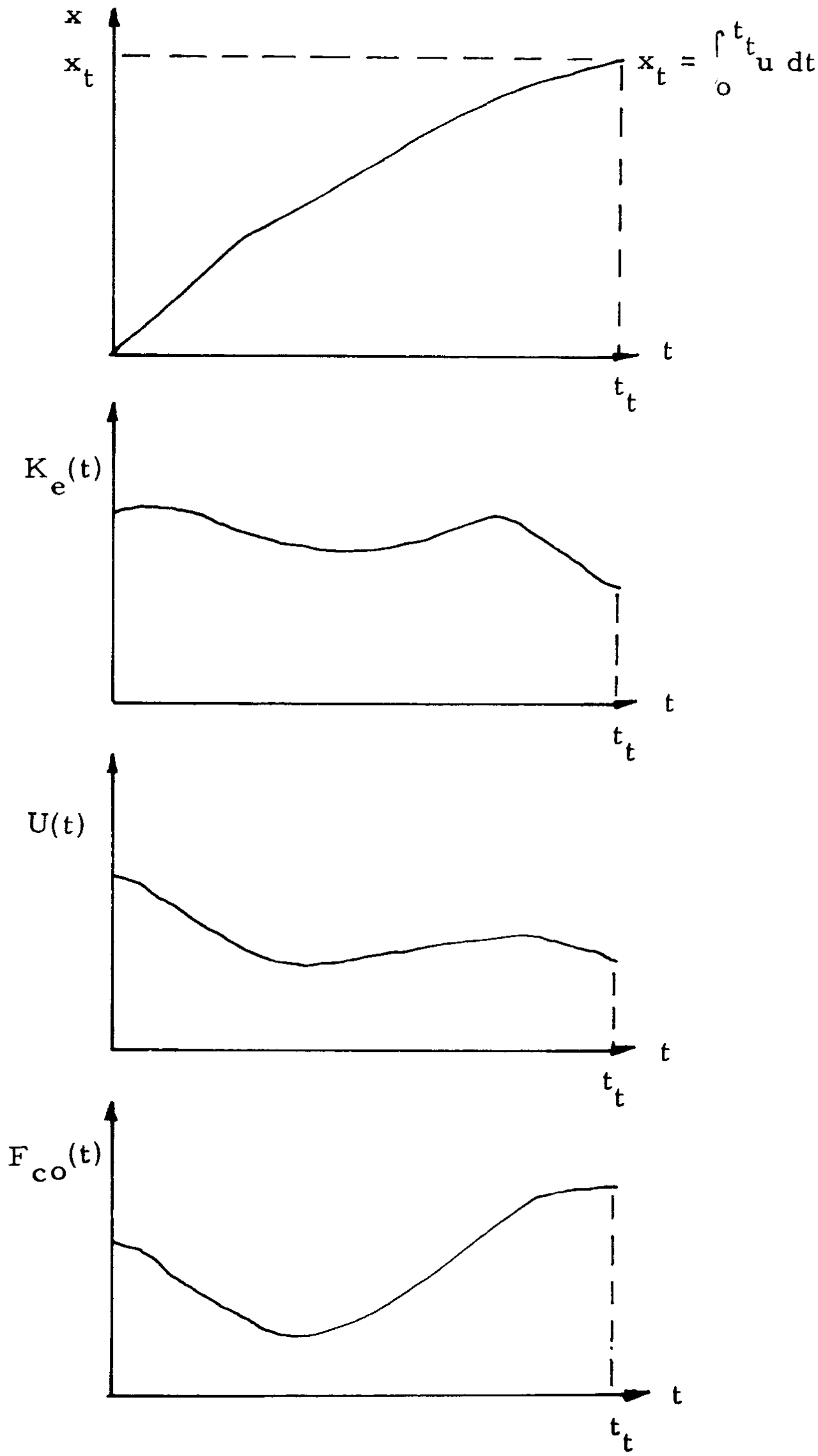

Figure 5.10 Representative sketches in cases of unsteady turbulent diffusion.

$$o \leq x \leq \int_o^{t_t} u(t)\, dt \tag{5.75}$$

Define a new independent variable ξ by

$$\xi = x - \int_o^t u\, dt \tag{5.76}$$

Equation (5.62) in (ξ, y, z, t) variables become:

$$\frac{\partial c}{\partial t} = \frac{\partial}{\partial y}(K_y \frac{\partial c}{\partial y}) + \frac{\partial}{\partial z}(K_z \frac{\partial c}{\partial z}) - K_d c \tag{5.77}$$

and the equations for the moments, Eqs. (5.66) and (5.67), become:

$$\frac{\partial c_o}{\partial t} = \frac{\partial}{\partial y}(K_y \frac{\partial c_o}{\partial y}) - K_d c_o \tag{5.78}$$

$$\frac{\partial c_2}{\partial t} = \frac{\partial}{\partial y}(K_y \frac{\partial c_2}{\partial y}) + 2K_z c_o - K_d c_2 \tag{5.79}$$

Equations (5.77) to (5.79) are all independent of the new variable ξ. However, the source condition is dependent upon ξ; i.e., Eqs. (5.71) to (5.73) apply at $\xi = -\int_o^t u dt$. Therefore, the number of independent variables has not been reduced by the ξ - transformation although the governing equations appear to be simpler. Along ξ = constant, we are following a certain part of the effluent field downstream. In particular, $\xi = 0$ represents the front of the effluent field, i.e., following the very first part of the release. Negative ξ values represent following later portions of release. Since longitudinal mixing (in x-direction) is neglected, there is no exchange between adjacent portions in the x-direction. Thus, we can treat the problem by investigating each portion of the release as it travels downstream. For the portion released at time $t = t_i$, the source distributions are $c_o(o, y, t_i)$ and $c_2(o, y, t_i)$. By solving Eqs. (5.78) and (5.79) we obtain the solution for this portion of the release. Note that x is related to the time variable t by:

$$x = \int_{t_i}^{t} u \, dt \tag{5.80}$$

By solving a number of cases with different t_i from 0 to t_t, the solution for the whole region of (x, t) is obtained.

5.4.3 Dimensionless Equations and Numerical Solutions

Dimensionless variables are defined as in Sec. 5.3.4. In addition to those, we also define:

$$t' = t \, x_t / u_o \tag{5.81}$$

The governing equations, (5.78), (5.79) and (5.80), in dimensionless forms are:

$$\frac{\partial c'_o}{\partial t'} = \frac{\partial}{\partial y'} (K'_y \frac{\partial c'_o}{\partial y'}) - K'_d c'_o \tag{5.82}$$

$$\frac{\partial c'_2}{\partial t'} = \frac{\partial}{\partial y'} (K'_y \frac{\partial c'_2}{\partial y'}) + 2K'_z c'_o - K'_d c'_o \tag{5.83}$$

and

$$x' = \int_{t'_i}^{t'} u' \, dt' \tag{5.84}$$

The boundary conditions are identical to those given by Eqs. (5.57) and (5.58) except $K'_e = K'_e(t)$.

Again, the Crank-Nicolson method was employed in solving this problem numerically. A Fortran IV program entitled "UTD" was prepared and listed in Appendix D to handle this particular mathematical model.

The unsteady problem (UTD) requires substantially more input data to specify the problem than the corresponding steady problem (PTD). In particular, it is necessary to specify the functions $F_{co}(t)$, $u(t)$ and $K_e(t)$, all quantities being dimensionless. Moreover, the program requires a substantially longer time on the computer particularly if the functions $F_{co}(t)$, $u(t)$ and $K_e(t)$ are specified for many values of t. Since the general basic model is the same as that used in PTD, it can be expected that similar results should obtain. Only a few cases have been run using UTD. The results are similar to those of PTD. These results are difficult to present in such a form as to give ready comparisons with those obtained from PTD, since the solution depends on the previous history of F_{co}, u, and K_e. Figure 5.11 shows one such comparison. The solid line in the figure is $c_o(x, o)$ from case PTD-CC-100. The points are from using UTD with the following functions for F_{co}, u, and K_e:

t	u	K_e	F_{co}
0	1.	0.0	1
0.2	1.	0	1
0.4	1.	0.1	0.5
0.6	2.	0.1	0.5
0.8	1.	0.2	0.8
1.0	0.5	0	1.0

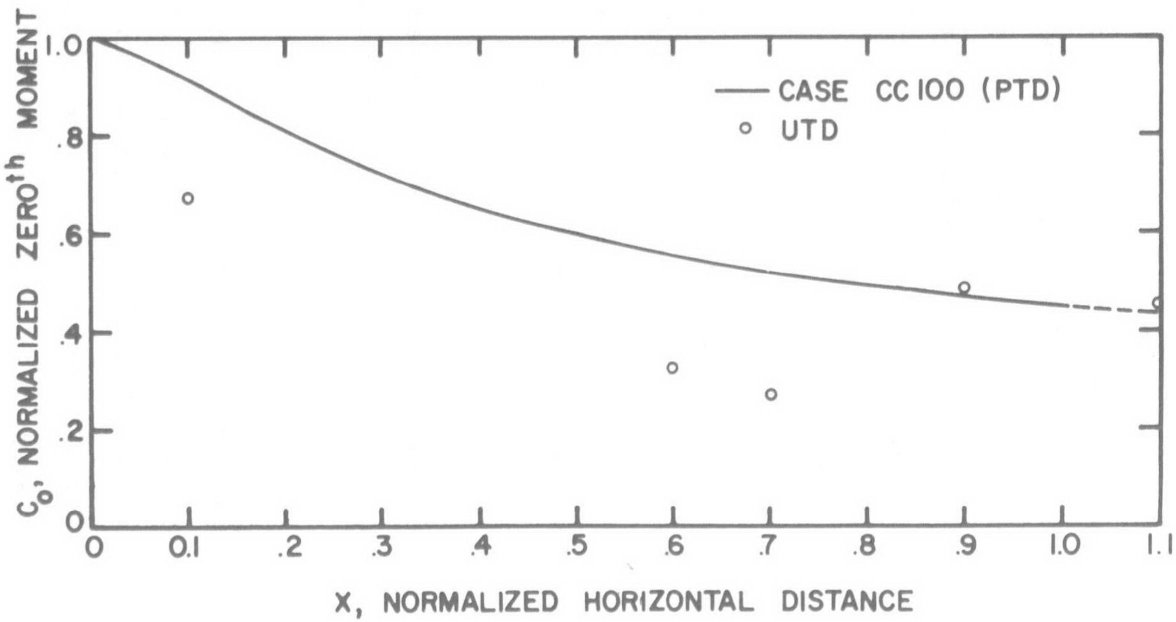

Figure 5.11 Comparison of PTD with UTD to illustrate effect of unsteady current, rate of heat discharged, and surface heat exchange coefficient.

5.5 Summary and Discussions

In this chapter, two mathematical models have been developed for the calculation of the distribution of excess temperature due to the effects of ambient turbulence, current, and surface heat exchange. Both models assume passive diffusion and ignore longitudinal dispersion. The first model (PTD) treats the case of a steady release into a steady unidirectional shear current while the second model (UTD) treats the case when the discharge, the ambient uniform current, and the surface heat exchange coefficient are time varying. Two computer programs (PTD and UTD) based on these models are listed in Appendices C and D. With these programs, the excess temperature distribution can be determined given the input conditions.

It should be pointed out that this model applies only after the initial phases of mixing (jet mixing and surface spreading) has subsided and the buoyancy of the discharge no longer influences the dynamics of the flow. The initial phases of mixing have been treated in earlier chapters of this report.

It was not possible to perform a detailed parametric study based on the models within the scope of this investigation. This should be done in the future.

Since in practical situations, the conditions are usually unsteady, the second model (UTD) is likely to be more useful. However, in that model the ambient current is assumed to be unidirectional and uniform whereas in practice, shear currents are likely to occur. The model should therefore be extended to include these effects. Such a model can be developed by using the concept of superposition. Thus, the case of an instantaneous release into a general environment should first be solved and the results superposed. This method has the further advantage of incorporating the longitudinal diffusion which is ignored in the present models.

It is recommended that this general model of unsteady passive turbulent diffusion in an arbitrary unsteady environment be developed in the future.

CHAPTER 6 APPLICATION OF THE MATHEMATICAL MODELS TO PRACTICAL PROBLEMS

In this report, several mathematical models and computer programs have been developed for the prediction of the excess temperature distribution in a large body of water resulting from the discharge of heat such as from power generation plants. Each of these models deals with a specific portion of the mixing phenomenon.

Although all these models are more general than previously existing ones, they cannot be regarded as complete. Moreover, no unified model is available which can calculate the excess temperature distribution from the beginning phase of discharge through the terminal stage of passive turbulent dispersion. It is the purpose of this chapter to provide a practical guideline by which the various models developed herein can be used in succession to arrive at the solution of practical problems.

Before discussing the practical application of these models, they will first be briefly summarized. In Chapter 3, two mathematical models have been developed. The first one (RBJ) solves the problem of mixing involved in a sub-surface discharge of heated water through a multiport diffuser from the discharge to the point when either the effluent reaches the surface of when it reaches its terminal level of ascent. This model is more general than previously available ones in that in includes jet interference and an arbitrary ambient density gradient. The second model developed in Chapter 3 deals with the time dependent surface spreading of the effluent. The primary purpose of that model is to provide time and length scales of the phenomenon. Application of this model requires several numerical coefficients which are as yet not available. These should be obtained by experiments in the future. In Chapter 4, the steady state surface buoyant jet discharged horizontally is analyzed. The two-dimensional case of a slot jet is analyzed in detail while the axisymmetric case is also investigated. The more realistic case of a slot jet of finite length is not solved and must await future studies. However, the two-dimensional case can be used in certain situations such as if the discharge slot is wide. In any case, the predictions based on the two-dimensional model should be conservative in the sense that the predicted temperature excess would be larger than the actual one, since the model does not include lateral mixing. In Chapter 5, again two models and computer programs are developed. The first one (PTD) examines the steady passive turbulent dispersion in a non-uniform current while the second one (UTD) examines the unsteady case. However, while PTD allows the current to vary with depth, UTD assumes a uniform, though time varying current. Previous models on this phase of dispersion assumes constant diffusities and uniform and steady conditions.

It is strongly recommended that before these models and computer programs are used in a practical situation, the individual using them thoroughly understand the assumptions involved in their derivation and their limitations. This can be achieved by studying the previous chapters of this report. With this in mind, the following sections of this chapter are prepared to aid in the practical applications of these models.

6.1 Subsurface Discharges

In the event the discharge of cooling water is made at depth, the program RBJ (Chapter 3) should first be used to obtain the buoyant jet portion of the mixing phenomenon. The reader is referred to Section 3.2.2 for a discussion on the use of this program. This program terminates the calculation either when the diluted effluent reaches the water surface or when it reaches its terminal level of ascent. This can be seen from the output of the program. In either case, the temperature excess, dilution ratio, and jet width at the end of this phase are available from the program output.

Having obtained these quantities, the program PTD (Chapter 5) should be used to continue the calculation. Besides the environmental conditions such as water depth, the diffusities, and current profiles the program PTD also requires knowledge of the initial conditions of h_o, y_o, and L_o, the source thickness, source level, and source width respectively. y_o should be taken as the terminal depth of ascent from RBJ if the pool is submerged or zero if the pool is surfaced. It should be noted that since, in PTD, the excess temperature is just being passively carried along, the flux of excess temperature, which is proportional to the product u L_o h_o C_{max} at the source of PTD, is known from the flux of excess temperature at the end of RBJ. Here u is the ambient current, C_{max} the excess temperature. Thus if we take C_{max} to be the same as provided by RBJ, then there is freedom in choosing only one of the two quantities L_o and h_o. Two choices are available. First, L_o may be chosen to be the total length of the diffuser plus the jet width. Second, h_o may be chosen to be half the jet width at the end of RBJ. It is proposed that separate calculations be made based on these choices and the worse of the two regarded as a conservative estimate for design purposes. The reader is referred to section 5.3.1.2 for a discussion of the environmental conditions. The program PTD uses dimensionless quantities in order to minimize the number of necessary inputs. These are defined in section 5.3.4. Also included in section 5.3.4 are example solutions which should serve as a guide on the use of the program. The output of the program include σ_z and C_{max} which are dimensionless plume width parameter and dimensionless plume width parameter and dimensionless centerline temperature excess, each normalized with respect to their values at the source center. From these and the output from RBJ, the actual temperature excess and plume width can be readily obtained.

6.2 Surface Discharge

In the event the discharge is made at the surface through a relatively wide discharge structure, the programs SBJ2 coupled with PTD can be used to provide an estimate of the excess temperature distribution. Since the program SBJ2 is based on a two-dimensional slot jet, the prediction would be more accurate the wider the actual discharge structure. In any event, the effect of lateral spreading (not included in SBJ2) is to widen the plume which would promote a faster rate of dispersion. Thus the use of SBJ2 constitutes a conservative approach.

The calculations based on SBJ2 should be carried out to the point of the internal hydraulic jump and from that point, the program PTD may be used using the conditions from SBJ2 after the jump as the source conditions for PTD. The source thickness for PTD may be chosen as the depth of the flowing layer from SBJ2. The source width L_o can then be obtained by a balance of the flux of excess temperature. In the event the source is inundated, the new source conditions can be obtained in the manner as described in example 2, section 4.4 This can then be used as the source condition for PTD. The event that SBJ2 would predict a jet all the way is not likely based on typical values of the relevant paramaters. In the unlikely event it is the case, then PTD is not needed. SBJ2 itself would probably provide a sufficient estimate of the temperature excess.

It should be reiterated that use of SBJ2 (two-dimensional) for a practical discharge structure (not two-dimensional) would result in overestimates of excess temperatures, thus leading to conservative designs. The three-dimensional problem analogous to SBJ2 should be analysed in the future to obtain a better prediction tool.

An alternative approach to the use of SBJ2 for the initial mixing stage, especially in the case of narrow discharge structures or in the event SBJ2 predicts a jet all the way, is to use simple submerged jet theory (e.g. Albertson, Et al (1950)) to calculate the dilution, based on which the excess temperature can be obtained. The actual temperature should be between the predictions based on these two alternatives (i.e. SBJ2-PTD and simple jet theory.)

REFERENCES

Abraham, G., "Jet Diffusion in Stagnant Ambient Fluid", Delft Hyd. Lab., Pub. No. 29 (1963).

Albertson, M. L., Dai, Y. B., Jensen, R. A., and Rouse, H., "Diffusion of Submerged Jets", Trans. ASCE, 115 (1950).

Bowden, K. F., "Turbulence", Chapter VI of "The Sea" Vol. I edited by M. N. Hill, Interscience Publishers, New York (1962).

Brooks, N. H., "Diffusion of Sewage Effluent in an Ocean Current", Waste Disposal in the Marine Environment, Pergamon Press, Inc., New York, New York.

Brooks, N. H. and Koh, R. C. Y., "Discharge of Sewage Effluent from a Line Source into a Stratified Ocean", XI Congress, Int'l Assoc. for Hydr. Res. (1965).

Defant, A., "Physical Oceanography", Vol. I, The MacMillan Co., New York, New York (1961).

Edinger, J. E. and Geyer, J. C., "Heat Exchange in the Environment", Research Project RP-49, Dept. of Sanitary Engineering and Water Resources, The John Hopkins University, Baltimore, Maryland, June (1965).

Edinger, J. E. and Polk, E. M., "Initial Mixing of Thermal Discharges into a Uniform Current", Report No. 1, National Center for Research and Training in the Hydraulic Aspects of Water Pollution Control, Department of Environmental and Water Resources Engineering, Vanderbilt University, Nashville, Tenn. Oct. (1969).

Ellison, T. H. and Turner, J. S., "Turbulent Entrainment in Stratified Flows", J. Fluid Mech., Vol. 6, Pt. 3, Oct. (1959).

Fan, L. N., "Turbulent Buoyant Jets into Stratified or Flowing Ambient Fluids", Rept. No. KH-R-15, W. M. Keck Lab. of Hydr. and Water Resources, Calif. Inst. of Tech., Pasadena, California (1967).

Foxworthy, J. E., "Eddy Diffusivity and the Four-thirds Law in Near-shore (Coastal Waters)", Allan Hancock Foundation, Rept. 68-1, Univ. of Southern California (1968).

Golubeva, V. N., "The Formation of the Temperature Field in a Stratified Sea", Bull. of Acad. of Sci. of the USSR, Geophy. Ser. (Transl. by F. Goodspeed), No. 5, pp. 4670-4671 (1964).

Harremos, P., "Diffuser Design for Discharge to a Stratified Water", The Danish Isotope Center, Copenhagen, Denmark, 18 pages (1967).

Hayashi, T. and Shuto, N., "Diffusion of Warm Water Jets Discharged Horizontally at the Water Surface", Proc. XII Cong., Int'l Assoc. for Hydr. Res. (1967).

Isayeva, L. S. and Isayev, I. L., "Determination of Vertical Eddy Diffusion in the Upper Layer of the Black Sea by a Direct Method", Issue No. 2, 1963 series, Soviet Oceanography Trans. of the Marine Hydro-physical Institute, Acad. of Sci. of the USSR, (Transl. by Scripta Technica, Inc.) pp. 22-24 (1963).

Jen, Y., Weigel, R., and Mobarek, J., "Surface Discharge of Horizontal Warm Water Jet", Proc. ASCE, J. Power Div., Vol. 92 (1966).

Keulegan, G. H., "Laminar Flow at the Interface of Two Liquids", J. Res. Nat. Bur. Stands., 32 (1944).

Kolesnikov, A. G., Ivanova, Z. S., and Boguslavska, S. G., "The Effect of Stability on the Intensity of Vertical Transfer in the Atlantic Ocean", Okeanologiya, Vol. 1, (4), English Translation (1961).

Kolesnikov, A. G., Panteleyev, N. A., and Pisarev, V. D., "Results of Direct Determination of the Intensity of Deep Turbulent Exchange in the Atlantic", Dokl. Akad. Nauk USSR, 155, No. 4, (Transl. by Scripta Technica, Inc.), pp. 3-6 (1964).

Lean, G. H. and Whillock, A. Z., "The Behavior of a Warm Water Layer Flowing Over Still Water", Eleventh International Congress, IAHR, Leningrad (1965).

Lofquist, K., "Flow and Stress Near an Interface Between Stratified Liquids", Physics of Fluids, 3 (1960).

Morton, B. R., Taylor, G. I., and Turner, J. S., "Turbulent Gravitational Convection From Maintained and Instantaneous Sources", Proc. Roy. Soc. London (A), 234 (1956).

Munk, W. H., Ewing, G. C., and Revelle, R. R., "Diffusion in Bikini Lagoon", Trans. Amer. Geophy. Union, 30, (1), pp. 59-66, February (1949).

Okubo, A., "A Review of Theoretical Models for Turbulent Diffusion in the Sea", J. of Ocean. Soc. of Japan, 20th Anniv. Vol. (1962).

Orlob, G. T., "Eddy Diffusion in Homogeneous Turbulence", J. Hyd. Div. Proc. ASCE, September (1959).

Orlob, G. T. and Selna, L. G., "Temperature Variations in Deep Reservoirs", J. Hyd. Div. Proc. ASCE, Feb. (1970).

Ozmidov, R. V., "Turbulent Exchange in a Stably Stratified Ocean", Bull. Acad. of Sci. of the USSR, Atm. and Oceanic Phys. Ser. 1, (Transl. by D. and V. Barcilon), pp. 493-497 (1965).

Parr, A. E., "On the Probable Relationship Between Vertical Stability and Lateral Mixing Processes", J. Conseil, perman. internat. explorat. mer., 11, No. 3 (1936).

Riley, G., "Parameters of Turbulence in the Sea", J. Marine Res., 10, No. 3 (1951).

Schlichting, H., "Boundary Layer Theory", McGraw Hill, New York, New York (1960).

Schuert, E. A., "Turbulent Diffusion in the Intermediate Waters of the North Pacific Ocean", J. Geophysical Research, 75 (1970).

Sharp, J. J., "Spread of Buoyant Jets at the Free Surface", J. Hyd. Div., Proc. ASCE, May and Sept. (1969).

Snyder, W. H., "A Field Test of the Four-Thirds Law of Horizontal Diffusion in the Ocean", M. S. Thesis Dissertation, U. S. Naval Postgrad. School, June (1967).

Stefan, H. and Schiebe, F. R., "Experimental Study of Warm Water Flow into Impoundments, Part I, II and III", Rept. 101, 102 and 103, St. Anthony Falls Hydr. Lab., Minneapolis, Minn. (1968).

Wada, A., "A Study on Phenomena of Flow and Thermal Diffusion Caused by Outfall of Cooling Water", Proc. 10th Conference on Coastal Engineering, Tokyo, Japan, Vol. II, Sept. (1966).

Yih, C. S., "Dynamics of Nonhomogeneous Fluids", The MacMillan Co. (1965).

APPENDIX A

The problem discussed in Chapter 3 on the dispersion in a row of buoyant jets can be solved using the program listed in this appendix. The numerical integration utilizes a fourth order Runge-Kutta scheme. To facilitate the use of the program, the following lists are prepared relating the names of variables used in the text to those used in the program.

Input:

In Text	In Program	Remarks
--	NC	number of points for specifying ambient
D_o	DO	diameter of individual jets
u_o	UO	velocity of jet discharge
T_1	TO	temperature of discharge
ρ_1	DEN1	density of discharge
θ_o	THETAO	angle of discharge
d	DJ	depth of discharge
L	SPACJ	jet spacing
--	D(I=1, NC)	depth at which ambient specified
T_a	TA(I=1, NC)	ambient temperature
ρ_a	DENA(I=1, NC)	ambient density
α_r	ALPHAR	
α_s	ALPHAS	
λ_r	LAMBDR	
λ_s	LAMBDS	
g	GRAVAC	gravitational acceleration

Output:

In Text	In Program	Remarks
x	X	
y	Y	
$2\sqrt{2}\,b$	JET WIDTH	
Q/Q_1	DILUTION	
T	JET TEMP	
ρ	JET DENSITY	
ρ_a	AMB DEN	
T_a	AMB TEMP	
$T - T_a$	DELTA T	

```
C       PROGRAM RBJ--ROW BUOYANT JET IN A STABLY DENSITY-STRATIFIED ,
C         STAGNANT ENVIRONMENT
        DIMENSION TA(50),D(50),DENA(50),ET(50),ED(50),YT(50)
        DIMENSION Y(6),YP(6)
        REAL LAMBDR,LAMBDS,M
        COMMON LAMBDR,LAMBDS,M,H,ALPHAR,ALPHAS,  NC,ET,ED,PAI,GRAVAC,YT,IK
       1,ICHEK,IQ,SPACJ
    204 READ (5,1) NC,DO,UO,TO,DEN1,THETAO,DJ,SPACJ
      1 FORMAT(1I10,7E10.5)
        IF (DO)  2,2,3
      2 CALL EXIT
      3 READ (5,10)  (D(I),TA(I),DENA(I),I=1,NC)
     10 FORMAT(3E10.5)
        READ (5,11) ALPHAR,ALPHAS,LAMBDR,LAMBDS,GRAVAC
     11 FORMAT(8E10.5)
        PAI=3.14159265
        DO 999 I=1,NC
    999 YT(I)=DJ-D(I)
        THETA=THETAO*PAI/180.
        ICHEK=0
        L=0
C       CHECK PHYSICAL UNITS
        IF (GRAVAC-900.) 97,97,98
     97 IF (GRAVAC-30.) 101,99,99
C       IN FPS UNITS
     99 WRITE (6,100) DO,UO,TO,DEN1,THETAO,DJ,SPACJ
    100 FORMAT (75H1ROW BUOYANT JETS IN AN ARBITRARILY DENSITY STRATIFIED
       1STAGNANT ENVIRONMENT///5X, 13HJET DIAMETER=,1F6.2,4HFEET,5X,
       223HJET DISCHARGE VELOCITY=,1F6.2,8HFEET/SEC/5X, 26HJET DISCHARGE T
       3EMPERATURE=,1F6.2,13HDEGREE FAHREN, 5X, 22HJET DISCHARGE DENSITY=,
       41F10.7, 11HGRAM PER ML/4X,18H JET DISCH. ANGLE=, 1F6.2,8H DEGREES/
       55X,20HJET DISCHARGE DEPTH=,1F6.2,4HFEET,   5X,16HJET SPACING C-C=,
       61F6.2,4HFEET)
        GO TO 110
C       IN MKS UNITS
    101 WRITE (6,102) DO,UO, TO, DEN1, THETAO,DJ, SPACJ
    102 FORMAT (75H1ROW BUOYANT JETS IN AN ARBITRARILY DENSITY STRATIFIED
       1STAGNANT ENVIRONMENT///5X, 13HJET DIAMETER=,1F6.2,6HMETERS,5X,
       223HJET DISCHARGE VELOCITY=,1F6.2,8HMET./SEC/5X, 26HJET DISCHARGE T
```

```
     3EMPERATURE=,1F6.2,13HDEGREE CENTIG, 5X, 22HJET DISCHARGE DENSITY=,
     41F10.7, 11HGRAM PER ML/4X,18H JET DISCH. ANGLE=, 1F6.2,8H DEGREES/
     55X,20HJET DISCHARGE DEPTH=,1F6.2,6HMETERS, 5X,16HJET SPACING C-C=,
     61F6.2,6HMETERS)
      GO TO 110
C     IN CGS UNITS
   98 WRITE (6,103) DO,UO, TO, DEN1, THETAO,DJ, SPACJ
  103 FORMAT (75H1ROW BUOYANT JETS IN AN ARBITRARILY DENSITY STRATIFIED
     1STAGNANT ENVIRONMENT///5X, 13HJET DIAMETER=,1F6.2,4H CM.,5X,
     223HJET DISCHARGE VELOCITY=,1F6.2,8H CM./SEC/5X, 26HJET DISCHARGE T
     3EMPERATURE=,1F6.2,13HDEGREE CENTIG, 5X, 22HJET DISCHARGE DENSITY=,
     41F10.7, 11HGRAM PER ML/4X,18H JET DISCH. ANGLE=, 1F6.2,8H DEGREES/
     55X,20HJET DISCHARGE DEPTH=,1F6.2,4H CM.,   5X,16HJET SPACING C-C=,
     61F6.2,4H CM.)
  110 WRITE (6,111)
  111 FORMAT (///5X,1HX,10X,1HY,12X,9HJET WIDTH,6X,8HDILUTION,6X,8HJET T
     1EMP,4X, 11HJET DENSITY,6X,8HAMB DEN ,5X, 8HAMB TEMP,4X,7HDELTA T)
      S=0.
C     TO FIND REFERENCE TEMPERATURE AND DENSITY
      IR=1
      IF (DJ-D(IR))  112,113,114
  113 TR=TA(IR)
      DENR=DENA(IR)
      GO TO 118
  112 IR=IR+1
      IF (DJ-D(IR)) 112,113,117
  114 WRITE (6,120)
  120 FORMAT(5X,53H INSUFFICIENT DATA ON AMBIENT DENSITY AND TEMPERATURE
     1)
      GO TO 204
  117 SL=(DJ-D(IR))/(D(IR-1)-D(IR))
      TR=TA(IR)+SL*(TA(IR-1)-TA(IR))
      DENR=DENA(IR)+SL*(DENA(IR-1)-DENA(IR))
C     INITIAL CONDITIONS
  118 Y(1)=PAI*DO*DO*UO*0.5
      M=Y(1)*UO*0.5
      VOLFJ=Y(1)
      H=M*COS(THETA)
      Y(2)=M*SIN(THETA)
```

```
      Y(3)=Y(1)*(DENR-DEN1)/DENR*0.5
      Y(4)=Y(1)*(TR-TO)/TR*0.5
      Y(5)=6.2*DO*COS(THETA)
      Y(6)=6.2*DO*SIN(THETA)
      IQ=0
      IP=0
      IK=2
      SQLAM=(1.+LAMBDR*LAMBDR)/(LAMBDR*LAMBDR)
      SQRLAM=SQRT(1.+LAMBDS*LAMBDS)/LAMBDS
C     CALCULATION OF DENSITY AND TEMPERATURE GRADIENTS
      NC1=NC-1
      DO 912 I=1,NC1
      I1=I+1
      DP1=YT(I1)-YT(I)
      ET(I)=(TA(I1)-TA(I))/(TR*DP1)
  912 ED(I)=(DENA(I1)-DENA(I))/(DENR*DP1)
C     CHOICE OF INTEGRATION STEP
      DS1=DO/20.
      DS2=DJ/2000.
      K=1
      IF (DS1-DS2) 301,301,302
  301 DS=DS1
      GO TO 303
  302 DS=DS2
C      INTEGRATION BY RUNGE-KUTTA METHOD
      K=1
  303 CALL RUNGS (S,DS,6,Y,YP,L)
  304 Y20=Y(2)
      CALL RUNGS (S,DS,6,Y,YP,L)
      IF (Y(2)*Y20) 20,21,21
   20 K=K+1
      IF (K-3) 21,22,22
   22 IF (ICHEK-1) 204,511,204
   21 CONTINUE
C     LOOP FOR TRANSITION POINT TWO
      IF (ICHEK-2) 513,514,204
  513 IF (ICHEK-1) 203,206,206
  203 TRANW=SPACJ
C     ROUND JET SOLUTION
```

```
  514 IF (Y(6)-DJ) 530,531,531
  531 WRITE (6,532)
  532 FORMAT (10X,20HTHIS IS FREE SURFACE)
      GO TO 204
  530 IF (IQ) 533,533,206
  533 M=SQRT(H*H+Y(2)*Y(2))
      WIDTH=2.*Y(1)/SQRT(PAI*M)
      IF (WIDTH-TRANW) 207,206,206
C     PRINT SPACING CONTROL
  207 SJP=2.*DO
      PI=IP*SJP
      IF (S-PI)  220,221,221
  220 GO TO 304
  221 IP=IP+1
      DENDIF=SQLAM*DENR*Y(3)/Y(1)
      TDIF=SQLAM*TR*Y(4)/Y(1)
      DILU=Y(1)/VOLFJ
      IF (DENDIF) 401,920,920
  401 DENDIF=DENDIF*0.5
      TDIF=0.5*TDIF
C     TO FIND AMBIENT DENSITY AND TEMPERATURE VALUES
  920 IY=2
  906 IF (Y(6)-YT(IY))  900,901,902
  901 DENAA=DENA(IY)
      TAA=TA(IY)
      IY=IY+1
      GO TO 909
  900 IY=IY-1
      IF (Y(6)-YT(IY)) 900,901,905
  905 IYY=IY+1
      SYY=(Y(6)-YT(IYY))/(YT(IY)-YT(IYY))
      TAA=SYY*(TA(IY)-TA(IYY))+TA(IYY)
      DENAA=SYY*(DENA(IY)-DENA(IYY))+DENA(IYY)
      GO TO 909
  902 IY=IY+1
      GO TO 906
  909 TJ=TAA-TDIF
      DENJ=DENAA-DENDIF
      TDIFM=-TDIF
```

```
      WRITE (6,222) Y(5), Y(6),WIDTH, DILU, TJ, DENJ,DENAA, TAA,TDIFM
  222 FORMAT (9G14.7)
      GO TO 304
C     SLOT JET SOLUITON
C     CHECK TRANSITION POINT ONE OR TWO
  206 IF (Y(6)-DJ) 522,511,511
  511 ICHEK=ICHEK+1
      IF (ICHEK-2) 512,512,204
C     TRANSITION POINT TWO
  512 S=SO
      Y(1)=Y1
      Y(2)=Y2
      Y(3)=Y3
      Y(4)=Y4
      Y(5)=Y5
      Y(6)=Y6
      IP=IPC
      IK=IKC
      IQ=0
      IY=IYC
      L=0
      K=KI
      WRITE (6,520)
  520 FORMAT (10X, 20HTRANSITION POINT TWO)
      GO TO 303
  522 IQ=1
      IF (ICHEK-1) 240,241,241
C     TRANSITION POINT ONE
  240 WRITE (6,1222)
 1222 FORMAT (10X, 20HTRANSITION POINT ONE)
C     STORE SOLUTIONS AS INITIAL CONDITIONS FOR TRANSITION POINT TWO
      SO=S
      Y1=Y(1)
      Y2=Y(2)
      Y3=Y(3)
      Y4=Y(4)
      Y5=Y(5)
      Y6=Y(6)
      TRANW=2.*ALPHAS*SPACJ/(PAI*ALPHAR)
```

```
      IPC=IP
      KI=K
      IKC=IK
      ICHEK=ICHEK+1
      IYC=IY
C     PRINT SPACING CONTROL
  241 PI=IP*SJP
      IF (S-PI)  304,501,501
  501 IP=IP+1
      M=SQRT(H*H+Y(2)*Y(2))
      WIDTH=Y(1)*Y(1)/(SQRT(PAI)*M*SPACJ)*2.
      DENDIF=SQRLAM*DENR*Y(3)/Y(1)
      TDIF=SQRLAM*TR*Y(4)/Y(1)
      DILU=Y(1)/VOLFJ
      IF (DENDIF) 402, 906,906
  402 CONST=0.5*SQRT(PAI*0.5)
      DENDIF=CONST*DENDIF
      TDIF=CONST*TDIF
      GO TO 906
      END
```

```
      SUBROUTINE  DERIVE (S,N,Y,YP)
      DIMENSION Y(6), YP(6)
      DIMENSION ET(50),ED(50),YT(50)
      REAL LAMBDR,LAMBDS, M
      COMMON LAMBDR,LAMBDS,M,H,ALPHAR,ALPHAS,  NC,ET,ED,PAI,GRAVAC,YT,IK
     1,ICHEK,IQ,SPACJ
C     COMPUTATION OF DENSITY AND TEMPERATURE GRADIENTS AT Y
  814 IF (Y(6)-YT(1)) 811,811,812
  812 IF(Y(6)-YT(NC)) 806,813,813
  811 EDD=ED(1)
      ETT=ET(1)
      GO TO 70
  813 EDD=ED(NC-1)
      ETT=ET(NC-1)
      GO TO 70
  806 IF (Y(6)-YT(IK)) 800,801,802
  801 EDD=(ED(IK)+ED(IK-1))*0.5
      ETT=(ET(IK)+ET(IK-1))*0.5
      IK=IK+1
      GO TO 70
  800 IK=IK-1
      IF(Y(6)-YT(IK)) 800,801,805
  805 EDD=ED(IK)
      ETT=ET(IK)
      IK=IK+1
      GO TO 70
  802 IK=IK+1
      IF (IK-NC) 814,814,807
  807 WRITE (6,808)
  808 FORMAT(10X,25H THIS IS THE FREE SURFACE)
      RETURN
   70 IF (IQ) 71,71,72
C     ROUND JET SOLUTION
   71 ENTRAN=2.*ALPHAR*SQRT(2.*PAI*M)
      CLAM=(1.+LAMBDR*LAMBDR)/2.
      GO TO 73
C     SLOT JET SOLUTION
   72 ENTRAN=2.*SQRT(2.)*ALPHAS*SPACJ*M/Y(1)
      CLAM=SQRT((1.+LAMBDS*LAMBDS)/2.)
```

```
   73 SQROTM=SQRT(Y(2)*Y(2)+H*H)
      YP(1)=ENTRAN
      YP(2)=CLAM*GRAVAC*Y(1)*Y(3)/SQROTM
      YP(3)=Y(1)*EDD*Y(2)/SQROTM
      YP(4)=Y(1)*ETT*Y(2)/SQROTM
      YP(5)=H/SQROTM
      YP(6)=Y(2)/SQROTM
      RETURN
      END
```

```
      SUBROUTINE  RUNGS (X,H,N,Y,YPRIME,INDEX)
      DIMENSION Y(7),YPRIME(7),Z(7),W1(7),W2(7),W3(7),W4(7)
CRUNGS - RUNGE-KUTTA SOLUTION OF SET OF FIRST ORDER O.D.E.  FORTRAN II
C     DIMENSIONS MUST BE SET FOR EACH PROGRAM
C     X   INDEPENDENT VARIABLE
C     H   INCREMENT DELTA X, MAY BE CHANGED IN VALUE
C     N   NUMBER OF EQUATIONS
C     Y   DEPENDENT VARIABLE BLOCK     ONE DIMENSIONAL ARRAY
C     YPRIME  DERIVATIVE BLOCK  ONE DIMENSIONAL ARRAY
C     THE PROGRAMMER MUST SUPPLY INITIAL VALUES OF  Y(1) TO Y(N)
C     INDEX  IS A VARIABLE WHICH SHOULD BE SET TO ZERO BEFORE EACH
C     INITIAL ENTRY TO THE SUBROUTINE, I.E., TO SOLVE A DIFFERENT
C     SET OF EQUATIONS OR TO START WITH NEW INITIAL CONDITIONS.
C     THE PROGRAMMER MUST WRITE A SUBROUTINE CALLED DERIVE WHICH COM-
C     PUTES THE DERIVATIVES AND STORES THEM
C     THE ARGUMENT LIST IS   SUBROUTINE DERIVE(X,N,Y,YPRIME)
      IF (INDEX) 5,5,1
    1 DO 2 I=1,N
      W1(I)=H*YPRIME(I)
    2 Z(I)=Y(I)+(W1(I)*.5)
      A=X+H/2.
      CALL DERIVE(A,N,Z,YPRIME)
      DO 3 I=1,N
      W2(I)=H*YPRIME(I)
    3 Z(I)=Y(I)+.5*W2(I)
      A=X+H/2.
      CALL DERIVE(A,N,Z,YPRIME)
      DO 4 I=1,N
      W3(I)=H*YPRIME(I)
    4 Z(I)=Y(I)+W3(I)
      A=X+H
      CALL DERIVE (A,N,Z,YPRIME)
      DO 7 I=1,N
      W4(I)=H*YPRIME(I)
    7 Y(I)=Y(I)+(((2.*(W2(I)+W3(I)))+W1(I)+W4(I))/6.)
      X=X+H
      CALL DERIVE (X,N,Y,YPRIME)
      GO TO 6
    5 CALL DERIVE (X,N,Y,YPRIME)

      INDEX=1
    6 RETURN
      END
```

APPENDIX B

The problem discussed in Chapter 4 on the two-dimensional surface buoyant jet can be solved using the program listed in this appendix. The reader should fully understand the investigation reported in Chapter 4 (Sec. 4.2) before attempting to use this program. To facilitate the use of the program, the following lists are prepared relating the names of variables used in the text to those used in the program.

Input:

In Text	In Program SBJ2	Remarks
e_o	E	entrainment coefficient
k	CAY	dimensionless surface heat exchange coefficient
F_o	F2	densimetric Froude number
$1/R$	EPS	inverse of Reynolds number
	XSTOP	value of x to stop integration
	D	control variable for step size
	D1	" " " " "

Output:

e_o	E	
F_o	F2	
x	X	dimensionless distance
T	T	dimensionless density deficiency
u	U	dimensionless velocity
h	H	dimensionless thickness
$F = F_o \frac{u^2}{Th}$	FR	local densimetric Froude number
h_2	H2	layer thickness after jump
F_2	FR2	Froude number after jump

```
C
C      PROGRAM SBJ2-TWO DIMENSIONAL SURFACE HORIZONTAL BUOYANT JET
C      ESP IS 1/RE
C
          DIMENSION Y(3),YP(3)
          COMMON E,CAY,F2,EPS,XSTOP,DX,DXP
        1 READ(5,10,END=999) E,CAY,F2,EPS,XSTOP,D1,D
       10 FORMAT(7F10.6)
          WRITE(6,1000) E,CAY,F2,EPS
     1000 FORMAT(1H1,1X,2HE=,F10.6,2HK=,F10.6,3HF2=,F10.3,4HEPS=,F10.6,///,
         17X,1HX,13X,1HT,13X,1HU,13X,1HH,13X,2HFR,12X,2HH2,12X,3HFR2)
          XPRINT=0.0
          IF(F2.LE.1.) XSTOP= 8./CAY
          IF(F2.LE.1.) D1=0.1
          IF(F2.LE.1.)  D=1./ 50./CAY
          DX=D1*D
          DXP=DX-0.00001
          X=0.0
          Y(1)=1.0
          Y(2)=1.0
          Y(3)=1.0
          N=3
          L=0
          CALL RUNGS(X,DX,N,Y,YP,L)
        3 CALL RUNGS(X,DX,N,Y,YP,L)
          IF(X.LE.XPRINT) GO TO 3
          IF(X.GE.10.*D) DX=0.2*D
          IF(X.GE.40.*D) DX=0.5*D
          IF(X.GE.100.*D) DX=D
          IF(X.GE.200.*D) DX=2.*D
          IF(X.GE.500.*D) DX=5.*D
          IF(X.GE.1000.*D) DX=10.*D
          IF(X.GE.D) DXP=10.*DX-0.00001
          FR=Y(2)*Y(2)/Y(1)/Y(3)*F2
          IF(FR.LE.0.) GO TO 1
          H2H1=(SQRT(1.+8.*FR)-1.)/2.
          FR2=FR/H2H1**3
          H2=H2H1*Y(3)
          XX=X+0.00001
```

```
      WRITE(6,100)XX,Y(1),Y(2),Y(3),FR,H2,FR2
  100 FORMAT(1H ,7G14.7)
      IF(F2.LT.1.) GO TO 11
      IF(FR.LE.1.) GO TO 1
   11 IF(X.GE.XSTOP) GO TO 1
      XPRINT=XPRINT+DXP
      GO TO 3
  999 CALL EXIT
      END
```

```
      SUBROUTINE  RUNGS (X,H,N,Y,YPRIME,INDEX)
      DIMENSION Y(3),YPRIME(3),Z(3),W1(3),W2(3),W3(3),W4(3)
CRUNGS - RUNGE-KUTTA SOLUTION OF SET OF FIRST ORDER O.D.E.  FORTRAN II
C     DIMENSIONS MUST BE SET FOR EACH PROGRAM
C     X   INDEPENDENT VARIABLE
C     H   INCREMENT DELTA X, MAY BE CHANGED IN VALUE
C     N   NUMBER OF EQUATIONS
C     Y   DEPENDENT VARIABLE BLOCK     ONE DIMENSIONAL ARRAY
C     YPRIME  DERIVATIVE BLOCK  ONE DIMENSIONAL ARRAY
C     THE PROGRAMMER MUST SUPPLY INITIAL VALUES OF  Y(1) TO Y(N)
C     INDEX  IS A VARIABLE WHICH SHOULD BE SET TO ZERO BEFORE EACH
C     INITIAL ENTRY TO THE SUBROUTINE, I.E., TO SOLVE A DIFFERENT
C     SET OF EQUATIONS OR TO START WITH NEW INITIAL CONDITIONS.
C     THE PROGRAMMER MUST WRITE A SUBROUTINE CALLED DERIVE WHICH COM-
C     PUTES THE DERIVATIVES AND STORES THEM
C     THE ARGUMENT LIST IS   SUBROUTINE DERIVE(X,N,Y,YPRIME)
      IF (INDEX) 5,5,1
    1 DO 2 I=1,N
      W1(I)=H*YPRIME(I)
    2 Z(I)=Y(I)+(W1(I)*.5)
      A=X+H/2.
      CALL DERIVE(A,N,Z,YPRIME)
      DO 3 I=1,N
      W2(I)=H*YPRIME(I)
    3 Z(I)=Y(I)+.5*W2(I)
      A=X+H/2.
      CALL DERIVE(A,N,Z,YPRIME)
      DO 4 I=1,N
      W3(I)=H*YPRIME(I)
    4 Z(I)=Y(I)+W3(I)
      A=X+H
      CALL DERIVE (A,N,Z,YPRIME)
      DO 7 I=1,N
      W4(I)=H*YPRIME(I)
    7 Y(I)=Y(I)+(((2.*(W2(I)+W3(I)))+W1(I)+W4(I))/6.)
      X=X+H
      CALL DERIVE (X,N,Y,YPRIME)
      GO TO 6
    5 CALL DERIVE (X,N,Y,YPRIME)
      INDEX=1
    6 RETURN
      END
```

```
      SUBROUTINE DERIVE(X,N,Y,YP)
      DIMENSION Y(3),YP(3)
      COMMON E,CAY,F2,EPS,XSTOP,DX,DXP
      EE=E*FUN(Y(1)*Y(3)/Y(2)/Y(2)/F2)
      YP(1)=-CAY*Y(1)/Y(2)/Y(3)-EE*Y(1)/Y(3)
      YP(3)=(-2.*EE-Y(3)*Y(3)*YP(1)/2./F2/Y(2)/Y(2)-EPS/Y(3)/Y(2))/(Y(1)
     1*Y(3)/F2/Y(2)/Y(2)-1.)
      YP(2)=Y(2)/Y(3)*(EE-YP(3))
      RETURN
      END
```

```
      FUNCTION FUN(X)
      IF(X.GE.0.85) FUN=0.
      IF(X.LT.0.85) FUN=(2./(1.+X/0.85)-1.)**1.75
      RETURN
      END
```

APPENDIX C

The problem discussed in Chapter 5 on the passive turbulent dispersion from a steady source can be solved using the program listed in this appendix. The numerical scheme used is based on the Crank-Nicolson method. To facilitate the use of the program, the following lists are prepared relating the names of variables used in the text to those used in the program.

Input:

In Text	In Program	Remarks
--	NEND	A program control number. If not equal to zero program will continue, otherwise the program will exit.
--	NDY	number of variations of y-mesh schemes
--	NDX	number of variations of x-step sizes
--	NEXP	number if variables $< 10^{-NEXP}$, it will take it zero
λ	LAMBDA	dimensionless quantity
y_o	YO	" "
h_o	HO	" "
u_o	UFS	" "
y_{e1}	YE1	" "
y_e	YE	" "
y_{K1}	YK1	" "
y_{K2}	YK2	" "
y_{K3}	YK3	" "
y_{K4}	YK4	" "
β_1	BETA1	" "
β_2	BETA2	" "
K_e	CKE	" "
K_d	CKD	" "

Input (continued):

In Text	In Program	Remarks
--	XDY(I)	x to change y-mesh scheme
--	NDYT(I)	number of y-mesh changes
--	NPR(I)	number of printout of the y-mesh lines
--	DY(I, J)	mesh size in y constant for NYC grids
--	NYC(I, J)	number of grids that y has mesh size DY
--	DX(I)	step size in x constant for NXC steps
--	NXC(I)	number of steps that x has step size DX
--	NPX	number of x steps for one printout

Output:

See Input List	LAMBDA	See Input List
"	YO	"
"	HO	"
"	YK1	"
"	YK2	"
"	YK3	"
"	YK4	"
"	BETA1	"
"	BETA2	"
"	UFS	"
"	YE1	"
"	YE	"
K_e	KE	dimensionless quantity
K_d	KD	" "
y	Y	" "
c_o	CO	" "
σ_z	SIGMAZ	" "
c_{max}	CMAX	" "

```
                 C       PROGRAM PTD -PASSIVE TURBULENT DIFFUSION OF A CONTINUOUS SOURCE
0001                     INTEGER OT
0002                     REAL LAMBDA
0003                     DIMENSION A(100),B(100),C(100),D(100),F(100),Y(100),CM(100,3),
                        1SOL(100,3),Y0(99),SZ(99),CMAX(99),  DY(9,9),  DX(9),NYC(9,9),
                        2NXC(9),NTAB(9),X1(9),X2(9),C0(99),U(99)
0004                     DIMENSION NDYT(9),YY(100),NPX(9),XDY(9),NPR(9)
0005                     COMMON LAMBDA,Y0,H0,YE1,YE,YK1,YK2,YK3,YK4,BETA1,BETA2,CKE,CKD,
                        1Y,CM,UFS
0006                     COMMON /HOLD/A,B,C,D,F,SOL,Y0,SZ,CMAX,C0
0007                     OT=6
0008                 100 READ (5,1)NEND,NDY,NDX,NEXP
0009                   1 FORMAT(10I5)
0010                     PAI=3.1415927
0011                     TESTXP=1./10.**NEXP
0012                     IF (NEND) 3,4,3
0013                   4 CALL EXIT
0014                   3 READ(5,2) LAMBDA,Y0,H0,UFS, YE1,YE,YK1,YK2,YK3,YK4,BETA1,BETA2,
                        1 CKE,CKD
0015                   2 FORMAT (8E10.5)
0016                     READ (5,834) (XDY(I),NDYT(I),NPR(I), I=1,NDY)
0017                 834 FORMAT (8(F5.1,I3,I2))
0018                 832 DO 24 I=1,9
0019                     DO 847 J=1,9
0020                     DY(I,J)=0.0
0021                 847 NYC(I,J)=0
0022                     X1(I)=0.0
0023                     X2(I)=0.0
0024                     DX(I)=0.0
0025                     NXC(I)=0.0
0026                  24 NTAB(I)=0
0027                  58 WRITE (OT,6) LAMBDA,Y0,H0,YK1,YK2,YK3,YK4,BETA1,BETA2,UFS,
                        1YE1,YE,CKE,CKD
0028                   6 FORMAT(9H1LAMBDA =,G12.5,//7H  Y0  =,G12.5,15X,5H H0 =,G12.5,//9H
                        1KY-PROF.,2X,4HYK1=,G12.5,2X,4HYK2=,G12.5,4HYK3=,G12.5,2X,4HYK4=,
                        2G12.5,2X,6HBETA1=,G12.5,2X,6HBETA2=,G12.5//9H U-PROF. ,2X,5HUFS =,
                        3G12.5,2X,4HYE1=,G12.5,2X,3HYE=,G12.5,//17H SURFACE EXCHANGE,5X,
                        45H KE =,G12.5,//13H DECAY COEFF.,10X,5H KD =,G12.5/)
0029                     NDY1=NDY-1
```

```
      DO 110 I=1,NDY1
      NSAV=NDYT(I)
      READ (5,5) (DY(J,I), NYC(J,I),J=1,NSAV)
      WRITE (OT,111) I, XDY(I)
      WRITE (OT,7) (DY(J,I), NYC(J,I),J=1,NSAV)
  111 FORMAT (I10,5X,6H    X =,G12.5)
  110 CONTINUE
      READ (5,55) (DX(I),NXC(I),NPX(I),I=1,NDX)
   55 FORMAT (4(E10.5,2I5))
    5 FORMAT (4(E10.5,I5,5X))
      WRITE (OT,7) (DX(I),NXC(I),I=1,NDX)
    7 FORMAT (5(G12.5,I5))
C     SET UP TABLE
      EKE=CKE*DY(1,1)
      Y(1)=-DY(1,1)
      Y(2)=0.
      K=2
      NSAV=NDYT(1)
      DO 10 I=1,NSAV
      DELY=DY(I,1)
      NUM=NYC(I,1)
      DO 15 J=1,NUM
      K=K+1
      Y(K)=Y(K-1)+DELY
   15 CONTINUE
   10 NTAB(I)=K
      NPRINT=NPR(1)+1
      NTAB(NSAV)=0
      M=K+1
      Y(M)=Y(K)+DELY
      M1=M-1
      M2=M1-1
      WRITE (OT,8) (Y(I),I=1,M)
    8 FORMAT (/19H TABLE OF INITIAL Y/(8G13.5))
      WRITE (OT,9) (NTAB(I),I=1,NSAV)
    9 FORMAT (/7H NTAB =,5I6)
C     SET UP SOURCE CONDITIONS
      DO 11 I=2,M1
      AY=ABS(Y(I)-Y0)
```

```
      ALPHA1=0.5*HO
      DO 13 J=1,3
   13 CM(I,J)=0.
      F(I-1)=CAY(I-1,I)
      U(I-1)=USUB(Y(I))
      IF (AY-ALPHA1)  12,11,11
   12 SAV1=SQRT(1.-(AY/ALPHA1)**2)
      CM(I,1)=SQRT(SAV1)
      CM(I,2)=SAV1*CM(I,1)
      CM(I,3)=CM(I,2)
      DO 11 J=1,3
      IF (ABS(CM(I,J))-TESTXP)  872,872,11
  872 CM(I,J)=0.0
   11 CONTINUE
C     SET BOUNDARY CONDITION AT X=0
      DO 14 J=1,3
      CM(1,J)=CM(3,J)-2.*CKE*DY(1,1)*CM(2,J)
   14 CM(M,J)=CM(M2,J)
C     LOOP ON NUMBER OF DELTA X-S
      X=0.
      IDY=2
C     PRINT SOURCE CONDITIONS
      L=1
      DO 17 I=2,NPRINT
      IF (ABS(CM(I,1))-1.0E-08) 17,17,16
   16 CO(L)=CM(I,1)
      YO(L)=Y(I)
      SZ(L)=SQRT(CM(I,2)/CM(I,1))
      CMAX(L)=CM(I,1)/SZ(L)
      L=L+1
   17 CONTINUE
      L=L-1
      WRITE (OT,90) X
   90 FORMAT(1H//3H X=,G12.5,//,5X,1HY,11X,2HCO,11X,7HSIGMA Z,7X,4HCMAX,
     1/)
      WRITE (OT,491) (YO(I),CO(I),SZ(I),CMAX(I),I=1,L)
  491 FORMAT (4G13.5)
      DO 50 NDXL=1,NDX
      DELX= DX(NDXL)
```

```
      NUM=NXC(NDXL)
      IF (ABS(X-XDY(IDY))-0.00001) 121,121,122
C     SET UP NEW Y TABLE
  121 YY(1)=-DY(1,IDY)
      YY(2)=0.
      EKE=CKE*DY(1,IDY)
      K=2
      NPRINT=NPR(IDY)+1
      NSAV=NDYT(IDY)
      DO 123 I=1,NSAV
      DELY=DY(I,IDY)
      NUMM=NYC(I,IDY)
      DO 124 J=1,NUMM
      K=K+1
      YY(K)=YY(K-1)+DELY
  124 CONTINUE
  123 NTAB(I)=K
      NTAB(NSAV)=0
      MSAV=M
      M=K+1
      YY(M)=YY(K)+DELY
      M1=M-1
      M2=M1-1
C     SET UP PROPER SOLUTION AT DISTANCE N*DX
C     LOOP ON YY
      IKK=2
      DO 126 I=2,M
      IK=IKK
      DO 127 J=IK,MSAV
      IKK=J
      IF (ABS(YY(I)-Y(J))-0.00001) 129,129,511
  511 IF (YY(I)-Y(J)) 128,129,127
  129 DO 131 IJ=1,3
  131 SOL(I,IJ)=CM(J,IJ)
      GO TO 126
  128 DO 132 IJ=1,3
  132 SOL(I,IJ)=(CM(J,IJ)-CM(J-1,IJ))*(YY(I)-Y(J-1))/(Y(J)-Y(J-1))+CM(J-
     11,IJ)
      GO TO 126
```

```
  127 CONTINUE
  126 CONTINUE
C     RESET BOUNDARY CONDITIONS
      DO 130 IJ=1,3
      SOL(M,IJ)=SOL(M2,IJ)
  130 SOL(1,IJ)=SOL(3,IJ)-2.*EKE*SOL(2,IJ)
      DO 133 I=1,M
      Y(I)=YY(I)
      DO 133 IJ=1,3
  133 CM(I,IJ)=SOL(I,IJ)
      DO 378 I=2,M1
      U(I-1)=USUB(Y(I))
  378 F(I-1)=CAY(I-1,I)
      IDY=IDY+1
C     SET UP MATRIX COEFFICIENTS FOR A CONSTANT DELTA X
  122 L=1
      IDYY=IDY-1
      X1(L)=0.5*DELX/DY(1,IDYY)**2
      DO 20 I=2,M1
      J=I-1
      IF (I-NTAB(L)) 21,22,21
   21 A(J)=-X1(L)*F(J)
      B(J)=X1(L)*(F(I)+F(J))+U(J)    +CKD*DELX
      C(J)=-X1(L)*F(I)
      GO TO 20
   22 X2(L)=DELX/(DY(L,IDYY)*DY(L+1,IDYY)*(DY(L,IDYY)+DY(L+1,IDYY)))
      A(J)=-X2(L)*F(J)*DY(L+1,IDYY)
      B(J)=X2(L)*(DY(L,IDYY)*F(I)+DY(L+1,IDYY)*F(J))+U(J)   +CKD*DELX
      C(J)=-X2(L)*F(I)*DY(L,IDYY)
      L=L+1
      X1(L)=0.5*DELX/DY(L,IDYY)**2
   20 CONTINUE
C     SET UP BOUNDARY CONDITIONS
      B(1)=B(1)-A(1)*EKE *2.
      C(1)=C(1)+A(1)
      A(M2)=A(M2)+C(M2)
C     TRIANGULATE MATRIX
      A(M2)=A(M2)/B(M2)
      DO 30 J=2,M2
```

```
          I=M2-J+1
          B(I)=B(I)-C(I)*A(I+1)
       30 A(I)=A(I)/B(I)
C         LOOP IN X-COORDINATE
          DO 51 NTIME=1,NUM
          X=X+DELX
C         LOOP OVER NUMBER OF EQUATIONS
          DO 52 NEQ=1,3
C         GENERATE NON-HOMOGENEOUS TERMS
          L=1
          DO 40 I=2,M1
          J=I-1
          I1=I+1
          IF (I-NTAB(L)) 41,42,41
       41 D(J)=CM(I,NEQ)*U(J)+X1(L)*(F(I)*(CM(I1,NEQ)-CM(I,NEQ))-F(J)*(CM(I,
         1NEQ)-CM(J,NEQ)))
          GO TO 43
       42 D(J)=CM(I,NEQ)*U(J)+X2(L)*(DY(L,IDYY)*F(I)*(CM(I1,NEQ)-CM(I,NEQ))-
         1DY(L+1,IDYY)*F(J)*(CM(I,NEQ)-CM(J,NEQ)))
          L=L+1
       43 CONTINUE
          GO TO (40,71,72),NEQ
       71 D(J)=D(J)+DELX*(CAYZ(I,CM)*(SOL(I,1)+CM(I,1)))
          GO TO 40
       72 D(J)=D(J)+DELX*(CAYZ(I,SOL)*(SOL(I,1)+CM(I,1)))
       40 CONTINUE
          D(M2)=D(M2)/B(M2)
          DO 66 J=2,M2
          I=M2-J+1
       66 D(I)=(D(I)-C(I)*D(I+1))/B(I)
C         COMPUTE SOLUTION VECTOR
          SOL(2,NEQ)=D(1)
          DO 67 I=2,M2
          IF (ABS(SOL(I,NEQ))-TESTXP) 881,881,67
      881 SOL(I,NEQ)=0.
       67 SOL(I+1,NEQ)=D(I)-A(I)*SOL(I,NEQ)
      882 SOL(M,NEQ)=SOL(M2,NEQ)
      883 CONTINUE
          SOL(1,NEQ)=SOL(3,NEQ)-2.*EKF*SOL(2,NEQ)
```

```
   52 CONTINUE
      DO 73 J=1,M
   73 SOL(J,2)=0.5*(SOL(J,2)+SOL(J,3))
      IF (MOD(NTIME,NPX(NDXL))) 98,54,98
C     COMPUTE INTEGRAL OF CO OVER DEPTH
   54 N1=3
      SUM=0.0
      DO 220 I=1,NSAV
      N2=NTAB(I)-1
      IF (I-NSAV) 221,222,221
  222 N2=M2
  221 SUM1=(SOL(N1-1,1)*U(N1-2)+SOL(N2+1,1)*U(N2))/2.
      DO 223 J=N1,N2
  223 SUM1=SUM1+SOL(J,1)*U(J-1)
      SUM=SUM1*DY(I,IDYY)+SUM
  220 N1=N2+2
C     COMPUTE DESIRED OUTPUT
      L=1
      DO 80 I=2,NPRINT
      IF (ABS(SOL(I,1))-1.0E-08) 80,80,81
   81 YO(L)=Y(I)
      CO(L)=SOL(I,1)
      SZ2=SOL(I,2)/SOL(I,1)
      IF (SZ2) 82,83,83
   82 SZ(L)=-SQRT(-SZ2)
      CMAX(L)=CO(L)/SZ(L)
      GO TO 76
   83 SZ(L)=SQRT(SZ2)
      CMAX(L)=CO(L)/SZ(L)
   76 L=L+1
   80 CONTINUE
      WRITE (OT,290) X,SUM
  290 FORMAT(1H1//7H    X =,G12.5,5X,8HI(CO*U)=,G12.5//5X,1HY,11X,3H CO,
     18X,7HSIGMA Z, 7X,4HCMAX,/)
      LM=L-1
      IF (LM-38) 94,94,95
   94 L1=1
      L2=L-1
      GO TO 96
```

```
   95 L1=1
      L2=38
   96 WRITE (OT,91)(YO(I),CO(I),SZ(I),CMAX(I),I=L1,L2)
   91 FORMAT (4G13.5)
      IF (L2-LM) 97,98,98
   97 L1=39
      L2=L-1
      WRITE (OT,99)
   99 FORMAT (1H1///)
      GO TO 96
C     SHIFT SOLUTION TO NEXT X-STEP
   98 DO 92 J=1,2
      DO 92 I=1,M
   92 CM(I,J)=SOL(I,J)
      DO 49 I=1,M
   49 CM(I,3)=CM(I,2)
   51 CONTINUE
   50 CONTINUE
      GO TO 100
      END

      FUNCTION CAY(I,J)
C     COMPUTE KY - VERTICAL DIFFUSION COEFFICIENT
C     UNIFORM CAY(=BETA2) IF YK4 IS NEGATIVE
      REAL LAMBDA
      DIMENSION Y(100),CM(100,3)
      COMMON LAMBDA,YO,HO,YE1,YE,YK1,YK2,YK3,YK4,BETA1,BETA2,CKE,CKD,
     1Y,CM,UFS
      P=(Y(I)+Y(J))/2.
      IF (YK4) 9,9,1
    1 IF (P-YK1) 2,2,3
    2 CAY=1.
      RETURN
    3 IF(P-YK2) 4,5,5
    4 CAY=(BETA1*(YK1-P)+(P-YK2))/(YK1-YK2)
      RETURN
    5 IF (P-YK3) 6,7,7
    6 CAY= BETA1
      RETURN
    7 IF (P-YK4) 8,9,9
    8 CAY=(BETA2*(YK3-P)+BETA1*(P-YK4))/(YK3-YK4)
      RETURN
    9 CAY=BETA2
      RETURN
      END
```

```
      FUNCTION USUB(Y)
      REAL LAMBDA
      DIMENSION Z(100),CM(100,3)
      COMMON LAMBDA,YO,HO,YE1,YE,YK1,YK2,YK3,YK4,BETA1,BETA2,CKE,CKD,
     1Z,CM,UFS
      IF (UFS) 10,10,11
   10 USUB=0.
      RETURN
   11 IF (Y-YE) 6,6,7
    6 IF (Y-YE1) 5,4,4
    5 USUB=UFS
      RETURN
    4 USUB=UFS*((Y-YE)/(YE1-YE))
      RETURN
    7 USUB=0.
      RETURN
      END
```

```
      FUNCTION CAYZ(L,CM)
C       COMPUTE KZ
      REAL LAMBDA
      COMMON LAMBDA,YO,HO,YE1,YE,YK1,YK2,YK3,YK4,BETA1,BETA2,CKE,CKD,
     1Y
      DIMENSION Y(100),CM(100,3)
      IF (ABS(CM(L,1))-1.0E-08) 1,1,2
    1 CAYZ=0.
      RETURN
    2 CAYZ=LAMBDA*(ABS(CM(L,2)/CM(L,1)))**0.666666667
      RETURN
      END
```

APPENDIX D

The problem discussed in Chapter 5 on the unsteady dispersion from a continuous source can be solved using the program listed in this appendix. The numerical scheme used is based on the Crank-Nicolson method.

Input:

In Text	In Program	Remarks
	NEND	see list in Appendix C
	NDY	" " " " "
	NDX	number of variation of t-step sizes
	NEXP	see list in Appendix C
	NT	number of times in specifying u, K_e, F_{co} values
	NXPR	number of variations of DXPR sizes
	LAMBDA	See list in Appendix C
	YO	"
	HO	"
	YK1	"
	YK2	"
	YK3	"
	YK4	"
	BETA1	"
	BETA2	"
	CKD	"
	XDY(I)	t to change y-mesh scheme
	NDYT(I)	see list in Appendix C
	NPR(I)	"
	TI(I)	times at which u, K_e, F_{co} specified

In Text	In Program	Remarks
u	U(I)	u at time TI(I)
K_e	CKE(I)	K_e at time TI(I)
$F_{co}(t)$	FC(I)	F_{co} at time TI(I)
	DXPR(I)	spacing in x for each printout, constant for NXPRC steps
	NXPRC(I)	see above
	DY(I, J)	y-mesh constant for NYC grids
	NYC(I, J)	number of grids that y has mesh size DY
	DX(I)	step size in t constant for NXC steps
	NXC(I)	number of steps that x has step size DX

Output:

	TI	See Input List
	U	"
	CKE	"
	FC	"
	LAMBDA	"
	YO	"
	HO	"
	YK1	"
	YK2	"
	YK3	"
	YK4	"
	BETA1	"
	BETA2	"
K_d	KD	
	XPR	x values for printout
	TPR	t values for printout
	Y	see output list for Appendix C
	CO	"
	SIGMZ	"
	CMAX	"

```
C      PROGRAM UTD--UNSTEADY TURBULENT DIFFUSION OF A CONTINUOUS SOURCE
       INTEGER OT
       REAL LAMBDA
       DIMENSION A(100),B(100),C(100),D(100),F(100),Y(100),CM(100,3),
      1SOL(100,3),YO(99),SZ(99),CMAX(99),  DY(9,9),  DX(9),NYC(9,9),
      2NXC(9),NTAB(9),X1(9),X2(9),CO(99),U(99)
       DIMENSION T(99),TI(99),CKE(99),FC(99),XI(99),DXPR(9),NXPRC(9),
      1TPR(99),XPR(99),SOLU(100,3)
       DIMENSION NDYT(9),YY(100),NPX(9),XDY(9),NPR(9)
       COMMON LAMBDA,YO,HO,        YK1,YK2,YK3,YK4,BETA1,BETA2,    CKD,
      1Y,CM
       COMMON /HOLD/A,B,C,D,F,SOL,YO,SZ,CMAX,CO
       OT=6
   100 READ (5,1)NEND,NDY,NDX,NEXP,NT,NXPR
     1 FORMAT(10I5)
       PAI=3.1415927
       TESTXP=1./10.**NEXP
       IF (NEND) 3,4,3
     4 CALL EXIT
     3 READ(5,2) LAMBDA,YO,HO,            YK1,YK2,YK3,YK4,BETA1,BETA2,
      1CKD,TF
     2 FORMAT (8E10.5)
       READ (5,834) (XDY(I),NDYT(I),NPR(I), I=1,NDY)
   834 FORMAT (8(F5.1,I3,I2))
       READ (5,835) (TI(I),U(I),CKE(I),FC(I),I=1,NT)
   835 FORMAT(4E10.5)
       TF=TI(NT)
       XI(1)=0.
       JS=2
       DO 730 I=2,NT
       XI(I)=XI(I-1)+0.5*(U(I)+U(I-1))*(TI(I)-TI(I-1))
   730 CONTINUE
       WRITE (6,336) (I,TI(I),U(I),CKE(I),FC(I),XI(I),I=1,NT)
   336 FORMAT (//12H TI,U,CKE,FC/(I5,5G13.5))
       READ (5,31) (DXPR(I),NXPRC(I),I=1,NXPR)
    31 FORMAT (4(E10.5,I10))
       K=2
       XPR(1)=0.
       DO 32 I=1,NXPR
```

```
      NXPRCC=NXPRC(I)
      DXPRC=DXPR(I)
      DO 33 J=1,NXPRCC
      XPR(K)=XPR(K-1)+DXPRC
      IF (XPR(K)-XI(NT)) 331,331,332
  331 K=K+1
   33 CONTINUE
   32 CONTINUE
  332 NXPR1=K-1
  832 DO 24 I=1,9
      DO 847 J=1,9
      DY(I,J)=0.0
  847 NYC(I,J)=0
      X1(I)=0.0
      X2(I)=0.0
      DX(I)=0.0
      NXC(I)=0.0
   24 NTAB(I)=0
   58 WRITE (OT,6) LAMBDA,YO,HO,YK1,YK2,YK3,YK4,BETA1,BETA2,
     1CKD
    6 FORMAT(9H1LAMBDA =,G12.5,//7H  YO  =,G12.5,15X,5H HO =,G12.5,//9H
     1KY-PROF.,2X,4HYK1=,G12.5,2X,4HYK2=,G12.5,4HYK3=,G12.5,2X,4HYK4=,
     2G12.5,2X,6HBETA1=,G12.5,2X,6HBETA2=,G12.5//13H DECAY COEFF.,10X,5H
     3 KD =,G12.5/)
      NDY1=NDY-1
      DO 110 I=1,NDY1
      NSAV=NDYT(I)
      READ (5,5) (DY(J,I), NYC(J,I),J=1,NSAV)
      WRITE (OT,111) I, XDY(I)
      WRITE (OT,7) (DY(J,I), NYC(J,I),J=1,NSAV)
  111 FORMAT (I10,5X,6H   X =,G12.5)
  110 CONTINUE
      READ (5,55) (DX(I),NXC(I),I=1,NDX)
   55 FORMAT (4(E10.5,I10))
    5 FORMAT (4(E10.5,I5,5X))
      WRITE (OT,7) (DX(I),NXC(I),I=1,NDX)
    7 FORMAT(5(G12.5,I10))
C     MAIN LOOP OVER TIME OF RELEASES
      NT1=NT-1
```

```
      DO 102 NTI=1,NT1
      XINTI=XI(NTI)
      DO 740 I=NTI,NT
  740 XI(I)=XI(I)-XINTI
      TPR(1)=0.
      J=JS
      NXPR11=NXPR1+1
      DO 38 I=2,NXPR11
   37 IF (XPR(I)-XI(J)) 34,36,35
   35 J=J+1
      IF(J-NT) 37,37,39
   36 TPR(I)=TI(J)
      GO TO 38
   39 TPR(1)=-1.2345
      NXPR2=I-1
      GO TO 1002
   34 TPR(I)=TI(J-1)+(TI(J)-TI(J-1))*(XPR(I)-XI(J-1))/(XI(J)-XI(J-1))
     1-TI(JS-1)
   38 CONTINUE
 1002 WRITE (6,333) (I,XPR(I),TPR(I),I=1,NXPR2)
  333 FORMAT (8H1XPR,TPR/(I5,2G15.5))
      MT=2
      TIN=TI(NTI)
      TF1=TF-TIN
      IF (TF1) 100,100,101
  101 FC1=FC(NTI)
      RKE=CKE(NTI)
C     SET UP TABLE
      EKE=RKE*DY(1,1)
      Y(1)=-DY(1,1)
      Y(2)=0.
      K=2
      NSAV=NDYT(1)
      DO 10 I=1,NSAV
      DELY=DY(I,1)
      NUM=NYC(I,1)
      DO 15 J=1,NUM
      K=K+1
      Y(K)=Y(K-1)+DELY
```

```
   15 CONTINUE
   10 NTAB(I)=K
      NPRINT=NPR(1)+1
      NTAB(NSAV)=0
      M=K+1
      Y(M)=Y(K)+DELY
      M1=M-1
      M2=M1-1
      WRITE (OT,8) (Y(I),I=1,M)
    8 FORMAT (/19H TABLE OF INITIAL Y/(8G13.5))
      WRITE (OT,9) (NTAB(I),I=1,NSAV)
    9 FORMAT (/7H NTAB =,5I6)
C     SET UP SOURCE CONDITIONS
      DO 11 I=2,M1
      AY=ABS(Y(I)-YO)
      ALPHA1=0.5*HO
      DO 13 J=1,3
   13 CM(I,J)=0.
      F(I-1)=CAY(I-1,I)
      IF (AY-ALPHA1)  12,11,11
   12 SAV1=SQRT(1.-(AY/ALPHA1)**2)
      CM(I,1)=SQRT(SAV1)*FC1
      CM(I,2)=SAV1*CM(I,1)
      CM(I,3)=CM(I,2)
      DO 11 J=1,3
      IF (ABS(CM(I,J))-TESTXP)  872,872,11
  872 CM(I,J)=0.0
   11 CONTINUE
C     SET BOUNDARY CONDITION AT X=0
      DO 14 J=1,3
      CM(1,J)=CM(3,J)-2.*EKE*CM(2,J)
   14 CM(M,J)=CM(M2,J)
C     LOOP ON NUMBER OF DELTA X-S
      X=0.
      IDY=2
C     PRINT SOURCE CONDITIONS
      L=1
      DO 17 I=2,NPRINT
      IF (ABS(CM(I,1))-1.0E-08) 17,17,16
```

```
   16 CO(L)=CM(I,1)
      YO(L)=Y(I)
      SZ(L)=SQRT(CM(I,2)/CM(I,1))
      CMAX(L)=CM(I,1)/SZ(L)
      L=L+1
   17 CONTINUE
      L=L-1
      WRITE (OT,90) TIN
   90 FORMAT(1H//15H1RELEASE TIME =,G12.5//,5X,1HY,11X,2HCO,11X,7HSIGMA
     1Z,7X,4HCMAX,/)
      WRITE (OT,491) (YO(I),CO(I),SZ(I),CMAX(I),I=1,L)
  491 FORMAT (4G13.5)
      DO 50 NDXL=1,NDX
      DELX= DX(NDXL)
      NUM=NXC(NDXL)
      IF (ABS(X-XDY(IDY))-0.00001) 121,121,122
C     SET UP NEW Y TABLE
  121 YY(1)=-DY(1,IDY)
      YY(2)=0.
      EKE=RKE*DY(1,IDY)
      K=2
      NPRINT=NPR(IDY)+1
      NSAV=NDYT(IDY)
      DO 123 I=1,NSAV
      DELY=DY(I,IDY)
      NUMM=NYC(I,IDY)
      DO 124 J=1,NUMM
      K=K+1
      YY(K)=YY(K-1)+DELY
  124 CONTINUE
  123 NTAB(I)=K
      NTAB(NSAV)=0
      MSAV=M
      M=K+1
      YY(M)=YY(K)+DELY
      M1=M-1
      M2=M1-1
C     SET UP PROPER SOLUTION AT DISTANCE N*DX
C     LOOP ON YY
```

```
      IKK=2
      DO 126 I=2,M
      IK=IKK
      DO 127 J=IK,MSAV
      IKK=J
      IF (ABS(YY(I)-Y(J))-0.00001) 129,129,511
  511 IF (YY(I)-Y(J)) 128,129,127
  129 DO 131 IJ=1,3
  131 SOL(I,IJ)=CM(J,IJ)
      GO TO 126
  128 DO 132 IJ=1,3
  132 SOL(I,IJ)=(CM(J,IJ)-CM(J-1,IJ))*(YY(I)-Y(J-1))/(Y(J)-Y(J-1))+CM(J-
     11,IJ)
      GO TO 126
  127 CONTINUE
  126 CONTINUE
C     RESET BOUNDARY CONDITIONS
      DO 130 IJ=1,3
      SOL(M,IJ)=SOL(M2,IJ)
  130 SOL(1,IJ)=SOL(3,IJ)-2.*EKE*SOL(2,IJ)
      DO 133 I=1,M
      Y(I)=YY(I)
      DO 133 IJ=1,3
  133 CM(I,IJ)=SOL(I,IJ)
      DO 378 I=2,M1
  378 F(I-1)=CAY(I-1,I)
      IDY=IDY+1
C     SET UP MATRIX COEFFICIENTS FOR A CONSTANT DELTA X
  122 L=1
      IDYY=IDY-1
      X1(L)=0.5*DELX/DY(1,IDYY)**2
      DO 20 I=2,M1
      J=I-1
      IF (I-NTAB(L)) 21,22,21
   21 A(J)=-X1(L)*F(J)
      B(J)=X1(L)*(F(I)+F(J))+1.00   +CKD*DELX
      C(J)=-X1(L)*F(I)
      GO TO 20
   22 X2(L)=DELX/(DY(L,IDYY)*DY(L+1,IDYY)*(DY(L,IDYY)+DY(L+1,IDYY)))
```

```
      A(J)=-X2(L)*F(J)*DY(L+1,IDYY)
      B(J)=X2(L)*(DY(L,IDYY)*F(I)+DY(L+1,IDYY)*F(J))+1.00 +CKD*DELX
      C(J)=-X2(L)*F(I)*DY(L,IDYY)
      L=L+1
      X1(L)=0.5*DELX/DY(L,IDYY)**2
   20 CONTINUE
      C(1)=C(1)+A(1)
      B1=B(1)
      A1=A(1)
      A(M2)=A(M2)+C(M2)
C     TRIANGULATE MATRIX
      A(M2)=A(M2)/B(M2)
      M3=M2-1
      DO 30 J=2,M3
      I=M2-J+1
      B(I)=B(I)-C(I)*A(I+1)
   30 A(I)=A(I)/B(I)
C     LOOP IN X-COORDINATE
      DO 51 NTIME=1,NUM
      X=X+DELX
      IF(X-TF1) 1001,1001,102
 1001 XT=X+TIN
      IR=1
  109 IF (XT-TI(IR)) 106,108,107
  107 IR=IR+1
      IF (IR-NT) 109,109,735
  735 IR=IR-1
  108 RKE=CKE(IR)
      GO TO 103
  106 IF (IR-1) 733,733,732
  733 RKE=CKE(1)
      GO TO 103
  732 RKE=CKE(IR)-(TI(IR)-XT)/(TI(IR)-TI(IR-1))*(CKE(IR)-CKE(IR-1))
  103 EKE=RKE*DY(1,IDYY)
C     SET UP BOUNDARY CONDITIONS
      B(1)=B1-A1*EKE *2.
      B(1)=B(1)-C(1)*A(2)
      A(1)=A1/B(1)
C     LOOP OVER NUMBER OF EQUATIONS
```

```
      DO 52 NEQ=1,3
C     GENERATE NON-HOMOGENEOUS TERMS
      L=1
      DO 40 I=2,M1
      J=I-1
      I1=I+1
      IF (I-NTAB(L)) 41,42,41
   41 D(J)=CM(I,NEQ)*1.00+X1(L)*(F(I)*(CM(I1,NEQ)-CM(I,NEQ))-F(J)*(CM(I,
     1NEQ)-CM(J,NEQ)))
      GO TO 43
   42 D(J)=CM(I,NEQ)*1.00+X2(L)*(DY(L,IDYY)*F(I)*(CM(I1,NEQ)-CM(I,NEQ))-
     1DY(L+1,IDYY)*F(J)*(CM(I,NEQ)-CM(J,NEQ)))
      L=L+1
   43 CONTINUE
      GO TO (40,71,72),NEQ
   71 D(J)=D(J)+DELX*(CAYZ(I,CM)*(SOL(I,1)+CM(I,1)))
      GO TO 40
   72 D(J)=D(J)+DELX*(CAYZ(I,SOL)*(SOL(I,1)+CM(I,1)))
   40 CONTINUE
      D(M2)=D(M2)/B(M2)
      DO 66 J=2,M2
      I=M2-J+1
   66 D(I)=(D(I)-C(I)*D(I+1))/B(I)
C     COMPUTE SOLUTION VECTOR
      SOL(2,NEQ)=D(1)
      DO 67 I=2,M2
      IF (ABS(SOL(I,NEQ))-TESTXP) 881,881,67
  881 SOL(I,NEQ)=0.
   67 SOL(I+1,NEQ)=D(I)-A(I)*SOL(I,NEQ)
      IF (ABS(SOL(M2+1,NEQ))-TESTXP) 882,882,883
  882 SOL(M2+1,NEQ)=0.0
  883 CONTINUE
      SOL(M,NEQ)=SOL(M2,NEQ)
      SOL(1,NEQ)=SOL(3,NEQ)-2.*EKE*SOL(2,NEQ)
   52 CONTINUE
      DO 73 J=1,M
   73 SOL(J,2)=0.5*(SOL(J,2)+SOL(J,3))
      IF (X-TPR(MT)) 98,301,301
  301 COEF=(X-TPR(MT))/DELX
```

```
      XPRR=XPR(MT)
      TPRR=TPR(MT)+TIN
      MT=MT+1
      DO 731 I=1,M
      SOLU(I,1)=SOL(I,1)-(SOL(I,1)-CM(I,1))*COEF
  731 SOLU(I,2)=SOL(I,2)-(SOL(I,2)-CM(I,2))*COEF
C     COMPUTE INTEGRAL OF CO OVER DEPTH
   54 N1=3
      SUM=0.0
      DO 220 I=1,NSAV
      N2=NTAB(I)-1
      IF (I-NSAV) 221,222,221
  222 N2=M2
  221 SUM1=(SOL(N1-1,1)+SOL(N2+1,1))/2.
      DO 223 J=N1,N2
  223 SUM1=SUM1+SOL(J,1)
      SUM=SUM1*DY(I,IDYY)+SUM
  220 N1=N2+2
C     COMPUTE DESIRED OUTPUT
      L=1
      DO 80 I=2,NPRINT
      IF (ABS(SOLU(I,1))-1.0E-08) 80,80,81
   81 YC(L)=Y(I)
      CO(L)=SOLU(I,1)
      SZ2=SOLU(I,2)/SOLU(I,1)
      IF (SZ2) 82,83,83
   82 SZ(L)=-SQRT(-SZ2)
      CMAX(L)=CO(L)/SZ(L)
      GO TO 76
   83 SZ(L)=SQRT(SZ2)
      CMAX(L)=CO(L)/SZ(L)
   76 L=L+1
   80 CONTINUE
      WRITE (OT,290) TIN,FC1,TPRR,XPRR,SUM
  290 FORMAT(1H1//18H TIME OF RELEASE =,G12.5,5X,20H AMOUNT OF RELEASE =
     1,G12.5,5X,7H TIME =,G12.5,5X,5H  X =,G12.5,5X,//8H I(CO) =,G12.5//
     25X,1HY,11X,3H CO,8X,7HSIGMA Z,7X,4HCMAX,/)
      LM=L-1
      IF (LM-38) 94,94,95
```

```
   94 L1=1
      L2=L-1
      GO TO 96
   95 L1=1
      L2=38
   96 WRITE (OT,91)(YO(I),CO(I),SZ(I),CMAX(I),I=L1,L2)
   91 FORMAT (4G13.5)
      IF (L2-LM) 97,98,98
   97 L1=39
      L2=L-1
      WRITE (OT,99)
   99 FORMAT (1H1///)
      GO TO 96
C     SHIFT SOLUTION TO NEXT X-STEP
   98 DO 92 J=1,2
      DO 92 I=1,M
   92 CM(I,J)=SOL(I,J)
      DO 49 I=1,M
   49 CM(I,3)=CM(I,2)
      IF(TPR(MT)) 102,51,51
   51 CONTINUE
   50 CONTINUE
  102 JS=JS+1
      GO TO 100
      END
```

```
      FUNCTION CAY(I,J)
C     COMPUTE KY - VERTICAL DIFFUSION COEFFICIENT
C     UNIFORM CAY(=BETA2) IF YK4 IS NEGATIVE
      REAL LAMBDA
      DIMENSION Y(100),CM(100,3)
      COMMON LAMBDA,YO,HO,        YK1,YK2,YK3,YK4,BETA1,BETA2,     CKD,
     1Y,CM
      P=(Y(I)+Y(J))/2.
      IF (YK4) 9,9,1
    1 IF (P-YK1) 2,2,3
    2 CAY=1.
      RETURN
    3 IF(P-YK2) 4,5,5
    4 CAY=(BETA1*(YK1-P)+(P-YK2))/(YK1-YK2)
      RETURN
    5 IF (P-YK3) 6,7,7
    6 CAY= BETA1
      RETURN
    7 IF (P-YK4) 8,9,9
    8 CAY=(BETA2*(YK3-P)+BETA1*(P-YK4))/(YK3-YK4)
      RETURN
    9 CAY=BETA2
      RETURN
      END
```



```
      FUNCTION CAYZ(L,CM)
C      COMPUTE KZ
      REAL LAMBDA
      COMMON LAMBDA,YO,HO,        YK1,YK2,YK3,YK4,BETA1,BETA2,     CKD
      DIMENSION CM(100,3)
      IF (ABS(CM(L,1))-1.0E-08) 1,1,2
    1 CAYZ=0.
      RETURN
    2 CAYZ=LAMBDA*(ABS(CM(L,2)/CM(L,1)))**0.666666667
      RETURN
      END
```

BIBLIOGRAPHIC: Tetra Tech, Inc., C. Y. Koh and Loh-Nien Fan, "Mathematical Models for the Prediction of Temperature Distributions From the Discharge of Heated Water into Large Bodies of Water", FWQA Publication No. 16130 DWØ10/70.

ACCESSION NO.

ABSTRACT: Mathematical models for heated water outfalls were developed for three flow regions. Near the source, the subsurface discharge into a stratified ambient water issuing from a row of buoyant jets was solved with the jet interference included in the analysis. The analysis of the flow zone close to and at intermediate distances from a surface buoyant jet was developed for the two-dimensional and axisymmetric cases. Far away from the source, a passive dispersion model was solved for a two-dimensional situation taking into consideration the effects of shear current and vertical changes in diffusivity.

A significant result from the surface buoyant jet analysis is the ability to predict the onset and location of an internal hydraulic jump. Prediction can be made simply from the knowledge of the source Froude number and a dimensionless surface exchange coefficient.

Parametric computer programs of the above models are also developed as a part of this study.

This report was submitted in fulfillment of Contract No. 14-12-570 under the sponsorship of the Federal Water Quality Administration.

KEY WORDS:

Mathematical mode
Thermal outfall

1 Accession Number	2 Subject Field & Group	
	Ø23C	**SELECTED WATER RESOURCES ABSTRACTS** INPUT TRANSACTION FORM

5 *Organization*

Tetra Tech, Inc.

6 *Title*

"Mathematical Models for the Prediction of Temperature Distributions Resulting From the Discharge of Heated Water into Large Bodies of Water"

10 *Author(s)*

C. Y. Koh and
Loh-Nien Fan

16 *Project Designation*

FWQA Contract #14-12-570; DWØ

21 *Note*

22 *Citation*

FWQA, R & D Report 16130DWØ10/70

23 *Descriptors (Starred First)*

*Mathematical Model, *Outfalls, *Thermal Pollution

25 *Identifiers (Starred First)*

Thermal outfalls

27 *Abstract*

Mathematical models for heated water outfalls were developed for three flow regions. Near the source, the subsurface discharge into a stratified ambient water issuing from a row of buoyant jets was solved with the jet interference included in the analysis. The analysis of the flow zone close to and at intermediate distances from a surface buoyant jet was developed for the two-dimensional and axisymmetric cases. Far away from the source, a passive dispersion model was solved for a two-dimensional situation taking into consideration the effects of shear current and vertical changes in diffusivity..

A significant result from the surface buoyant jet analysis is the ability to predict the onset and location of an internal hydraulic jump. Prediction can be made simply from the knowledge of the source Froude number and a dimensionless surface exchange coefficient.

Parametric computer programs of the above models are also developed as a part of this study.

This report was submitted in fulfillment of Contract No. 14-12-570 under the sponsorship of the Federal Water Quality Administration.

Abstractor Shirazi, Mostafa A.

Institution EPA/Federal Water Quality Administration

WR:102 (REV. JULY 1969)
WRSIC

SEND TO: WATER RESOURCES SCIENTIFIC INFORMATION CENTER
U.S. DEPARTMENT OF THE INTERIOR
WASHINGTON, D. C. 20240

★ GPO: 1969—359-339